

SLAC - PUB - 3665  
May 1985  
(T/E)

# The Higgs Boson In $e^+e^-$ Annihilation Experimental Status And Perspectives\*

ANDREAS S. SCHWARZ

*Stanford Linear Accelerator Center  
Stanford University, Stanford, California, 94305*

## ABSTRACT

The current experimental status of the Higgs particle of the standard model of electroweak interaction is reviewed. Special emphasis is put on the possible production in the decays of heavy vector resonances like the  $J/\Psi$  and the  $\Upsilon$ . Extensions of the simple Higgs sector with their phenomenological implications are discussed. An overview concerning Higgs production at  $Z^0$  factories like the SLC and LEP is given.

*Submitted for Publications*

---

\* Work supported by the Department of Energy, contract DE-AC03-76SF00515

# TABLE OF CONTENTS

Abstract . . . . .	1
1. Introduction . . . . .	2
2. The Standard Model and the Higgs mechanism . . . . .	3
3. The properties of the Higgs boson . . . . .	9
4. Nonstandard Higgs models . . . . .	12
5. Search for the standard Higgs in $e^+e^-$ annihilation . . . . .	15
5.1 Continuum production . . . . .	16
The direct process $e^+e^- \rightarrow H^0 \rightarrow \text{hadrons}$ . . . . .	16
The Bremsstrahlung off final state quarks . . . . .	17
The process $e^+e^- \rightarrow H^0\gamma$ . . . . .	17
Two photon physics and the Higgs boson . . . . .	18
5.2 The standard Higgs and heavy vector resonances . . . . .	18
The Bremsstrahlung off the $J/\Psi$ . . . . .	19
$\Psi' \rightarrow H^0 + J/\Psi$ . . . . .	19
The Wilczek mechanism $V(q\bar{q}) \rightarrow \gamma H^0$ . . . . .	20
$J/\Psi \rightarrow \gamma\xi(2.2)$ . . . . .	22
$\Upsilon \rightarrow \gamma\zeta(8.3)$ . . . . .	29
The mixing with the $^3P_0$ state of quarkonium . . . . .	35
B mesons and the standard Higgs . . . . .	37
6. Search for the nonstandard Higgs in $e^+e^-$ annihilation . . . . .	39
7. The $Z^0$ , Toponium and the Higgs boson . . . . .	43
$Z^0 \rightarrow \gamma + H^0$ . . . . .	44
$Z^0 \rightarrow Z^{0*} H^0 \rightarrow l^+l^- H^0$ . . . . .	45
$Z^{0*} \rightarrow Z^0 H^0$ . . . . .	46
$Z^0 \rightarrow H^+ H^-$ . . . . .	47
Toponium and the Higgs boson . . . . .	48
8. Conclusions . . . . .	49
List of References . . . . .	51
List of Figures . . . . .	57

# 1. Introduction

The recent discovery of the intermediate vector bosons  $W^\pm$  and  $Z^0$  (Ref. 1) at CERN as the carriers of the weak interaction has constituted a remarkable success of the standard model of electroweak interaction<sup>[2]</sup>. A very basic ingredient in this theory is the requirement of local gauge invariance under  $SU(2)\times U(1)$  transformations together with the method of spontaneous symmetry breaking<sup>[3]</sup>. It is this combination, which gives mass to the  $W^\pm$  and  $Z^0$  bosons. An immediate result in the standard model is the predicted existence of a scalar neutral massive particle, the Higgs boson. The following Chapter is a brief review of the basic ingredients of the standard model to indicate the key role, the Higgs mechanism is playing. In Chapter 3, the general properties of the standard Higgs particle will be discussed, followed in Chapter 4 by some remarks on the possible extensions of the minimal Higgs sector leading, among other things, to the prediction of charged Higgs bosons. In Chapter 5, I will give an overview on the possible promising signatures of the standard Higgs in  $e^+e^-$  interactions and the actual searches performed so far, whereas Chapter 6 will deal with the experimental search for charged Higgs bosons. Finally in Chapter 7, an outlook is attempted at the possibilities to discover the standard Higgs boson at the  $Z^0$  factories like the SLC<sup>[4]</sup> and LEP<sup>[6]</sup>. Though this seems not to be of immediate importance for the current experimental searches in  $e^+e^-$  annihilation, it might give some hints on the possible strategy one may have to pursue at  $e^+e^-$  storage rings currently in operation.

## 2. The Standard Model and the Higgs mechanism

Since the weak interactions among leptons were known to involve transitions  $\nu_e \leftrightarrow e$ ,  $\nu_\mu \leftrightarrow \mu$  etc., it was quite natural, to put the leptons into 'generations' or (weak isospin) doublets which can be described by the group SU(2):

$$\begin{pmatrix} \nu_e \\ e^- \end{pmatrix} \quad \begin{pmatrix} \nu_\mu \\ \mu^- \end{pmatrix} \quad \begin{pmatrix} \nu_\tau \\ \tau^- \end{pmatrix}, \dots \text{ with "weak charge" } \begin{pmatrix} +1/2 \\ -1/2 \end{pmatrix} \quad (2.1)$$

and equivalently for the quarks

$$\begin{pmatrix} u \\ d \end{pmatrix} \quad \begin{pmatrix} c \\ s \end{pmatrix} \quad \begin{pmatrix} t \\ b \end{pmatrix} \quad (2.2)$$

All experimental evidence so far is consistent with the assumption that charged weak currents involve only the lefthanded lepton components. The righthanded states do not participate in the charged weak interaction and hence have the weak charge 0. The additional assumption which was put into the model was, therefore, that the leptons and quarks form lefthanded weak isodoublets and righthanded weak isosinglets:

$$\begin{pmatrix} \nu_e^L \\ e_L^- \end{pmatrix} \text{ and } e_R^- \quad (2.3)$$

The known relationship between weak charge (weak isospin)  $I_3$  and electromagnetic charge  $Q$

$$Q = I_3 + \frac{Y}{2} \quad (2.4)$$

( $Y$  is the "weak hypercharge" associated with the one parameter group U(1), see also Table 1), gave the hint that the weak and electromagnetic interactions could be combined somehow to an interaction governed by the larger symmetry group SU(2)xU(1). If one now required that the Lagrangian describing the weak

and electromagnetic interactions is locally gauge invariant under  $SU(2) \times U(1)$  rotations, this lead immediately to the existence of one isotriplet gaugefield  $\vec{A}_\mu$  (corresponding to the generators of the weak isospin group associated with  $\vec{I}$ ) and one isosinglet gauge field  $B_\mu$  (associated with the hypercharge symmetry  $Y$ )<sup>[3]</sup>.

**Table 1:** Tabulation of the values of weak isospin  $I_3$ , electric charge  $Q$  and weak hypercharge  $Y$  for leptons (from Ref.3).

	$e_L$	$\nu_e^L$	$e_R$	$\nu_e^R$	$\mu_L$	$\nu_\mu^L$	$\mu_R$	$\nu_\mu^R$
$I_3$	-1/2	1/2	0	0	-1/2	1/2	0	0
$Y$	-1	-1	-2	0	-1	-1	-2	0
$Q$	-1	0	-1	0	-1	0	-1	0

The generalized Gell-Mann-Nishijima formula (2.4) implies that the physical photon (coupling only to the charge  $Q$ ) must be some linear combination of one component of each  $\vec{A}_\mu$  and  $B_\mu$ . The two gauge fields  $\vec{A}_\mu$  and  $B_\mu$  correspond hence to the introduction of four vector bosons described by<sup>[3]</sup>

$$W_\mu^+ = \frac{1}{\sqrt{2}}(A_{\mu_1} - iA_{\mu_2})$$

$$W_\mu^- = \frac{1}{\sqrt{2}}(A_{\mu_1} + iA_{\mu_2}) \quad (2.5)$$

$$Z_\mu = \cos \theta_W A_{\mu_3} - \sin \theta_W B_\mu$$

$$A_\mu = \sin \theta_W A_{\mu_3} + \cos \theta_W B_\mu$$

where  $\theta_W$  (the "Weinberg angle") is an adjustable parameter in the theory.  $W_\mu^\pm$  can be identified with the mediators of the weak charged currents involved in

reactions like the  $\beta$ - decay

$$p \rightarrow n + e^+ + \nu_e \quad (2.6)$$

and  $A_\mu$  can be identified with the photon of QED. Thus one important prediction of this model is the existence of a fourth vector boson, the  $Z^0$  (described by  $Z_\mu$ ), which introduces a new kind of weak interaction, the neutral weak current e.g.

$$e^- + \nu_\mu \rightarrow e^- + \nu_\mu \quad (2.7)$$

The Weinberg angle  $\theta_W$ , which can be determined by the interaction (2.7), describes the mixing of  $\vec{A}_\mu$  and  $B_\mu$  to produce the photon and the  $Z^0$ .

Unfortunately this theory, elegant as it was, was not complete, as it predicts the carriers of the weak interaction to be massless. This is in sharp contrast to experiment, as the *weak* force was known to be very short ranged indicating a force carrier with a very large mass instead. It is possible to introduce masses 'by hand' into the Lagrangian describing the interaction, but this would break the original local gauge invariance, leading to a theory which is not renormalizable and hence uncalculable.

Here is where the concept of "spontaneous symmetry breaking" enters<sup>[3]</sup>. It was known from the description of ferromagnetic materials, that it was possible to have the peculiar situation in which the Lagrangian describing a system could be perfectly symmetric but that the ground state (or vacuum state of the system) had a non zero value and thus was 'hiding' (=spontaneously breaking) the internal symmetry. The requirement of this spontaneous breakdown of the symmetry in the ground state leads to the appearance of a field of massless scalar particles for each degree of freedom in which the theory is spontaneously broken, the Goldstone bosons<sup>[6]</sup>.

— A very important additional ingredient was the observation that the presence of gauge fields (like e.g.  $\vec{A}_\mu, B_\mu$ ) evades the Goldstone theorem<sup>[7]</sup> by absorbing the degrees of freedom associated with the Goldstone bosons into additional

degrees of freedom for the gauge quanta. This mechanism (the Higgs mechanism) was exactly what was needed. If it would be possible to find a suitable transformation that would identify the degrees of freedom associated with the Goldstone bosons with the longitudinal polarisation degrees of freedom of some of the (up to now) massless gauge quanta, the corresponding gauge quanta would acquire a mass. At the same time the massless Goldstone bosons would disappear. So essentially the trick was to require local gauge symmetry under  $SU(2) \times U(1)$  rotations as before *but in a vacuum which has a groundstate or vacuumstate with nonzero expectation value*.

In the "standard model"<sup>[2]</sup> this mechanism of mass generation is realized by introducing a single complex doublet (under weak isospin) of scalar fields<sup>[3]</sup> \*

$$\phi = \frac{1}{\sqrt{2}} \begin{pmatrix} \phi_1 + i\phi_2 \\ \phi_3 + i\phi_4 \end{pmatrix} ; \phi_i \text{ real} \quad (2.8)$$

In order now to get spontaneous symmetry breaking, one has to introduce a potential (self-interactions) for the  $\phi$  field

$$V(\phi) = \mu^2(\phi^\dagger\phi) + \lambda(\phi^\dagger\phi)^2 \quad (2.9)$$

with  $\lambda > 0$ . If one now takes  $\mu^2$  to be negative, the system is in the spontaneously broken mode<sup>[3]</sup>. The vacuum expectation value  $v$  of  $\phi$  is determined by

$$(\phi^\dagger\phi)_{vac} = \frac{-\mu^2}{2\lambda} \quad (2.10)$$

Taking

$$\phi_{vac} = \frac{1}{\sqrt{2}} \begin{pmatrix} 0 \\ v \end{pmatrix} \quad (2.11)$$

---

\* Since all lefthanded fermions are in doublets and all righthanded fermions are in singlets, only Higgs doublets can contribute masses to all fermions<sup>[3]</sup>.

gives for the vacuum expectation value

$$v = \left[ \frac{-\mu^2}{\lambda} \right]^{1/2} . \quad (2.12)$$

Three of the four real field components  $\phi_i$  are identified as massless Goldstone bosons (corresponding to the spontaneous breakdown of  $SU(2)$ ). If one now requires the Lagrangian to be invariant under local  $SU(2) \times U(1)$  gauge transformations, four vector fields appear, as discussed before (see eq.(2.5)). The three degrees of freedom associated with the Goldstone bosons are absorbed as helicity 0 degrees of freedom for 3 of the 4 gauge fields thus giving mass to the three corresponding gauge quanta ( $W^\pm, Z^0$ ). The fourth gauge quantum remains massless (the photon),  $U(1)$  remains unbroken. The fourth real component of the introduced scalar isodoublet does not disappear but remains as a physical scalar massive particle: the Higgs boson. Thus the inevitable consequence of spontaneous symmetry breaking is the appearance of a massive scalar physical particle.

Since the mass of the  $W^\pm$  and  $Z^0$  have been created by the spontaneous symmetry breaking mechanism, they are naturally related to the vacuum expectation value of the Higgs field,  $v$ , which is responsible for the symmetry breaking:

$$m = \frac{gv}{2} . \quad (2.13)$$

Specifically for the  $W^\pm$  and the  $Z^0$  mass one has

$$m_W^2 = \frac{g^2 v^2}{4} \quad (2.14)$$

and

$$m_Z^2 = \frac{g^2 v^2}{4 \cos^2 \theta_W} \quad (2.15)$$

where  $g$  is the  $SU(2)$  semiweak coupling constant

$$g \sin \theta_W = |e| = (4\pi\alpha)^{1/2} . \quad (2.16)$$

The lepton and quark masses arise through a Yukawa type coupling of the lep-

ton/quark fields to the vacuum expectation value of the Higgs field<sup>[5,6]</sup> similar to eq. (2.13)

$$m_f = \frac{g_f v}{2} \quad (2.17)$$

The coupling constants  $g_f$  are 'free' parameters in the standard model and are fixed by the experimentally determined masses of the particles. Because the masses of the fermions span a huge range, the same applies to the couplings  $g_f$  to the Higgs field. The origin of this fact remains unanswered.

The known strength of the charged weak current processes at low energies (like the  $\mu$  decay) fixes the strength of the weak coupling:

$$\frac{G_F}{\sqrt{2}} = \frac{g^2}{8M_W^2} \quad (2.18)$$

where  $G_F = 1.166 \times 10^{-5} \text{ GeV}^{-2}$  is the Fermi weak coupling constant. Therefore, the value of the vacuum expectation value can be determined as

$$v^2 = \frac{1}{\sqrt{2}G_F} \approx (246 \text{ GeV})^2 \quad (2.19)$$

Combining (2.16) with (2.18) and (2.14) with (2.15) results in two rather important predictions of the standard model (see also the chapter on nonstandard Higgs models) in lowest order:

$$\rho \equiv \frac{m_W^2}{m_Z^2 \cos^2 \theta_W} = 1 \quad (2.20)$$

and

$$m_W^2 = \left( \frac{\pi \alpha}{\sqrt{2}G_F} \right) \frac{1}{\sin^2 \theta_W} \approx \frac{[37.3 \text{ GeV}/c^2]^2}{\sin^2 \theta_W} \quad (2.21)$$

The measurement of  $\sin^2 \theta_W$  in neutral current processes hence lead to a prediction of the masses of the intermediate vector bosons, which for  $\sin^2 \theta_W =$

$(0.217 \pm 0.014)$  (Ref. 9) in lowest order resulted in

$$m_W = (80.0 \pm 2.5) \text{ GeV}/c^2 \quad \text{and} \quad m_Z = (90.4 \pm 2.9) \text{ GeV}/c^2 \quad . \quad (2.22)$$

The recent discovery of the  $W^\pm$  and  $Z^0$  bosons at (within error) the predicted masses is an impressive confirmation of the standard model of the electroweak interactions. All current experimental evidence (culminating in the discovery of the  $W^\pm$  and  $Z^0$ ) is consistent with this model. The Higgs particle is the only essential ingredient of the standard model which has not yet been found.

### 3. The properties of the Higgs boson

In the following I will briefly outline the properties of the Higgs boson as predicted by the standard model of electroweak interactions<sup>[2,3,8]</sup>.

- Because the Higgs field provides the helicity 0 degree of freedom for the  $W^\pm$  and the  $Z^0$  bosons (hence giving them mass), the Higgs boson must be a scalar particle ( $J = 0$ ).
- It has to be electrically neutral because in the standard model the photon can stay massless only if the *neutral* part of the complex isodoublet Higgs field has a nonvanishing vacuum expectation value.
- The mass of the Higgs boson, obviously a most important parameter for the discussion of any experimental signature, is given by<sup>[8]</sup>

$$m_{H^0}^2 = -2\mu^2 = 2\lambda v^2 \quad . \quad (3.1)$$

At present there is no experimental information on the magnitude of the parameter  $\lambda$ , which describes the quartic selfcoupling of the Higgs field (see — eq.(2.9)). This makes it evidently difficult to search for the Higgs particle. Theoretical efforts to derive bounds on the mass of the Higgs have resulted in the allowed range  $O(7 \text{ GeV}/c^2) \leq m_{H^0} \leq O(1 \text{ TeV}/c^2)$  in the minimal

model<sup>[10]</sup>. The situation gets even less restrictive if one introduces more than one Higgs doublet (see below). Phenomenological arguments from macroscopic, atomic and nuclear physics require  $m_{H^0} > O(15\text{MeV})$ <sup>[11]</sup>. The most stringent lower limit stems from an analysis of experimental results on the decay  $K^+ \rightarrow \pi^+ H^0 \rightarrow \pi^+ \mu^+ \mu^-$  (Ref.12). The authors conclude that the mass of the standard Higgs boson must be larger than  $\approx 325 \text{ MeV}/c^2$ . As in the following we want to discuss the experimental search for the Higgs particle in  $e^+e^-$ -annihilation, we will for simplicity assume  $m_{H^0}$  to be an unknown.

- The Higgs boson is coupled to any particle proportional to the particle mass, provided the particle received its mass via spontaneous symmetry breaking. The coupling  $g_{X\bar{X}H^0}$  is determined by (2.17):

$$g_{X\bar{X}H^0} = \frac{2m_{X(\bar{X})}}{v} \approx \frac{m_{X(\bar{X})}}{123\text{GeV}/c^2}$$

where  $X$  denotes any fermion or boson and  $m$  is measured in  $\text{GeV}/c^2$ .

Table 2 gives a short overview over the expected coupling strengths normalized to the coupling to the  $Z^0$ . The fact that the  $H^0$ - $X\bar{X}$  coupling is proportional to the mass of the particles involved has thus important consequences for its production and decay:

1. It will have the largest branching ratio to the heaviest possible pair of fermions. Table 3 shows an overview over the expected main decay modes derivable from this rule.
2. Because the lepton masses for different generations ( $e, \mu, \tau, \dots$ ) are grossly different, the Higgs coupling does not obey lepton universality.
3. The Higgs will have a very poor coupling to  $e^+e^-$ ,  $u\bar{u}$ ,  $d\bar{d}$  resulting in the unfortunate fact that  $\sigma(e^+e^- \rightarrow H^0 + \text{anything})$  and  $\sigma(p\bar{p} \rightarrow H^0 + \text{anything})$  are in general expected to be small.
4. There is *no* coupling (in lowest order) to  $\gamma\gamma$ ,  $g\bar{g}$  ( $g$ =gluons).

**Table 2:** A comparison of coupling strengths of the neutral standard Higgs  $H^0$ . The values have been normalized to the value for the  $Z^0 Z^0 H^0$  coupling.

Coupling	$m_X$ in GeV/c <sup>2</sup>	$g_{X\bar{X}H^0}$
$Z^0 Z^0 H^0$	$\approx 93$	1.00 -
$W^+ W^- H^0$	$\approx 82$	$\approx 0.88$
$b\bar{b}H^0$	$\approx 4.9$	$\approx 0.053$
$\mu^+ \mu^- H^0$	$\approx 0.106$	$\approx 1.1 \times 10^{-3}$
$e^+ e^- H^0$	$\approx 0.0005$	$\approx 5.5 \times 10^{-6}$

These four predictions on one hand provide a good signature for the Higgs boson. On the other hand the miniscule production rate in  $e^+e^-$  or  $p\bar{p}$  reactions (at least for the presently available storage rings) as well as the predominant decay to high mass particles with their large final state particle multiplicities make it a formidable task to prove or disprove its existence.

5. The width of the Higgs boson is determined by the number of channels it can couple to and hence by its mass. For  $m_{H^0} < m_{Z^0}$  one gets

$$\Gamma_{tot} = m_{H^0} \frac{G_F}{4\sqrt{2}\pi} \sum_{i=1}^{N_f} N_C m_f^2 \left[ 1 - \frac{4m_f^2}{m_{H^0}^2} \right]^{\frac{3}{2}} \quad N_C = \begin{cases} 1 & \text{for leptons} \\ 3 & \text{for quarks} \end{cases} \quad (3.2)$$

(For  $m_{H^0} \geq 2m_{W^\pm}$  this changes due to the additional open channels to the intermediate vector bosons). Hence for  $m_{H^0} \approx 1$  GeV/c<sup>2</sup> one gets  $\Gamma_{tot} \sim O(10)$  eV and for  $m_{H^0} \approx 40$  GeV/c<sup>2</sup> one gets  $\Gamma_{tot} \sim O(2)$  MeV. Therefore, unless  $m_{H^0}$  gets very big, the Higgs should show up as a very narrow resonance. Fig. 1 shows the corresponding lifetime of the Higgs boson as a function of Higgs mass<sup>[11]</sup>. One can see that above masses of  $m_{H^0} \approx 2m_\mu$  it will be too short lived to produce any separate decay vertex.

A short glimpse at Table 2 could lead to the somewhat premature conclusion, that one should wait for the turn-on of  $Z^0$ -factories like the SLC ( $\approx 1987$ ) or LEP

( $\approx 1989$ ), especially in view of the totally unknown mass of the Higgs boson. It turns out however, that in spite of the miniscule coupling to  $e^+e^-$  nevertheless the  $e^+e^-$ -storage rings promise to offer the sensitivity necessary for a dedicated Higgs search in the intermediate energy range. The reason is the production of bound states of heavy quarks below threshold like the  $J/\Psi$ ,  $\bar{\Psi}'$ ,  $\bar{\Psi}''$  and  $\Upsilon(nS)$  (see section 5.2).

**Table 3:** An overview over the expected main decay modes of the standard neutral Higgs boson for different assumptions on its mass (Ref.11).

Mass range for $H^0$	Dominant decay mode
$m_e < m_{H^0}$	$e^+e^-$ (and $\gamma\gamma$ through virtual loops)
$2m_\mu < m_{H^0} < 2m_\pi$	$\mu^+\mu^-$ final states
$2m_\pi < m_{H^0} < 1 \text{ GeV}$	$\pi^+\pi^-$ final states
$1 \text{ GeV} < m_{H^0} < 4 \text{ GeV}$	strange particles
$4 \text{ GeV} < m_{H^0} < 10 \text{ GeV}$	$c\bar{c}$ ( $\tau\bar{\tau}$ suppressed due to colour)
$10 \text{ GeV} < m_{H^0} < m_{Z^0}$	$b\bar{b}$ (and eventually $t\bar{t}$ )

#### 4. Nonstandard Higgs models

Many predictions of the standard model have by now been tested by experiment. An important relation connected to the isospin structure of the Higgs sector (namely the introduction of one single complex Higgs field in a doublet to spontaneously break the  $SU(2)\times U(1)$  symmetry) is the  $\rho$  parameter (eq. (2.20))

$$\rho = \frac{m_W^2}{m_Z^2 \cos^2 \theta_W} \equiv 1 \quad . \quad (4.1)$$

Taking the average experimental values for  $m_W$  and  $m_Z$  of<sup>[13]</sup>

$$m_W = (82.2 \pm 1.8) \text{ GeV}/c^2 \quad \text{and} \quad m_Z = (93.2 \pm 1.5) \text{ GeV}/c^2 \quad (4.2)$$

together with the result on  $\sin^2 \theta_W$  from deep inelastic neutrino scattering<sup>[9]</sup>

$\sin^2 \theta_W = (0.217 \pm 0.014)$ , one gets the experimental value

$$\rho = (0.99 \pm 0.08) \quad (4.3)$$

in excellent agreement with the predictions of the simple standard model. Corrections to this value can come from calculable radiative corrections<sup>[13]</sup> to the lowest order formula (eq. (4.1)) as well as from virtual effects from as yet undiscovered high mass leptons.

The remarkable closeness of  $\rho$  to the prediction of the simplest form of the standard model puts some constraints on attempted extensions regarding the Higgs sector. Such extensions are, e.g., always implied in the building of grand unified theories<sup>[14]</sup>. A study of possibilities to enlarge the Higgs sector by the introduction of additional scalar Higgs fields<sup>[8,15]</sup> leads to the result that  $\rho$  always remains exactly one (in lowest order) for an arbitrary number of Higgs fields, *provided they are doublets*. The introduction of, e.g., weak isospin triplets, however, is theoretically unappealing, as complicated relations between the individual vacuum expectation values have to occur to bring  $\rho$  in agreement with the experimental findings. It is thus usually assumed, that the dominant Higgs multiplets are doublets.

The simplest extension of the standard model is thus the introduction of 2 complex Higgs doublets<sup>[8]</sup>:

$$\begin{pmatrix} \phi_1 + i\phi_2 \\ \phi_3 + i\phi_4 \end{pmatrix} \quad \text{and} \quad \begin{pmatrix} \psi_1 + i\psi_2 \\ \psi_3 + i\psi_4 \end{pmatrix} \quad (4.4)$$

The  $SU(2) \times U(1)$  symmetry is now broken by the presence of two nonzero vacuum expectation values  $v_\phi$  and  $v_\psi$ . One of the doublets gives as before masses to the  $W^\pm$  and  $Z^0$  with one remaining neutral scalar physical Higgs boson  $H^0$ . However, one now gets 4 additional physical Higgs bosons, two of which are charged:  $\Phi^0, h^0, H^+$  and  $H^-$ .  $H^0$  and  $\Phi^0$  are scalar ( $J^P = 0^+$ ) whereas  $h^0, H^\pm$  are (in general) pseudoscalar particles ( $J^P = 0^-$ ).

Although one has now even more parameters to adjust, one can still expect a general correlation of the Higgs couplings to the masses of the quarks and leptons like in the standard model<sup>[16]</sup>. So most of the preceding discussion will be more or less valid also for these extended models.

The main impact of the introduction of additional doublets to the Higgs sector on phenomenology is

1. The possibility of stronger (or weaker) couplings than predicted from the standard model.
2. The appearance of charged Higgs particles.

Stronger (or weaker) couplings can result from the assumption that the Higgs field responsible for the masses of the intermediate vector bosons is not the same one that provides the masses of the fermions (an attractive idea, if one recalls the huge scale of couplings otherwise involved)\*. So even if the sensitivity of present experiments seems not to be good enough to pin down the standard Higgs boson, it is nevertheless worthwhile to look for any hints in existing data samples. It turns out however<sup>[17]</sup> that radiative corrections and mixing effects would not allow the two vacuum expectation values to be too different from another, hence limiting possible enhancements to at most an order of magnitude.

From the experimental point of view, the appearance of charged Higgs bosons is very appealing as charged Higgs bosons can be pair produced in  $e^+e^-$ -interactions via their electromagnetic coupling, hence requiring much less sensitivity. This is one of the reasons why most of the experimental literature devoted to Higgs searches is dealing with charged Higgs bosons (see Chapter 6).

---

\* This can also be achieved in a model, where one doublet is responsible for the masses of the "up"-type quarks and the other is responsible for the masses of the "down"-type quarks (Ref.17).

## 5. Search for the standard Higgs in $e^+e^-$ annihilation

The remarks in the preceding chapters on the properties and couplings of the standard Higgs to leptons and quarks could lead to the immediate conclusion that  $e^+e^-$ -colliders are not very well suited to produce the Higgs boson copiously. Unfortunately, the prospects of  $p\bar{p}$  colliders look even dimmer (at least for  $m_{H^0} < 2m_W$ <sup>[18]</sup>). Fig.2 shows some of the possible diagrams involved in the production of the Higgs boson in  $p\bar{p}$  collisions together with the estimated cross sections as a function of the Higgs mass and for different c.m. energies<sup>[19]</sup>. The dominant graphs include gluon fusion involving virtual quark loops (Fig.2a) and bremsstrahlung off a heavy final state quark line (Fig.2b). (Note that  $H^0 \not\rightarrow gg$  in lowest order due to  $m_g = 0$ ). The dominant production mechanism is hence probably via gluon-gluon fusion<sup>[16]</sup> resulting in

$$\sigma(p\bar{p} \rightarrow H^0 + X) \approx 10 \text{ pb for } m_{H^0} \leq 30 \text{ GeV}/c^2, \quad (5.1)$$

at  $\sqrt{s} \geq 400 \text{ GeV}$  (see Fig.2a). This is clearly too small for observation given the present luminosity of the CERN- $p\bar{p}$  collider: The total luminosity accumulated there since startup in 1983 is only about  $550 \text{ nb}^{-1}$ .

Unfortunately in addition to the very high luminosities needed, the expected decay signatures of the produced Higgs boson are hardly distinguishable from less interesting events in hadronic interactions. This problem may partly be solved by processes like that depicted in Fig. 2b where the additional heavy quarks might constitute a useful signature.

In the following I want therefore concentrate on the possibilities of neutral Higgs boson production in  $e^+e^-$  annihilation. First a brief overview on the continuum production is given, followed by a more detailed discussion of the special role of heavy vector resonances like the  $J/\Psi$  and the  $\Upsilon$  and a comparison with experimental results<sup>[20]</sup>.

## 5.1 CONTINUUM PRODUCTION

### The direct process $e^+e^- \rightarrow H^0 \rightarrow \text{hadrons}$

The production mechanism  $e^+e^- \rightarrow H^0 H^0$  is forbidden due to Bose symmetry. The easiest production mechanism in the continuum is therefore the process

$$e^+e^- \rightarrow H^0 \rightarrow \text{hadrons} \quad (5.2)$$

(see Fig. 3a). The cross section for this process is given roughly by<sup>[21]</sup>

$$\sigma(e^+e^- \rightarrow H^0) \simeq \frac{4\pi}{m_H^2} \frac{\Gamma(H^0 \rightarrow e^+e^-)}{\Gamma(H^0 \rightarrow \text{all})} \quad (5.3)$$

Taking the width of the Higgs as defined by eq.(3.2) and making the simplified assumption that the total width is dominated by decays to quarks, the contribution from direct Higgs production to the R-value ( $\equiv \sigma_{had}/\sigma_{\mu\mu}$ ) is given by

$$\Delta R(e^+e^- \rightarrow H^0) \approx \frac{1}{\alpha^2} \left( \frac{m_e^2}{\sum m_Q^2} \right) \quad (5.4)$$

where the sum runs over all quarks that are kinematically possible in the decay of the Higgs. This gives roughly

$$\Delta R \simeq 1.5 \times 10^{-3} \quad \text{for } 2m_D < m_{H^0} < 2m_B$$

$$\Delta R \simeq 1.7 \times 10^{-4} \quad \text{for } 2m_B < m_{H^0} < 2m_T$$

Fig.4 shows the  $R$  values from selected experiments<sup>[22]</sup> with systematic errors less than 7%. The smallest systematic error on this number is reported by the MAC collaboration<sup>[23]</sup> :  $\pm 2.3\%$ . It is clear that from a measurement of  $R$  alone one would not notice any contribution due to the production of a Higgs boson. One could imagine that the detection of specific decay modes like  $H^0 \rightarrow \tau^+\tau^-$  or  $H^0 \rightarrow b\bar{b}$  could help, but the contribution due to the normal continuum process  $e^+e^- \rightarrow \gamma^* \rightarrow f\bar{f}$  of  $\Delta R = 1/3$  for  $b$ -quarks and  $\Delta R = 1$  for  $\tau$ -pairs will kill the signal.

### The Bremsstrahlung off final state quarks

Another continuum process one can envision is the Bremsstrahlung of the Higgs off a quark line<sup>[24]</sup> as shown in Fig.3b, where  $f$  denotes a fermion. Clearly this depends on the mass of the Higgs as well as on the mass of the final state quark. Fig.5 summarizes the results of a calculation<sup>[24]</sup> of the total cross sections for  $e^+e^- \rightarrow f\bar{f}H^0$  at  $\sqrt{s} = 40$  GeV for Higgs masses up to  $25 \text{ GeV}/c^2$  and fermion masses between  $1.5$  and  $15 \text{ GeV}/c^2$ . Note that for quarks one has to multiply the shown cross sections with the factor  $3Q^2$  (where  $Q$  is the charge of the radiating quark). If one adds the contributions of all the known fermions, the authors of Ref. 24 find a total inclusive cross section at  $\sqrt{s}=40$  GeV of

$$\sigma(e^+e^- \rightarrow \sum f\bar{f}H^0) = 2.1 \times 10^{-4} \text{ pb} \quad (5.5)$$

for an assumed Higgs mass of  $5 \text{ GeV}/c^2$ . If one considers achievable luminosities for storage rings like PEP or PETRA of at most  $O(1 - 10) \text{ pb}^{-1}$  per day and in addition the necessity to *identify* the Higgs boson through its decay (which will lead to an additional suppression), one can safely ignore this process in the further discussion.

### The process $e^+e^- \rightarrow H^0\gamma$

Because of the large coupling of the standard Higgs boson to the intermediate vector bosons one could a priori assume that the excitation of virtual  $Z^0$ 's or  $W^\pm$  's could yield a sizeable cross section via the process shown in Fig. 3c. The advantage of this process would be the kinematic correlation of photon and Higgs particle. A detailed calculation however gives<sup>[21]</sup>

$$\Delta R(e^+e^- \rightarrow H^0\gamma) \simeq 4.8 \times 10^{-10} s(1 - \frac{m_H^2}{s})^3 \cdot |I|^2 \quad (5.6)$$

where  $|I|^2 \simeq 5$  at  $\sqrt{s} = 30$  GeV thus leading to<sup>[21]</sup>  $\Delta R \approx O(10^{-6})$  for  $m_{H^0} \leq 20 \text{ GeV}/c^2$  and  $20\text{GeV} \leq \sqrt{s} \leq 90\text{GeV}$ . This is even harder to measure than the process of direct  $H^0$  production discussed before.

## Two photon physics and the Higgs boson

For increasing c.m. energy the two photon process  $e^+e^- \rightarrow e^+e^-X$  becomes increasingly important. Although the Higgs boson does not couple in lowest order to photons because they are massless, higher order processes like those in Fig.3d could become sizeable. These processes have been calculated<sup>[25]</sup> and the resulting cross section is

$$\sigma(e^+e^- \rightarrow e^+e^-H^0) \simeq \frac{GF\alpha^4}{\sqrt{2}\pi^3} \left[ \ln \frac{\sqrt{s}}{2m_e} \right]^2 \cdot \Phi \left( \frac{\sqrt{s}}{m_{H^0}} \right) \cdot |I|^2 \quad (5.7)$$

where  $|I|^2 \sim O(1)$  for 3 generations of fermions and  $m_{H^0}^2 \ll m_{W^\pm}^2$ , and

$$\Phi(x) = -(2+x^2)^2 \ln x - (1-x^2)(3+x^2) \quad (5.8)$$

is a phase space factor<sup>[25]</sup>. For  $m_{H^0} \simeq 10 \text{ GeV}/c^2$  and  $\sqrt{s} \sim 30 \text{ GeV}$  this gives  $\sigma(e^+e^- \rightarrow e^+e^-H^0) \simeq O(10^{-5})pb$  and even at LEP energies of  $\sqrt{s} \sim 200 \text{ GeV}$  the cross section is only of  $O(10^{-4})pb$ , again a depressingly small number.

In conclusion the continuum production of the Higgs in  $e^+e^-$  annihilations is negligible. Any limits on the production in the continuum from current experiments would not even come close to the theoretical predictions to test the standard model.

## 5.2 THE STANDARD HIGGS AND HEAVY VECTOR RESONANCES

The miniscule cross sections discussed above even for heavy quark production seem depressing. However Nature provided us with 'amplifiers' for heavy quark production, namely the vector resonances  $\rho, \phi, J/\Psi, \Upsilon$  and their excited states. Indeed, as will be shown below, some of them will be the most promising places to look for the neutral Higgs boson(s). One important advantage of the vector resonances is that the Zweig rule<sup>[26]</sup> leads to a suppression of competing hadronic decay modes and thus effectively enhances the decay branching ratio to the Higgs

boson. Before however discussing the main decay mode via the so-called Wilczek mechanism<sup>[27]</sup>, I will shortly cover some early other ideas<sup>[11]</sup> involving heavy vector resonances which appeared in the literature.

### The Bremsstrahlung off the $J/\Psi$

This process<sup>[11]</sup> is illustrated in Fig. 6a. A rough estimate of the cross section gives

$$\frac{\sigma(V \rightarrow H^0 V)}{\sigma(V \rightarrow \mu^+ \mu^-)} \simeq 0.048 \frac{m_V^2}{m_p^2} \frac{\Gamma(V \rightarrow e^+ e^-)}{m_{H^0}} \quad (5.9)$$

where  $m_{H^0}$  is expressed in units of  $\text{MeV}/c^2$  and the cross section has been evaluated at the optimal energy  $\sqrt{s} = m_V + \sqrt{2}m_{H^0}$ . For the  $J/\Psi$  resonance the corresponding contribution to  $R_{had}$  for this process is approximately

$$\Delta R(e^+ e^- \rightarrow \text{"}J/\Psi\text{"} \rightarrow J/\Psi + H^0) \approx \frac{1.6 \times 10^{-3}}{m_{H^0}} \quad (5.10)$$

where  $m_{H^0}$  is in  $\text{MeV}$ . This value again is very small and in addition the signal lacks a distinct signature. If one considers tagging the  $J/\Psi$  by its decay into lepton pairs this diminishes the signal further but provides a rather clean signature. This process does not really fully exploit the advantage of the vector resonances because one has to sit in the continuum above the  $J/\Psi$  requiring a dedicated Higgs search experiment.

### $\Psi' \rightarrow H^0 + J/\Psi$

This process is in principle possible<sup>[11]</sup> if the Higgs mass is smaller than the mass difference  $m(\Psi') - m(J/\Psi)$ . As discussed above (see also Table 3) a Higgs boson with a mass exceeding  $2m_\pi$  should (in this process) decay predominantly into 2 pions. Tagging the  $J/\Psi$  by its decay into leptons would lead to the signature  $\Psi' \rightarrow \pi\pi l^+ l^-$  and the invariant mass calculated from the two pions should

show a peak at the Higgs mass. Unfortunately the estimated cross section<sup>[11]</sup>

$$\frac{\Gamma(\Psi' \rightarrow H^0 + J/\Psi)}{\Gamma(\Psi' \rightarrow \text{all})} \simeq O(10^{-4}) \quad (5.11)$$

is too small, the background due to the normal hadronic transition  $\Psi' \rightarrow \pi^+\pi^-J/\Psi$  with a branching ratio of  $(0.33 \pm 0.02)$ <sup>[28]</sup> is orders of magnitude larger. (An interesting option however would be the case where  $m_{H^0} < 2m_\pi$  leading to e.g.  $\Psi' \rightarrow \mu^+\mu^-l^+l^-$  final states).

#### The Wilczek mechanism $V(q\bar{q}) \rightarrow \gamma H^0$

The rate for this process<sup>[27]</sup>, normalized to the rate for the process  $V(q\bar{q}) \rightarrow \mu^+\mu^-$  as described by the Feynman diagrams of Fig. 6b has been calculated to be

$$\frac{\Gamma(V \rightarrow \gamma H^0)}{\Gamma(V \rightarrow \mu^+\mu^-)} = \frac{Br(V \rightarrow \gamma H^0)}{Br(V \rightarrow \mu^+\mu^-)} = \frac{G_F m_V^2}{4\sqrt{2}\pi\alpha} \left[ 1 - \frac{m_{H^0}^2}{m_V^2} \right] \quad (5.12)$$

This has to be modified slightly if one takes into account the dependence of the amplitude for  $V \rightarrow \gamma H^0$  on the mass of the Higgs<sup>[29,30]</sup>. This modification can be accomplished by adding to (5.12) a factor  $F(m_{H^0}^2, m_V^2)$ , which can be approximated to a good degree by<sup>[29]</sup>

$$F(m_{H^0}^2, m_V^2) \approx \left( 1 - \frac{m_{H^0}^2}{m_V^2} \right) \quad (5.13)$$

This modification will get important when the Higgs mass approaches the vector resonance mass  $m_V$ .

In Table 4, the predicted branching ratios  $Br(V \rightarrow \gamma H^0)$  for the vector resonances up to the  $\Upsilon(3S)$  are listed. As expected from the properties of the Higgs coupling, the  $\Upsilon$ -system seems to be the most promising place to look for the Higgs boson produced via the Wilczek mechanism. An additional advantage is the wide range of Higgs masses spanned. On the other hand, one has of course to take into account the relative production cross section (which on the  $J/\Psi$  is roughly

$\sigma_{had}^{vis}(J/\Psi) \simeq 2500 \text{ nb}$  at SPEAR<sup>[31]</sup> to be compared with  $\sigma_{had}^{vis}(\Upsilon) \simeq 20 \text{ nb}$  at CESR<sup>[32]</sup> ) and the performance of the machine, given by the delivered integrated luminosity per day. The experimentally significant figure of merit is therefore the (storage ring dependent) quantity

$$f = \sigma_{had}^{vis} \cdot Br(V \rightarrow \gamma H^0) \cdot \int_{day} Ldt \quad (5.14)$$

which is just the expected number of events of the process of interest produced per day of running. A rough estimate using the above figures gives thus

$$f^{SPEAR} \rightarrow \begin{cases} 160 \text{ pb} \cdot \int_{day} Ldt & \text{for the } J/\Psi \\ 4.9 \text{ pb} \cdot \int_{day} Ldt & \text{for the } \Psi' \end{cases}$$

and

$$f^{CESR} \rightarrow \begin{cases} 4.8 \text{ pb} \cdot \int_{day} Ldt & \text{for the } \Upsilon(1S) \\ 1.2 \text{ pb} \cdot \int_{day} Ldt & \text{for the } \Upsilon(2S) \\ 0.7 \text{ pb} \cdot \int_{day} Ldt & \text{for the } \Upsilon(3S) \end{cases}$$

(The corresponding value for DORIS is  $f^{DORIS} \approx 1/2 \cdot f^{CESR}$  due to the larger beam width at DORIS II). Currently achievable luminosities lie around  $O(50) \text{ nb}^{-1}/\text{day}$  for the  $J/\Psi$ <sup>[33]</sup> and  $O(1000) \text{ nb}^{-1}/\text{day}$  for CESR/DORIS. Thus from the experimental point of view the  $\Psi$ -system and the  $\Upsilon$ -system are quite competitive.

The possibility of the Wilczek mechanism suggests that every new narrow resonance\* discovered in the radiative decays of the  $J/\Psi$  or  $\Upsilon$  should be studied very carefully under the assumption that it might be a Higgs boson. The situation gets a little bit more complicated due to the fact that the  $J/\Psi$  and (to a lesser extent also the  $\Upsilon$ ) are also expected to be sources of glueballs produced

---

\* The resolution of normal particle physics experiments ( $\sim O(10 \text{ MeV})$ ) is much larger than the expected width of the Higgs boson (see Chapter 3), which is of  $O(\text{eV})$  to  $O(1 \text{ MeV})$ .

via the process shown in Fig.6c. However, the distinct couplings of the Higgs boson should make a separation possible by looking at the decay modes of the new state.

**Table 4:** The predicted branching ratio for the decay  $V \rightarrow \gamma H^0$  via the Wilczek mechanism for various heavy vector resonances  $V$ .<sup>† \*</sup>

Resonance V	Br( $V \rightarrow l^+l^-$ ) [%]	Br( $V \rightarrow \gamma H^0$ ) $\times [1 - m_{H^0}^2/m_V^2]^{-q}$
$\rho$	$(6.7 \pm 1.2) \times 10^{-5}$	$\approx 3.6 \times 10^{-9}$
$\omega$	$(6.7 \pm 0.4) \times 10^{-5}$	$\approx 3.7 \times 10^{-9}$
$\phi$	$(2.5 \pm 0.3) \times 10^{-4}$	$\approx 2.3 \times 10^{-8}$
$\Psi(3.096)$	$(7.4 \pm 1.2) \times 10^{-2}$	$\approx 6.4 \times 10^{-5}$
$\Psi(3.685)$	$(0.8 \pm 0.2) \times 10^{-2}$	$\approx 9.8 \times 10^{-6}$
$\Upsilon(9.460)$	$(2.9 \pm 0.2) \times 10^{-2}$	$\approx 2.4 \times 10^{-4}$
$\Upsilon(10.025)$	$(1.6 \pm 0.3) \times 10^{-2}$	$\approx 1.4 \times 10^{-4}$
$\Upsilon(10.355)$	$(2.0 \pm 0.7) \times 10^{-2}$	$\approx 1.9 \times 10^{-4}$

In the following I want to discuss the results of several experimental searches for the Higgs in radiative  $J/\Psi$  and  $\Upsilon$  decays with special emphasis on 2 possible candidates, the  $\xi(2.2)$ , seen by the Mark III collaboration<sup>[34]</sup> at SPEAR and the  $\zeta(8.3)$ , seen by the Crystal Ball collaboration at DORIS II<sup>[35]</sup>. This will be followed by a discussion of the interesting possibility that the standard  $J^P = 0^+$  (the nonstandard  $J^P = 0^-$ ) Higgs might mix with the  $^3P_0$  ( $^1S_0$  or  $\eta_b$ ) state of quarkonium<sup>[30]</sup> providing a possible enhancement factor for its production.

### $J/\Psi \rightarrow \gamma \xi(2.2)$

In the summer of 1983, the Mark III collaboration announced the evidence

<sup>†</sup> The resonances above charm (bottom) threshold have not been considered as the rates are smaller by several orders of magnitude due to competing decay channels.

\* The values for  $Br(V \rightarrow l^+l^-)$  are taken from Ref.28, and lepton universality is assumed.

for a new state with mass of  $2.2 \text{ GeV}/c^2$  discovered in an analysis of  $\approx 2.6 \times 10^6$   $J/\Psi$  decays<sup>[84]</sup>. The state, called  $\xi(2.2)$ , was observed in the radiative decays of the  $J/\Psi$  in the process

$$J/\Psi \rightarrow \gamma \xi(2.2) \rightarrow \gamma K^+ K^- \quad (5.15)$$

as a 4.6 standard deviation effect. Fig.7a shows the  $K^+ K^-$  invariant mass spectrum<sup>[86]</sup>. In addition to the new state  $\xi(2.2)$  also the  $f'(1525)$  and  $\Theta(1690)$  are evident. Fig.7b shows the invariant  $K_S^0 K_S^0$  mass spectrum for events of the type  $J/\Psi \rightarrow \gamma K_S^0 K_S^0$ . Also here one might see a slight indication of the new state. Fitting the  $K^+ K^-$  spectrum above  $2.0 \text{ GeV}/c^2$  with a Breit Wigner convoluted with a gaussian over a quadratic background gave the following resonance parameters<sup>[86]</sup>:

$$m_\xi = (2218 \pm 3 \pm 10) \text{ MeV}/c^2$$

$$\Gamma_\xi < 40 \text{ MeV} \quad (95\% \text{ C.L.}) \quad (5.16)$$

$$B(J/\Psi \rightarrow \gamma \xi) \cdot Br(\xi \rightarrow K^+ K^-) = (5.8 \pm 1.8_{stat} \pm 1.5_{syst}) \times 10^{-5} .$$

This state hence has several rather remarkable properties: Besides its unexpectedness, its width is consistent with the understanding of the detector resolution<sup>[84]</sup> and thus much less than expected for an ordinary hadronic state with mass in the  $2 \text{ GeV}/c^2$  range<sup>[87]</sup>. The evidence of the decay mode  $K_S^0 K_S^0$  (though statistically not convincing) hints to a possible spin-parity assignment of  $J^P = 0^+, 2^+, 4^+, \dots$ . A detailed spin analysis however is complicated by the background due to the decay  $J/\Psi \rightarrow K^{*+} K^- \rightarrow K^+ K^- \pi^0$ , where the  $\pi^0$  is misidentified as a photon or one of the decay photons escapes detection. The above facts together with the knowledge about the Wilczek mechanism (eq. (5.12)) lead naturally to theoretical speculations regarding the possibility of a Higgs particle assignment<sup>[88]</sup> for the  $\xi(2.2)$ .

However there exist to date several obstacles to this interpretation, both from experimental and from theoretical side. The Mark III collaboration reports<sup>[36]</sup> on one difficulty which they had in their analysis, namely that the number of observed events in the  $\xi$ -region recorded in the 1982 running period ( $\simeq 0.9 \times 10^6$   $J/\Psi$  decays) is somewhat less than the expected number based on a datasample recorded in 1983 ( $\simeq 1.8 \times 10^6$   $J/\Psi$  decays). The two resulting spectra are shown in Fig.8 together with the scaled expectation from the 1983 data sample superimposed on the 1982 data. The effect however corresponds to only about 2.2 standard deviations discrepancy between the two data samples and is thus not fatal yet.

Another experimental result is more puzzling. The DM2 collaboration, running on the  $J/\Psi$  at the storage ring DCI reported at the 1984 Leipzig conference their results<sup>[39]</sup> on the  $\gamma K^+ K^-$  final state in  $J/\Psi$  decays based on an analyzed data sample of  $\simeq 4.4 \times 10^6$   $J/\Psi$  's (from in total  $8.6 \times 10^6$   $J/\Psi$  events). Fig. 9 shows their invariant  $K^+ K^-$  and  $K_S^0 K_S^0$  invariant mass distributions. The  $\xi(2.2)$  seen by Mark III is not visible in their spectra. Using the quoted Mark III results (eq.(5.16)) and their known detection efficiencies, they computed that they should have seen 23  $\xi$  events in the  $K^+ K^-$  mass spectrum over a background of 30 events in a 40 MeV/c<sup>2</sup> mass interval. The nonobservation of the  $\xi$  signal corresponds to a 3 standard deviations effect<sup>[39]</sup>.

The most recent experimental information comes again from the DM2 group at DCI. They extended the above analysis to their full datasample of  $\sim 8.6 \times 10^6$   $J/\Psi$  -decays and still see no evidence<sup>[40]</sup> for the  $\xi(2.2)$ . Fig. 10 shows the corresponding spectra for the invariant  $K^+ K^-$  and  $K_S^0 K_S^0$  mass for their full data sample. They derive an upper limit of

$$Br(J/\Psi \rightarrow \gamma\xi) \cdot Br(\xi \rightarrow K^+ K^-) < 1.5 \times 10^{-5}$$

$$Br(J/\Psi \rightarrow \gamma\xi) \cdot Br(\xi \rightarrow K^0 \bar{K}^0) < 3.0 \times 10^{-5}$$

(at 95% C.L.) in disagreement with the findings of Mark III. The Mark III col-

laboration is taking data on the  $J/\Psi$  right now (April 1985) and hopes to double their initial data sample<sup>[41]</sup>, so the situation of the  $\xi(2.2)$  on the experimental side will soon be clarified.

If one wants to interpret the  $\xi$  as a possible Higgs candidate, there are obstacles from the theoretical side as well. Besides the 'low' mass of the  $\xi(2.2)$ , the measured product branching ratio  $Br(J/\Psi \rightarrow \gamma\xi) \cdot Br(J/\Psi \rightarrow K^+K^-) = (5.8 \pm 1.8 \pm 1.5) \times 10^{-5}$  is in clear disagreement with the expectations from the Wilczek mechanism of  $Br(J/\Psi \rightarrow \gamma\xi(2.2)) \simeq 1.6 \times 10^{-5}$  (the correction factor  $F(m_V^2, m_\xi^2)$  (eq.(5.13)) has been taken into account). This discrepancy gets even larger if one considers that the  $K^+K^-$  decay cannot be the only decay mode of the  $\xi(2.2)$  (e.g. the  $K^0\bar{K}^0$  is equally likely and indications for the decay into  $K_S^0 K_S^0$  have been observed). Indeed, if the observed  $K^+K^-$  final state stems from the Higgs coupling to an  $s\bar{s}$  pair ( $s$  is the strange quark) with subsequent fragmentation, it is quite natural to expect that  $Br(\xi(2.2) \rightarrow K^+K^-)$  will be much smaller than 100%.

Thus the  $\xi(2.2)$  cannot be the standard Higgs boson. As mentioned in Chapter 4 however, the possible enlargement of the Higgs sector by additional weak isospin doublets leads among others to the possibility of enhanced Higgs-fermion couplings. Because the nonstandard Higgs interpretation of the  $\xi(2.2)$  has important and testable consequences also for the  $\Upsilon$ -system, in the following a short overview over the most popular theoretical attempts<sup>[88]</sup> will be given.

By introducing two doublets in the Higgs sector, one has in general two non zero vacuum expectation values, e.g.  $v_\phi$  and  $v_\psi$ . The decay rate for  $V \rightarrow \gamma H$  (eq.(5.12)) gets now modified to<sup>[42]</sup>

$$\frac{\Gamma(V \rightarrow \gamma H)}{\Gamma(V \rightarrow \mu^+ \mu^-)} = \frac{Br(V \rightarrow \gamma H)}{Br(V \rightarrow \mu^+ \mu^-)} = \tan^2 \beta \cdot \frac{G_F m_V^2}{4\sqrt{2}\pi\alpha} \left[ 1 - \frac{m_H^2}{m_V^2} \right] \cdot F \quad (5.17)$$

where  $\tan \beta \equiv v_\phi/v_\psi$  is the ratio of vacuum expectation values for the two Higgs fields.

Depending on the model, one can now get an enhancement or suppression of the corresponding rate<sup>[38,42]</sup>. One possibility is that the two Higgs doublets are decoupled, so that one of them gives masses to the  $W^\pm$  and  $Z^0$  as before and the other gives masses to quarks and leptons. In this case the rate for  $\Upsilon$  decays should be enhanced by the same factor as that 'observed' in the  $J/\Psi$  decays (provided the  $\xi(2.2)$  is a Higgs). Assuming that  $\Gamma(\xi \rightarrow K^+K^-) \simeq 1/6 \Gamma(\xi \rightarrow \text{all})$ <sup>[38]</sup> one gets a needed enhancement of about 10-20 depending on the assumption about  $F(m_V^2, m_{H^0}^2)$ . Thus in this approach the branching ratio for  $\Upsilon \rightarrow \gamma\xi(2.2)$ ,  $\xi(2.2) \rightarrow \text{all}$  should be  $\sim (2.4 - 4.8) \times 10^{-3}$  leading to

$$Br(\Upsilon(1S) \rightarrow \gamma\xi) \cdot Br(\xi \rightarrow K^+K^-) \simeq (4.0 - 8.0) \times 10^{-4}$$

$$Br(\Upsilon(2S) \rightarrow \gamma\xi) \cdot Br(\xi \rightarrow K^+K^-) \simeq (2.3 - 4.6) \times 10^{-4}$$

Both the CUSB and the CLEO collaborations operating at the storage ring CESR have analyzed their data with respect to these predictions<sup>[43]</sup>. Fig.11 shows the spectrum of the invariant  $K^+K^-$  invariant mass for events of the type  $\Upsilon(1S) \rightarrow \gamma K^+K^-$  from the CLEO group. They derive<sup>[43]</sup> from this an upper limit of (90 % C.L.)

$$Br(\Upsilon(1S) \rightarrow \gamma\xi) \cdot Br(\xi \rightarrow K^+K^-) < 2 \times 10^{-4}$$

$$Br(\Upsilon(2S) \rightarrow \gamma\xi) \cdot Br(\xi \rightarrow K^+K^-) < 9 \times 10^{-5}$$

The CUSB group<sup>[44]</sup> derived an upper limit for  $Br(\Upsilon \rightarrow \gamma\xi) \cdot Br(\xi \rightarrow \text{all})$  by looking at their inclusive photon spectrum of  $\sim 112,000$   $\Upsilon(1S)$  decays (Fig.12). Plotted is the variable  $z = E_\gamma/E_{\text{beam}}$ . The resulting limit (at 90% C.L.) they arrived at is

$$Br(\Upsilon(1S) \rightarrow \gamma\xi) \cdot Br(\xi \rightarrow \text{all}) < 6 \times 10^{-4}$$

to be compared with the predicted 0.2-0.5%. Thus if one assumes that the  $\xi$  is a Higgs particle, the two doublet model with identical couplings for charge 2/3 and charge -1/3 quarks ( $c$  and  $b$ ) is ruled out by experiment.

In another class of models<sup>[45]</sup> however, one vacuum expectation value is responsible for the charge 2/3 quarks and the other is responsible for the charge -1/3 quarks. An observed enhancement in the  $J/\Psi$  system would thus lead to a *suppression of the same size* in the  $\Upsilon$  system<sup>[46]</sup>. Because the present experiments taking data at the  $\Upsilon$  do not yet have enough sensitivity to rule out even the predictions of the standard model (see Table 4), this specific class of extended Higgs models cannot be ruled out by the  $\Upsilon$  decay processes discussed so far.

A much more severe constraint on this class of models comes from measurements involving  $B$ -meson decays: Although the Lagrangian in these models contains no flavor changing neutral couplings, these can arise from one loop diagrams involving charge 2/3 quark loops like that in Fig.13 leading to the possible decay process<sup>[47]</sup>

$$b \rightarrow s + h^0 \quad . \quad (5.18)$$

This one-loop process is dominated by the coupling to the virtual  $t$  quark. Since in this model all charge 2/3 quarks experience the same coupling enhancement, this can be deduced from the comparison of the  $J/\Psi$  data with the simple Wilczek formula prediction. In addition the branching ratio for the process (5.18) also depends on the mass of the charged Higgs boson (see Fig.13). It turns out<sup>[38]</sup>, that for a wide range of parameters the resulting branching ratio for the process  $b \rightarrow s + h^0$  is of the order of 50 % (!). For a reasonable choice of parameters one gets the prediction<sup>[43]</sup>

$$Br(B \rightarrow h^0 + X) \cdot Br(h^0 \rightarrow K^+K^-) > 3.5 \times 10^{-3} \cdot \left(\frac{M_t}{21}\right)^4 \quad (5.19)$$

Fig.14 shows the invariant  $K^+K^-$  mass spectrum observed on the  $\Upsilon(4S)$  resonance (which is a  $B$ -meson factory) from the CLEO collaboration<sup>[48]</sup>. The data corresponds to about 44,000  $B\bar{B}$  events. The CLEO group derived from this an

upper limit of

$$Br(B \rightarrow \xi + \text{anything}) \cdot Br(\xi \rightarrow K^+ K^-) < 3 \times 10^{-3} .$$

This limit holds<sup>[43]</sup> approximately for the whole region of masses between 2 and 3 GeV/c<sup>2</sup>. The nonobservation of the toponium ground state at PETRA<sup>[48]</sup> leads to the lower limit of  $M_t \geq 23$  GeV/c<sup>2</sup>. Thus also this extended Higgs model seems very unlikely.

Another additional constraint along the same line of thought comes from the upper limit on dimuon events in  $B$  decays of<sup>[49]</sup>

$$Br(B \rightarrow \mu^+ \mu^- + \text{anything}) < 0.31 \% \quad (90\% \text{ C.L.})$$

which is a factor of about 10 down from the theoretical estimate<sup>[43,47]</sup> of  $Br(b \rightarrow sh^0) \cdot Br(h^0 \rightarrow \mu^+ \mu^-) \simeq 5\%$ .

Triggered by the theoretical speculations about the Higgs particle assignment to the  $\xi(2.2)$ , the Mark III collaboration has searched<sup>[36]</sup> for various additional decay modes in their data, including the decay  $\xi \rightarrow \mu^+ \mu^-$  (see Table 5). This specific decay mode is rather important as it is expected to be rather big ( $\sim 4 - 16$  % of  $Br(h^0 \rightarrow s\bar{s})$  depending on the mass of the strange quark), and would clearly provide a very strong case for a Higgs interpretation, as the decay rate of ordinary hadrons to  $\mu^+ \mu^-$  should be miniscule. The quoted upper limit on this mode (Table 5) is<sup>[36]</sup>

$$\frac{Br(\xi \rightarrow \mu^+ \mu^-)}{Br(\xi \rightarrow s\bar{s})} < 6\% \cdot \frac{Br(\xi \rightarrow K\bar{K})}{Br(\xi \rightarrow s\bar{s})}$$

(using the measured branching ratio for  $\xi \rightarrow K^+ K^-$  and assuming  $Br(\xi \rightarrow K^+ K^-) \equiv Br(\xi \rightarrow K^0 \bar{K}^0)$ ). This additional slight disagreement with the Higgs assumption is almost as severe as the facts mentioned before, as one now would have to make the additional assumption that the Higgs field(s) couple also differently to leptons and quarks.

**Table 5:** Various upper limits on possible decay modes of the  $\xi(2.2)$  from the Mark III collaboration (Ref.36).

Decay mode	Upper limit (90 % C.L.)
$Br(J/\Psi \rightarrow \gamma\xi(2.2)) \cdot Br(\xi(2.2) \rightarrow \mu^+\mu^-)$	$< 7.3 \times 10^{-6}$
$Br(J/\Psi \rightarrow \gamma\xi(2.2)) \cdot Br(\xi(2.2) \rightarrow \pi^+\pi^-)$	$< 3 \times 10^{-5}$
$Br(J/\Psi \rightarrow \gamma\xi(2.2)) \cdot Br(\xi(2.2) \rightarrow K^*K)$	$< 2.5 \times 10^{-4}$
$Br(J/\Psi \rightarrow \gamma\xi(2.2)) \cdot Br(\xi(2.2) \rightarrow K^*\bar{K}^*)$	$< 3 \times 10^{-4}$
$Br(J/\Psi \rightarrow \gamma\xi(2.2)) \cdot Br(\xi(2.2) \rightarrow \eta\eta)$	$< 7 \times 10^{-5}$
$Br(J/\Psi \rightarrow \gamma\xi(2.2)) \cdot Br(\xi(2.2) \rightarrow p\bar{p})$	$< 6 \times 10^{-5}$

Thus in conclusion, the explanation of the  $\xi(2.2)$  as a Higgs boson (standard or non standard) is very unlikely. On the other hand the experimental problems mentioned before as well as the non observation of the  $\xi(2.2)$  in any other channel but  $K^+K^-$  (and eventually  $K_S^0 K_S^0$ ) make almost *any* interpretation of this resonance very problematic.

### $\Upsilon \rightarrow \gamma\zeta(8.3)$

As if history would repeat itself at a different place, in the summer of 1984, this time the Crystal Ball collaboration reported evidence for a narrow massive state in the radiative decays of the  $\Upsilon(1S)$ <sup>[35]</sup>. The state with a mass of  $\sim 8.3$  GeV/c<sup>2</sup>, called  $\zeta$ , was observed in about 100,000  $\Upsilon(1S)$  decays in two independent sets of data: One in which  $\zeta \rightarrow$  multiple hadrons and one which was strongly biased towards  $\zeta \rightarrow$  two low multiplicity jets. The best estimate for mass and width of the new state was reported to be

$$M = (8322 \pm 8 \pm 24) \text{ MeV}/c^2$$

$$\Gamma < 80 \text{ MeV} \quad (90\% \text{C.L.}) \quad (5.20)$$

$$Br(\Upsilon(1S) \rightarrow \gamma\zeta) \sim 0.5 \%$$

Fig.15 shows the inclusive photon spectrum around  $E_\gamma=1$  GeV for hadronic events with high multiplicity. The spectrum was fit in the region of  $E_\gamma$  between 750 MeV and 1604 MeV using the known line shape of the Crystal Ball (with variable amplitude and mean) superimposed on a 3rd order polynomial background. The fit yielded a significance of 4.2 standard deviations for the observed signal. The estimated branching ratio for the high multiplicity analysis was<sup>[35]</sup>

$$Br(\Upsilon(1S) \rightarrow \gamma\zeta) \cdot Br(\zeta \rightarrow \text{hadrons}) = (0.47 \pm 0.11_{\text{stat}} \pm 0.26_{\text{syst}})\%$$

The bulk of the systematic error is coming from the uncertainties in the photon detection efficiency which varies rather strongly for different assumptions on the decay modes of the  $\zeta$  particle.

In a second independent analysis the group looked for low multiplicity decays motivated in fact by a possible Higgs interpretation of the signal. The resulting photon spectrum in the  $\zeta$ -region is shown in Fig.16. The fit similar to that in Fig.15 yielded a 3.3 standard deviation signal with parameters for mass and width which were in excellent agreement with the values obtained from the high multiplicity analysis. Because the results of the two analyses were statistically independent, the combined significance for the signal was greater than 5 standard deviations<sup>[35]</sup>.

The Crystal Ball collaboration also looked for the possible contributions from  $\Upsilon(1S) \rightarrow \gamma\zeta \rightarrow \gamma\tau^+\tau^-$  followed by the decays  $\tau^\pm \rightarrow e^\pm\nu\bar{\nu}$ ,  $\tau^\mp \rightarrow \mu^\mp\bar{\nu}\nu$  and also  $\Upsilon(1S) \rightarrow \gamma\zeta \rightarrow \gamma e^+e^-$  resulting in simple final states. The non observation of any signal in these decay modes was converted into upper limits (90 % C.L.) of

$$Br(\Upsilon(1S) \rightarrow \gamma\zeta) \cdot Br(\zeta \rightarrow \tau^+\tau^-) < 0.2\%$$

$$Br(\Upsilon(1S) \rightarrow \gamma\zeta) \cdot Br(\zeta \rightarrow e^+e^-) < 3 \times 10^{-4}$$

The result on  $\zeta \rightarrow \tau^+\tau^-$  (see also Fig. 17) is compatible with the signal from the

low multiplicity analysis even for the extreme assumption  $Br(\zeta \rightarrow \tau^+\tau^-) = 100\%$ .

The Crystal Ball collaboration studied very carefully<sup>[35,50]</sup> the possibility that the signal, while statistically significant, resulted from some trigger bias, background effects and/or software procedural biases. One of the very important tests (but as turned out also obstacles) for the  $\zeta$  signal was the analysis of the  $\Upsilon(2S)$  data with the same cuts as were used in the  $\Upsilon(1S)$  analysis. The  $\Upsilon(2S)$  data are very well suited for several reasons

1. The  $\Upsilon(2S)$  is very near in c.m. energy, so the background photon spectrum should show a similar behaviour as in the  $\Upsilon(1S)$  decays.
2. The data sample on the  $\Upsilon(2S)$  ( $\sim 60 \text{ pb}^{-1}$ ) had about twice the number of resonance events and four times the number of hadronic events giving the possibility to test whether the signal seen in the  $\Upsilon(1S)$  would somehow be correlated to specific topologies of the events.
3. The known decays  $\Upsilon(2S) \rightarrow \pi\pi\Upsilon(1S)$  and  $\Upsilon(2S) \rightarrow \gamma\gamma\Upsilon(1S)$  with a summed branching ratio of  $\sim 42\%$ <sup>[51,52]</sup> and the subsequent decay  $\Upsilon(1S) \rightarrow \gamma\zeta$  should result in a (slightly Doppler broadened) signal for the  $\zeta$ . The Crystal Ball group estimated<sup>[35]</sup> the expected number of events in the peak as  $53 \pm 13$  events.

Fig.18 shows the obtained inclusive photon spectrum from the  $\Upsilon(2S)$ . The corresponding fit shows a smooth dependence in the region of  $E_\gamma$  from 800 to 2000 MeV. The first conclusion therefore was, that the  $\zeta$  was not created by the cuts used in the analysis. The nonobservation of the expected signal due to the transitions to the  $\Upsilon(1S)$  at  $E_\gamma \simeq 1070 \text{ MeV}$  was not harmful, as a fit to the region of interest gave an upper limit of 70 counts consistent with the expectations<sup>[35]</sup>.

In addition, depending on the origin of the  $\zeta$ , one could expect to see at some level the *direct* decay  $\Upsilon(2S) \rightarrow \gamma\zeta$ , which for a  $\zeta$ -mass of  $8.3 \text{ GeV}/c^2$  would correspond to a peak in the inclusive photon spectrum at  $E_\gamma \simeq 1560 \text{ MeV}$ . No such signal can be observed (Fig.18). The resulting ratio of direct branching

ratios of the fits to the  $\Upsilon(1S)$  and  $\Upsilon(2S)$  spectra gave thus an upper limit of

$$\frac{Br(\Upsilon(2S) \rightarrow \gamma\zeta)}{Br(\Upsilon(1S) \rightarrow \gamma\zeta)} < 0.22 \quad (90\% \text{ C.L.}) \quad (5.21)$$

The announcement of a state with such a high mass in the radiative decays of the  $\Upsilon(1S)$  caused considerable excitement and suggested to a number of theorists the possibility that this state might indeed be a Higgs boson<sup>[53]</sup>. Again, like in the case of the  $\xi(2.2)$  the branching ratio of  $\sim 0.5\%$  was far too high compared to the expectations for the standard Higgs ( $\sim (1.2 - 5) \times 10^{-5}$ ) leading to a discussion very similar to that in the  $\xi(2.2)$  case. Much of the theoretical work addressing the question of whether the  $\xi(2.2)$  was a Higgs particle lead (as discussed above) to testable predictions for the next heavier family of quark-antiquark boundstates, the  $\Upsilon$  system. Unfortunately, for the  $\zeta(8.3)$  the next family of vector resonances (toponium) has yet to be found. There is however one result in the Crystal Ball data that created severe doubts in a possible Higgs interpretation: the nonobservation of the direct decay  $\Upsilon(2S) \rightarrow \gamma\zeta$ . In fact, this result turned out to be a problem for almost any reasonable interpretation of the  $\zeta$ -origin.

Any explanation of the  $\zeta$  requires that the  $b\bar{b}$ -quarks building the  $\Upsilon(1S)$  annihilate<sup>[54,55]</sup> thus producing the  $\zeta$ . One example of this fundamental process is the Wilczek mechanism discussed above (Fig.6b). Therefore the production rate from any  $\Upsilon$ -resonance should be proportional to the wave function of the  $b\bar{b}$ -system at the origin,  $|\Psi(0)|^2$ , which can be measured by e.g.  $\Upsilon(nS) \rightarrow \mu^+\mu^-$ . The different masses of the  $\Upsilon(nS)$  states should be taken care of by different phase space factors for the decay. Indeed in the case of the Wilczek mechanism one gets the prediction

$$\frac{Br(\Upsilon(2S) \rightarrow \gamma\zeta)}{Br(\Upsilon(1S) \rightarrow \gamma\zeta)} = \frac{m_{\Upsilon'}^2}{m_{\Upsilon}^2} \cdot \frac{\Phi_{\Upsilon'}}{\Phi_{\Upsilon}} \cdot \frac{Br(\Upsilon' \rightarrow \mu^+\mu^-)}{Br(\Upsilon \rightarrow \mu^+\mu^-)} \quad (5.22)$$

where  $\Phi_{\Upsilon} = (1 - m_{\zeta}^2/m_{\Upsilon}^2) \cdot F(m_{\zeta}^2, m_{\Upsilon}^2)$  (eq. (5.12)). Using  $Br(\Upsilon' \rightarrow \mu^+\mu^-) = (1.6 \pm 0.3)\%$  and  $Br(\Upsilon \rightarrow \mu^+\mu^-) = (2.9 \pm 0.2)\%$  (Ref.28,56) gives for the ratio

(eq.(5.22))

$$\frac{Br(\Upsilon(2S) \rightarrow \gamma\zeta)}{Br(\Upsilon(1S) \rightarrow \gamma\zeta)} = \begin{cases} 0.85 \pm 0.17 & \text{for } F(m_\zeta^2, m_\Upsilon^2) = 1 \\ 1.18 \pm 0.24 & \text{for } F(m_\zeta^2, m_\Upsilon^2) = (1 - \frac{m_\zeta^2}{m_\Upsilon^2}) \end{cases}$$

evidently in rather strong disagreement with the experimental findings (5.21).

After the announcement of the  $\zeta(8.3)$  in the summer 1984, a large effort was mounted by groups both at CESR and at DORIS II to check these results independently both by analyzing data already taken and also by accumulating new data samples on the  $\Upsilon(1S)$ . The Crystal Ball obtained  $22 \text{ pb}^{-1}$  of additional data (corresponding to  $\sim 200,000$  hadronic  $\Upsilon$ -decays) whereas the CUSB group accumulated about 340,000 new  $\Upsilon$ -decays into addition to their 112,000  $\Upsilon$  decays they already had. In an earlier analysis of the inclusive photon spectrum of these 112,000 hadronic decays, published before the announcement of the evidence for the  $\zeta(8.3)$ <sup>[44]</sup>, they derived an upper limit (90 % C.L.) for the branching ratio  $Br(\Upsilon(1S) \rightarrow \gamma H^0)$  as a function of the mass recoiling against the photon<sup>[57]</sup> as displayed in Fig.19 (curve (a)). Unfortunately their results just stopped before the mass of the  $\zeta(8.3)$ . At the Leipzig conference<sup>[58]</sup> they enlarged the region of considered photon energies slightly to enclose the  $\zeta$  (Fig.20) yielding a 90 % C.L. upper limit of 0.2% for the production of the  $\zeta^*$ . Indicated also is the Crystal Ball value for  $Br(\Upsilon \rightarrow \gamma\zeta) \cdot Br(\zeta \rightarrow \text{hadrons})$ . As discussed before, the big systematic error on the branching ratio of almost 50% is mainly due to the unknown decay characteristics of the  $\zeta$ . The large photon energy involved ( $E_\gamma \approx 1/9\sqrt{s}$ ) leads to strong kinematical correlations which are modeled differently in e.g. a  $\gamma g g$  Monte Carlo compared to a  $\gamma X, X \rightarrow c\bar{c}$  Monte Carlo.

The preliminary analysis of the CUSB collaboration based on their newest data of  $\approx 340,000$  decays gives an upper limit for the product branching ratio of  $Br(\Upsilon \rightarrow \gamma\zeta) \cdot Br(\zeta \rightarrow \text{hadrons}) < 0.14 - 0.20\%$  (90% C.L.)<sup>[59]</sup> depending on the detector configuration. This result has been added to Fig. 20 (shaded area).

---

\* Note that there is a slight disagreement between Fig.19 and Fig.20 at lower recoil masses.

Although not directly relevant to the question of the existence of the  $\zeta$ , for completeness I want to also mention the CUSB results<sup>[44]</sup> on a search for the Higgs boson in radiative  $\Upsilon$  decays involving explicit final states. Fig.21 (curve (a)) shows the 90% C.L. upper limit for the product branching ratio  $Br(\Upsilon \rightarrow \gamma H^0) \cdot Br(H^0 \rightarrow 2 \text{ charged particles})$  which is especially important for low mass Higgs particles like the  $\xi(2.2)$  which cannot decay into  $c\bar{c}$  or  $\tau^+\tau^-$ .

The ARGUS collaboration<sup>[60]</sup> analyzed their data with respect to a possible  $\tau^+\tau^-$  final state of the  $\zeta(8.3)$ . To suppress the QED background of radiative  $\tau$ -pair production they looked for  $\Upsilon(2S)$ -decays of the form  $\Upsilon(2S) \rightarrow \pi^+\pi^-\Upsilon(1S)$ ,  $\Upsilon(1S) \rightarrow \gamma\tau^+\tau^-$  using the hadronic transition to tag the  $\Upsilon(1S)$  by requiring the recoil mass against the 2 pions to lie in the  $\Upsilon$  mass range. The  $\tau$ 's were detected by their decay into one charged particle and neutrinos ( $\tau \rightarrow \mu\nu\bar{\nu}, e\nu\bar{\nu}, \pi\nu, K\nu$ ). They did not see any sign of a signal, yielding an upper limit of  $Br(\Upsilon(1S) \rightarrow \gamma\zeta) \cdot Br(\zeta \rightarrow \tau^+\tau^-) < 0.1\%$  (90 % C.L.) (see Fig.22) thus improving the upper limit set by the Crystal Ball collaboration (Fig.17) by about a factor of two.

If one now combines the most stringent upper limits obtained for the  $\tau^+\tau^-$  final state by the ARGUS collaboration and compares it with the branching ratio for the  $\zeta$ -decay into hadrons from the Crystal Ball collaboration (eq.(5.20)) one gets for the fraction of the decay  $\zeta \rightarrow \tau^+\tau^-$  with respect to  $\zeta \rightarrow \text{hadrons}$

$$\frac{Br(\zeta \rightarrow \tau^+\tau^-)}{Br(\zeta \rightarrow \text{hadrons})} \ll (0.21 \pm 0.05_{stat} \pm 0.12_{syst})$$

which would still be consistent with even the hypothesis that the  $\zeta(8.3)$  is a neutral Higgs particle with standard couplings to  $\tau^+\tau^-$ .

The main problem, regarding the  $\zeta$  comes from the Crystal Ball collaboration itself. They analyzed their new data with the same cuts that were used for the 'high multiplicity'  $\zeta$  analysis which lead to the 4.2 standard deviation signal reported above. (The low multiplicity analysis has not been completed yet<sup>[50]</sup>). Fig.23 shows the corresponding inclusive photon spectrum from the new data.

No evidence for the  $\zeta$  is apparent. Superimposed is the best fit with mean constrained to  $\pm 1.0\%$  of that expected for the  $\zeta$ , resulting in  $-29 \pm 29$  counts. The disagreement between this new result and the previous one is about 4.0 standard deviations<sup>[50]</sup>. When they combine all their  $\Upsilon(1S)$  data they get an upper limit of

$$Br(\Upsilon \rightarrow \gamma\zeta) \cdot Br(\zeta \rightarrow \text{hadrons}) < 0.19 \% \quad (90\% \text{ C.L.})$$

Fig.24 shows the upper limit derived from their new data alone.

In conclusion, though the future of the  $\zeta(8.3)$  as well as the  $\xi(2.2)$  look rather dim, they proved to be very interesting in several aspects. They gave an opportunity to rethink the current wisdom regarding the Higgs in the standard model and its extensions. They also showed what amount of "stretchability" the ideas regarding the Higgs couplings really have and where the limitations lie. The fact, that current experiments are very near the required sensitivity to test the standard Higgs via the Wilczek mechanism points to the need for a dedicated Higgs search experiment running on the  $\Upsilon(1S)$  to either find the Higgs or to rule out standard Higgs particles with masses below  $9.4 \text{ GeV}/c^2$ . This would be a big step forward compared to the current mass limit of  $O(0.33) \text{ GeV}/c^2$ .

#### The mixing with the $^3P_0$ state of quarkonium

A very interesting possibility to enhance the decay rate due to the Wilczek mechanism is the mixing of the Higgs particle with the  $^3P_0$  ( $0^{++}$ ) states of quarkonia (Ref.30), which may provide sizeable enhancement effects when the Higgs boson mass is close to the quark-antiquark threshold. The same applies in principle to possible mixing of the nonstandard pseudoscalar neutral Higgs boson with the  $^1S_0$  ( $\eta_b$ ) states. This option is of special importance to an approach of achieving spontaneous symmetry breaking in a dynamical way through radiative corrections rather than by having a nonzero  $-\mu^2\phi^2$  term in the potential<sup>[61]</sup>. In

this case the Higgs mass turns out to be fixed to<sup>[30]</sup>

$$m_{H^0}^2 = \frac{3\alpha^2}{8\sqrt{2}G_F} \left[ \frac{2 + \sec^4\theta_W}{\sin^4\theta_W} - O\left(\frac{m_f^4}{m_W^4}\right) \right] . \quad (5.23)$$

Using the world average value of  $\sin^2\theta_W = (0.220 \pm 0.006)^{[62]}$  yields thus a predicted value of the Higgs mass of

$$m_{H^0} \sim (9.55 \pm 0.23) \text{ GeV}/c^2 . \quad (5.24)$$

Radiative corrections to eq.(5.23) are expected to be  $O(1\%)^{[30]}$ . Thus the  $1^3P_0$ -state of bottomonia with mass  $m[{}^3P_0(b\bar{b})] \approx 9.86 \text{ GeV}/c^2$  (Ref. 52) is only a few hundred  $\text{MeV}/c^2$  away. In that case, the rate for  $V \rightarrow \gamma H^0$  (here  $V \equiv \Upsilon'$ ) should have a characteristic dipole behaviour which leads to a suppression of the rate<sup>[29,30]</sup>. Fig.25 (taken from Ref.30) shows the modified rate for the direct decay without mixing as the dash-dotted curve. On the other hand, when the Higgs mass approaches the mass of the  ${}^3P_0$  state, the mixing as sketched in Fig.26 has to be considered as well. The corresponding result is shown in Fig.25 as the dashed curve. It is evident that the mixing can enhance the rate  $\Upsilon' \rightarrow \gamma H^0$  by an appreciable amount. Note that the parameters used in the calculations (like the masses of the  ${}^3P_0$  states, the leptonic widths of the resonances etc.) have not been updated to the current experimental status. The values chosen in Ref.30 however are reasonably close to the experimental reality.

One can therefore conclude that a sizeable enhancement is expected when the Higgs mass lies in the vicinity of the  ${}^3P_0$  states of bottomonium. This is an experimentally interesting option not only because the required sensitivity for a detection of the Higgs is less, but also because the  ${}^3P_0$  states decay favorably into two gluon final states. This would open the possibility of copious Higgs production in hadronic collisions<sup>[19,30]</sup> through gluon-gluon fusion, which as discussed earlier otherwise is pretty much suppressed. The mixing with the  ${}^3P_0$  states on the other hand puts some challenge to experiment, as the Higgs now has to be

distinguished from the  ${}^3P_0$  state itself which is produced far more copiously. The  $\tau^+\tau^-$  final state of the Higgs seems to be the most promising in this respect.

### B mesons and the standard Higgs

The existence of the  $\Upsilon(4S)$  as a  $B$ -meson factory offers another possibility to search for the standard neutral Higgs<sup>[63]</sup>. Although the mass of the  $B$  meson limits the region of accessible Higgs masses to  $m_{H^0} \leq 4.5 \text{ GeV}/c^2$ , detailed calculations show<sup>[63]</sup>, that in some cases the corresponding branching ratio is larger than the value according to the Wilczek mechanism discussed before.

The Higgs boson coupling in the standard model is flavor conserving. Therefore the decay  $b \rightarrow H^0 + X$  must occur in higher order. Fig.27a shows the corresponding Feynman diagrams with Fig. 27b as a specific example involving the top quark mass. Hence though the process is higher order, the involvement of very heavy quarks might yield appreciable rates. Fig.27 also indicates, that the resulting branching ratio will depend on the (as yet unknown) top quark mass. The "bremsstrahlungs" diagrams (Fig.27c) are found to be negligible<sup>[63]</sup> for the  $b$ -quark decay.

The ratio for the inclusive rate  $B \rightarrow H^0 X$  to the inclusive rate  $B \rightarrow e\nu X$  has been calculated<sup>[63]</sup> to be

$$\begin{aligned} \frac{\Gamma(B \rightarrow H^0 X)}{\Gamma(B \rightarrow e\nu X)} &= \frac{|V_{tb}V_{ts}^*|^2}{|V_{bc}|^2} \frac{27\sqrt{2}}{64\pi^2} G_F m_b^2 \left(\frac{m_t}{m_b}\right)^4 \Phi(\text{masses}) \\ &\approx 1.7 \times 10^{-5} \left(\frac{m_t}{m_b}\right)^4 \left[1 - \frac{m_{H^0}^2}{m_b^2}\right] \end{aligned}$$

for  $m_b \leq 4.5 \text{ GeV}/c^2$ . (The  $V_{ab}$  are the Kobayashi-Maskawa matrix elements taken from Ref.28 and  $\Phi$  is a phase space factor). The semileptonic branching ratio has been measured<sup>[32]</sup> to be

$$\frac{\Gamma(B \rightarrow l\nu X)}{\Gamma(B \rightarrow \text{all})} = (11.7 \pm 0.5)\% \quad (5.25)$$

leading to the prediction

$$\frac{\Gamma(B \rightarrow H^0 X)}{\Gamma(B \rightarrow \text{all})} \approx 2.0 \times 10^{-6} \left( \frac{m_t}{m_b} \right)^4 \left[ 1 - \frac{m_{H^0}^2}{m_b^2} \right] \quad (5.26)$$

which becomes quickly sizeable for increasing top quark mass. The current lower limit for the mass of the top quark from PETRA<sup>[46]</sup> of  $m_t \gtrsim 23 \text{ GeV}/c^2$  gives  $Br(B \rightarrow H^0 X) > 1.4 \times 10^{-3} \cdot \Phi$ , and for  $m_t \simeq 45 \text{ GeV}/c^2$  the branching ratio gets as large as 2.0%. For top meson decays, a look at the Feynman graphs involved (Fig.27) shows, that the heaviest quark mass involved in the coupling would be that of the bottom quark. Also the ratio of Kobayashi-Maskawa matrix elements is much smaller, yielding negligible values for the corresponding branching ratio.

No *specific* experimental investigation of this process has yet been published. The experimental signature depends of course on the Higgs mass, as this determines the final states. For a mass small enough to allow a sizeable branching fraction to  $\mu$ -pairs, this process would lead to a signature that resembles that of flavor changing neutral currents (FCNC)<sup>[63]</sup>. This signature has been investigated by the CLEO collaboration<sup>[49]</sup> which published an upper limit on  $Br(b \rightarrow l^+ l^- X) < 0.31\%$  and

$$\frac{Br(B \rightarrow l^+ l^- X)}{Br(B \rightarrow l \nu X)} < 0.029 \quad 90\% C.L. \quad (5.27)$$

The interpretation of this result in terms of a possible Higgs production is however not so easy, as the performed cuts used in the analysis were tailored to the FCNC assumption. An attempt to translate the above results into upper limits for Higgs production (as a function of the top quark mass) has been performed in Ref.63. Their result is shown in Fig.28. Due to the many uncertainties in the underlying assumptions like the assumed branching ratio for  $H^0 \rightarrow \mu^+ \mu^-$ , experimental acceptance factors etc., this figure is only illustrative. But it shows in a nice way what one could achieve with a reanalysis of the data which has the Higgs possibility in mind. So the conclusion here is that a detailed analysis of already

existing data with respect to the just discussed decay mode may give important restrictions on the mass of the standard Higgs particle in a region below  $\simeq 4.5$  GeV/c<sup>2</sup>.

## 6. Search for the nonstandard Higgs in $e^+e^-$ annihilation

As discussed briefly already in Chapter 4, almost any attempt of grand unified theory building leads to an enlargement of the simple Higgs sector. The introduction of additional Higgs fields lead to the appearance of new physical Higgs bosons, some of which are charged. Also considerably more freedom in the choice of couplings between the Higgs particles and leptons and quarks can be achieved. In general however one can still expect a correlation of the Higgs couplings with the masses of the fermions. The properties of the neutral Higgs bosons are therefore expected to be similar to those discussed in the previous sections. Therefore I will in the following concentrate on the properties of charged Higgs particles. The additional freedom concerning the couplings of the Higgs particles to fermions unfortunately complicates the predictions concerning the decay patterns and hence the experimental search.

Before however discussing the search for charged Higgs bosons in greater detail, there are some constraints on the mass which can already be deduced from its very general properties. Firstly, because of its charge, the Higgs couples to two quarks which have different flavor and its decays will thus look very much like decays involving the  $W^\pm$  bosons (as it couples to the weak doublets in the same way). However, because its coupling is 'semiweak' ( $\Gamma \sim G_F$  instead of  $\Gamma \sim G_F^2$ ), an order of magnitude estimate comparing the decay  $q \rightarrow H^- q'$  with  $q \rightarrow W^- q'$  shows, that the process involving the (on shell) Higgs particle is preferred by several orders of magnitude, as only one weak vertex is involved in the decay. This leads naturally to important phenomenological consequences. As an example consider an extension of the standard model with two complex Higgs fields (see also Chapter 4). The SU(2)xU(1) symmetry gets broken by the

presence of two non zero vacuum expectation values,  $v_\phi$  and  $v_\psi$ . One possible scenario is now, that mass is given to the upper (lower) partners of the SU(2) doublets by  $v_\phi$  ( $v_\psi$ ) only. Assuming that the charged Higgs has a mass below the mass of the  $\tau$ , this would result in<sup>[64]</sup>

$$\frac{\Gamma(\tau \rightarrow \pi \nu_\tau)}{\Gamma(\tau \rightarrow H \nu_\tau)} \sim \frac{G_F f_\pi^2 \tan^2 \beta}{(1 - m_H^2/m_\tau^2)^2} \ll 1 \quad (6.1)$$

where  $\tan \beta = v_\phi/v_\psi$ . This is obviously not consistent with experiment as the  $\tau$ -decays follow very nicely the pattern predicted by the standard model<sup>[28] \*</sup>. Hence charged Higgs bosons with  $m_{H^\pm} \lesssim m_\tau$  are ruled out already.

Similarly, for the bottom system the above assumptions lead to the rough estimate<sup>[64]</sup>

$$\frac{\Gamma(b \rightarrow H^- q)}{\Gamma(b \rightarrow W^- q)} \sim \frac{6\pi^2}{G_F m_b^2} \left[ \cot^2 \beta + \left(\frac{m_c}{m_b}\right)^2 \tan^2 \beta \right] \geq 10^5 \quad (6.2)$$

which would mean that the  $b$ -decays are totally dominated by their decay to the Higgs particle. The total rate  $\Gamma(b \rightarrow W q)$  can be calculated<sup>[65]</sup>

$$\begin{aligned} \Gamma(b \rightarrow W q) &\simeq \frac{G_F^2 m_b^5}{192\pi^3} [7.69 |V_{bu}|^2 + 3.07 |V_{bc}|^2] \\ &\simeq O(10^{-4}) \text{ eV} \end{aligned} \quad (6.3)$$

leading to lifetimes  $\tau_B \simeq 10^{-12} - 10^{-13}$  sec. If the mass of the charged Higgs would be below the  $b$ -quark mass, the lifetime of the  $b$  would be much smaller. The generally very good agreement of the  $B$ -meson properties with the standard model predictions without a light charged Higgs<sup>[32]</sup> and especially the very nice results on the measurement of the  $B$ -lifetime<sup>[66]</sup> of  $\sim 10^{-12}$  sec thus rules out charged Higgs bosons with  $m_{H^\pm} \lesssim 4.5 \text{ GeV}/c^2$  (Ref.67). If the recent evidence

---

\* Note that  $\beta \approx \pi/2$  (which would mean that  $H^\pm$  decouple from the leptons) is ruled out by data on D-decays (Ref. 64).

for the top quark seen in  $p\bar{p}$ -collisions by the UA1-collaboration<sup>[68]</sup> is confirmed, the observed consistency of its decay pattern involving only  $W^\pm$  exchange could increase this limit to  $m_{H^\pm} \not\prec (m_t - m_b)$ .

From the experimental point of view, the most important model independent property of the charged Higgs is of course the charge itself, as this leads to the attractive possibility of pair production via an intermediate virtual photon (Fig.29a). The differential cross section for pair production of a scalar particle in  $e^+e^-$  annihilation is given by<sup>[69]</sup>

$$\frac{d\sigma}{d\Omega} = \frac{\alpha^2}{8s} \beta^3 \sin^2\theta \quad (6.4)$$

where  $\theta$  is the production angle with respect to the beam axis, and  $\beta = p_H/E_H$ . Normalized to the pointlike cross section this gives

$$R_{H^+H^-} = \frac{1}{4}\beta^3 = \frac{1}{4} \left[ 1 - \frac{4m_H^2}{s} \right] \quad (6.5)$$

for the contribution to the  $R$ -value, which counts the fundamental charged degrees of freedom. For  $s \gg 4m_H^2$  this contributes  $\Delta R = 0.25$ . Given the sensitivity of current  $e^+e^-$  experiments for this value of  $O(5\%)$ <sup>[22]</sup>, such a step in  $R$  should in principle be visible, provided the Higgs particle decays predominantly hadronically. Unfortunately the value 0.25 is reached only very slowly above threshold and competes with variations of  $R$  due to electroweak interference and higher order QCD corrections<sup>[22,70]</sup>.

In general also the charged Higgs bosons are expected to couple to the fermions proportional to their masses. Fig.30 shows the expected dominant decay modes of the charged Higgs (not including the top quark)<sup>[71]</sup>. The decay mode  $H^+ \rightarrow c\bar{b}$  is on one hand Cabibbo suppressed as the involved Kobayashi-Maskawa matrixelement is small<sup>[28]</sup> †, but this is partly overcome by the speciality of the

---

† We follow<sup>[72]</sup> the theoretical prejudice that the Higgs will favour coupling among members of a common generation, like  $c\bar{s}$ , but will suppress cross generation couplings.

Higgs coupling favouring high masses. A rough estimate<sup>[73]</sup> gives

$$\frac{\Gamma(H^+ \rightarrow c\bar{b})}{\Gamma(H^+ \rightarrow c\bar{s})} \sim (m_b/m_c)^2 \sin^2 \theta_3 \quad (6.6)$$

which is very small for the currently accepted values of  $\sin \theta_3 \lesssim 0.05$ <sup>[74]</sup>. So in general it is sufficient to consider only the decays  $H^+ \rightarrow c\bar{s}$  and  $H^+ \rightarrow \tau^+ \nu_\tau$ . Unfortunately, the relative proportions of these two decay modes depend on the details of the specific model chosen<sup>[73,76]</sup>. Actual experimental searches were performed under variable assumptions about the relative decay rate to leptons and quarks which may be parameterized by<sup>[76]</sup>

$$x \equiv \frac{\Gamma(H^+ \rightarrow c\bar{s}, c\bar{b})}{\Gamma(H^+ \rightarrow \tau^+ \nu_\tau)} \quad (6.7)$$

A sketch of the typical event shapes for the extreme cases  $x \ll 1$ ,  $x \simeq 1$  and  $x \gg 1$  is shown in Fig.31 (from Ref.76) demonstrating the variable complexity of the events. The results of the various searches performed are summarized<sup>[76]</sup> in Fig.32 which shows the combined limits on the mass of the charged Higgs as a function of its branching ratio into  $\tau^\pm \nu_\tau$ . Note that this is directly correlated to limits on the branching ratio into  $(c\bar{b}, c\bar{s})$  as  $B_{had} + B_\tau \simeq 1$  is assumed.

In conclusion, one can say that charged Higgs particles with the discussed couplings do not exist for masses  $m_H \lesssim 13 \text{ GeV}/c^2$ . It is possible to push this limit up towards  $m_H \lesssim 23 \text{ GeV}/c^2$ , when the most recent data taken at the storage ring PETRA will be fully analyzed.

## 7. The $Z^0$ , Toponium and the Higgs boson

One of the most exciting possibilities for  $e^+e^-$  annihilation in the near future is the direct production of the  $Z^0$  at  $e^+e^-$  colliding beam facilities like the SLC<sup>[4]</sup> and LEP<sup>[5]</sup>. The large coupling of the standard Higgs particle to the intermediate vector bosons (Table 2) and the expected large rate of  $Z^0$  bosons produced leads to the expectation that the  $Z^0$  will be a very promising place to look for the Higgs. The expected cross section for  $Z^0$  production is given by<sup>[3]</sup>

$$\sigma_{tot}(s) = \frac{12\pi s}{m_{Z^0}^2} \cdot \frac{\Gamma(Z^0 \rightarrow e^+e^-)\Gamma(Z^0 \rightarrow \text{all})}{(s - m_{Z^0}^2)^2 + (m_Z \Gamma_Z^{tot})^2} \quad (7.1)$$

The width of the  $Z^0$  is given by<sup>[16]</sup>

$$\begin{aligned} \Gamma(Z^0 \rightarrow \text{all}) = \frac{G_F m_Z^3}{24\sqrt{2}\pi} \left\{ \right. & \left[ 1 + (1 - 4 \sin^2 \theta_W)^2 \right] N_{l^-} + 2 N_\nu \\ & + 3 \left[ 1 + \left( 1 - \frac{8}{3} \sin^2 \theta_W \right)^2 \right] N_{2/3} \\ & \left. + 3 \left[ 1 + \left( 1 - \frac{4}{3} \sin^2 \theta_W \right)^2 \right] N_{-1/3} \right\} \quad (7.2) \end{aligned}$$

where  $N_{l^-}$  is the number of charged leptons with  $m_l < m_Z/2$ ,  $N_\nu$  is the number of neutrinos and  $N_{2/3}$  ( $N_{-1/3}$ ) is the number of charge 2/3 (-1/3) quarks with  $m_q < m_Z/2$ . Using  $\sin^2 \theta_W = 0.22$  and the measured<sup>[13]</sup> mass of the  $Z^0$  of  $(93.2 \pm 1.5)$  GeV/c<sup>2</sup> this gives

$$\Gamma(Z^0 \rightarrow \text{all}) \simeq 976 \times N_D \quad [\text{MeV}]$$

$$\Gamma(Z^0 \rightarrow \mu^+ \mu^-) \simeq 90 \times N_D \quad [\text{MeV}]$$

where  $N_D$  is the number of weak doublets (generations) with mass lighter than half the  $Z^0$  mass. The total width of the  $Z^0$  is hence much larger than the beam

widths of the SLC or LEP, which will be of  $O(100)$  MeV<sup>[4,5]</sup>. The peak cross section (normalized to the pointlike cross section  $\sigma_{\mu\mu}$ ) is therefore simply<sup>[16]</sup>

$$R_{Z^0}^{peak} \simeq \frac{9}{\alpha^2} \frac{\Gamma(Z^0 \rightarrow e^+e^-)}{\Gamma(Z^0 \rightarrow \text{all})} = \frac{9}{\alpha^2} Br(Z^0 \rightarrow e^+e^-) \quad (7.3)$$

For  $Br(Z^0 \rightarrow e^+e^-) \simeq 3\%$  this gives  $R_{Z^0}^{peak} \simeq 5000$  ! The projected luminosity values at the  $Z^0$  factories are<sup>[4,5]</sup>

$$L^{SLC} \simeq 10^{30} \text{ cm}^{-2} \text{ sec}^{-1}$$

$$L^{LEP} \simeq 10^{32} \text{ cm}^{-2} \text{ sec}^{-1}$$

To give an idea of the  $Z^0$  rates to be expected, a luminosity of  $L = 10^{30} \text{ cm}^{-2} \text{ sec}^{-1}$  (corresponding to  $\sim 86 \text{ nb}^{-1}/\text{day}$ ) would yield approximately 4300  $Z^0$ 's per day. In the following, I will briefly discuss some of the more promising production modes for the standard Higgs involving the  $Z^0$  boson and a possibly existing toponium resonance<sup>[20]</sup>.

### $Z^0 \rightarrow \gamma + H^0$

This process offers a rather clean signature. Representative diagrams for this process (which is of higher order) are displayed in Fig.33 (Ref.77). The main contribution comes from the  $W^\pm$  - boson loop

$$\frac{\Gamma(Z^0 \rightarrow \gamma H^0)}{\Gamma(Z^0 \rightarrow \mu^+ \mu^-)} \simeq 7.8 \times 10^{-5} \left(1 - \frac{m_{H^0}^2}{m_{Z^0}^2}\right)^3 \left(1 + 0.17 \frac{m_{H^0}^2}{m_{Z^0}^2}\right) \quad (7.4)$$

Fig.34 shows this rate calculated as a function of Higgs mass (full line). The branching ratio of this process is hence of  $O(10^{-6})$ . A detailed analysis of the large QED background<sup>[77]</sup> showed that this process is not a good way to search for the Higgs.

$$\underline{Z^0 \rightarrow Z^{0*} H^0 \rightarrow l^+ l^- H^0}$$

This process (Fig.35a) is the dominant production mechanism<sup>[16]</sup> when sitting on top of the  $Z^0$  as it takes full advantage of the sizeable  $Z^0 Z^0 H^0$  coupling. The  $l^+ l^-$  pair is produced by the virtual  $Z^0$ . The differential rate has been calculated by Bjorken<sup>[78]</sup> to be

$$\frac{1}{\Gamma(Z^0 \rightarrow \mu^+ \mu^-)} \frac{d\Gamma(Z^0 \rightarrow H^0 \mu^+ \mu^-)}{dx} = \frac{\alpha}{4\pi \sin^2 \theta_W \cos^2 \theta_W} \cdot F(x, m_{H^0}/m_{Z^0})$$

with

$$F(x, y) = \frac{\left[1 - x + \frac{x^2}{12} + \frac{2}{3}y^2\right] [x^2 - 4y^2]^{1/2}}{[x - y^2]^2} \quad (7.5)$$

where  $x = 2E_{H^0}/m_{Z^0}$ . If one integrates this differential rate in the kinematic limits  $2m_{H^0}/m_{Z^0} \leq x \leq 1 + m_{H^0}^2/m_{Z^0}^2$ , one gets the dashed curve in Fig.34. Unfortunately, again one gets a pretty small branching ratio. For Higgs masses bigger than 40-50 GeV/c<sup>2</sup> the production rate is too small for the projected luminosities at the SLC and even at LEP, even if one assumes 100 % detection efficiency.

The signal consists of the decay products of the Higgs particle and a lepton pair (for ease of detection preferentially a  $\mu^+ \mu^-$  or  $e^+ e^-$  pair) recoiling against the Higgs particle. A detailed study<sup>[79]</sup> shows that the possible background due to lepton production of weak heavy quark decays peaks at low invariant masses for the lepton pair, in contrary to the signal, thus making a separation without a big loss in efficiency reasonably easy. The situation gets worse with decreasing invariant mass (corresponding to increasing Higgs mass).

An important further background, especially for the  $H^0 e^+ e^-$  mode, comes from the two photon production of hadrons where both scattered electrons enter the detector<sup>[79]</sup>. These events also have a high invariant mass for the leptons. The corresponding recoil mass<sup>[79]</sup> is shown in Fig.36 for a Monte Carlo generation of the two photon process  $e^+ e^- \rightarrow e^+ e^- X$  (full histogram) and  $Z^0 \rightarrow e^+ e^- H^0$

(dashed curve,  $m_{H^0} = 10 \text{ GeV}/c^2$ ). One can see that the background from two photon processes limits the sensitivity of the discussed method to Higgs bosons with masses bigger than  $\simeq 10 \text{ GeV}/c^2$ .

### $Z^{0*} \rightarrow Z^0 H^0$

This process (Fig.35b) is in principle very similar to the one just discussed, involving the Bremsstrahlung of the Higgs particle off the  $Z^0$  (which this time however is virtual). Hence one has to sit at c.m. energies above the  $Z^0$ . The cross section has been calculated<sup>[20,80]</sup>

$$\sigma(e^+e^- \rightarrow Z^0 H^0) = \frac{G_F^2 m_{Z^0}^4}{48\pi} \cdot \frac{1}{2} [1 + (1 - 4 \sin^2 \theta_W)^2] \cdot f(s, m_{Z^0})$$

where

$$f(s, m) = \frac{8K}{\sqrt{s}} \left[ \frac{K^2 + 3m^2}{(s - m^2)^2} \right]$$

and  $K$  is the c.m. momentum of the Higgs (or the  $Z^0$ ). This cross section, normalized to the point cross section, is plotted in Fig.37 for different c.m. energies and as a function of the Higgs mass<sup>\*</sup>. The production cross section peaks at  $\sqrt{s} = m_{Z^0} + \sqrt{2}m_{H^0}$ <sup>[77]</sup>:

$$R^{max} = \frac{\sigma(e^+e^- \rightarrow Z^0 H^0)}{\sigma_{\mu\mu}} = \frac{3}{64} \left( \frac{m_{Z^0}}{38\text{GeV}} \right)^4 \frac{m_{Z^0}}{2\sqrt{2}m_{H^0}} [1 + (1 - 4 \sin^2 \theta_W)^2]$$

which for a Higgs mass of  $10 \text{ GeV}/c^2$  is  $R^{max} \sim 5.6$  corresponding to  $\simeq 3-4$  events per day with a luminosity of  $10^{30} \text{ cm}^{-2} \text{ sec}^{-1}$ , quite a sizeable number. The mass of the Higgs particle is then determined by<sup>[77]</sup>

$$m_{H^0}^2 = (\sqrt{s} - E_{Z^0})^2 - p_{Z^0}^2 \quad (7.6)$$

where  $E_{Z^0}$  ( $p_{Z^0}$ ) is the energy (momentum) of the  $Z^0$ . Clearly, for an unambiguous detection of this decay one will have to identify the  $Z^0$  by its decay into  $e^+e^-$  or

---

\* The 'error bars' in Fig. 37 reflect the dependence on  $\sin^2 \theta_W$  when varied between 0.22 and 0.29 (see Ref. 16).

$\mu^+\mu^-$ . This unfortunately lowers the rate considerably. Also the determination of the Higgs mass is complicated due to the large width of the  $Z^0$ .

As in the previous case, the background from heavy quark decays, which is of similar size as the signal, peaks at low invariant masses of the lepton pair and is manageable. Another very attractive feature is, that one is in principle sensitive to Higgs masses in the range  $0 < m_{H^0} \leq (\sqrt{s} - m_{Z^0})$  and the main limitation on possible masses comes from the c.m. energy reachable. At LEP (phase II, see Ref.5) one may thus be able to search for Higgs bosons with masses as large as  $100 \text{ GeV}/c^2$ .

An unattractive feature however is that one has to sit above the  $Z^0$  to look for the Higgs particle, which at least in the startup phases of the SLC and LEP seems to be rather unlikely. One would envision a high statistics scan up to the highest possible c.m. energy. In view of the importance of the Higgs particle on the other hand this is of course a worthwhile enterprise.

### $Z^0 \rightarrow H^+H^-$

Below the  $Z^0$ -pole the cross section for pair production of charged Higgs bosons is dominated by the one photon exchange diagram. This changes dramatically as one approaches the  $Z^0$ . In this case the cross section gets modified by the increased importance of the  $Z^0$ -exchange (Fig.29b) to<sup>[77]</sup>

$$\frac{\sigma(e^+e^- \rightarrow H^+H^-)}{\sigma(e^+e^- \rightarrow \mu^+\mu^-)} = \frac{\beta_H^3}{4} \cdot \left\{ 1 - \frac{2s\chi vv_H}{(s/m_{Z^0}^2 - 1) + \Gamma_{Z^0}^2/(s - m_{Z^0}^2)} + \frac{s^2\chi^2(v^2 + a^2)v_H^2}{(s/m_{Z^0}^2 - 1) + \Gamma_{Z^0}^2/m_{Z^0}^2} \right\}$$

where  $\beta_H = p_H/e_H$  as before,  $a = -1$ ,  $v = v_H = -1 + 4\sin^2\theta_W$  and  $\chi \equiv G_F/(8\sqrt{2}\pi\alpha)$ . A rough sketch of the calculated cross section<sup>[77]</sup> involving the  $Z^0$ -exchange is shown in Fig.38. Compared to the total peak cross section at the  $Z^0$  of  $\simeq 50 \text{ nb}$  the production of charged Higgs bosons appears to be miniscule.

Compared with the continuum cross section however, the  $Z^0$  is the best place to look for charged Higgs particles with masses less than  $m_{Z^0}/2$ . An assumed luminosity of  $10^{30}\text{cm}^{-2}\text{sec}^{-1}$  would give  $\simeq 1.5$  events/day. At higher c.m. energies other production mechanisms seem more promising<sup>[16,77]</sup>.

### Toponium and the Higgs boson

The recently reported evidence for the top quark<sup>[68]</sup> with a mass between 30 and 60  $\text{GeV}/c^2$  suggests that the bound states of the top-quark and its antiparticle (toponium) might lie in the vicinity of the  $Z^0$  peak. The negative results of the top searches at PETRA place a lower limit<sup>[48]</sup> on the mass of  $m_t \gtrsim 23 \text{GeV}/c^2$ .

When the mass of the toponium groundstate is comparable with the mass of the intermediate vector bosons, the characteristics of its decay pattern change drastically from the picture known from the  $J/\Psi$  and the  $\Upsilon$  resonances. The main contributions to the decay of e.g. the  $\Upsilon(1S)$  are shown in Fig.39a. In this case the  $Z^0$ -exchange is still negligible. The weak decays involving the  $W^\pm$  bosons play almost no role. As one approaches the  $Z^0$  and the  $W^\pm$  poles, the importance of the  $Z^0$  exchange diagrams and of the weak decays involving the  $W^\pm$  bosons (Fig.39b) gain importance. For toponium masses exceeding the  $Z^0$  mass, the weak (spectator like) decay of one of the constituent heavy quarks in fact will dominate all other decay modes. This situation is depicted in Fig.40a, which shows the widths for the various possible decays as a function of top quark mass<sup>[81]</sup>. Also shown is the expected width for Higgs production by the Wilczek mechanism for a Higgs boson with a mass of  $O(10\text{GeV}/c^2)$ . As expected it rises slowly ( $\sim m_t^2$ ) with increasing top quark mass. However the branching ratio actually decreases due to the opening of competing decay channels<sup>[81]</sup> as shown in Fig.40b. This applies in fact to all decay modes which are not connected to the  $W^\pm$  and the  $Z^0$ . For top quark masses around 50-60  $\text{GeV}/c^2$  however the branching ratio for  $V(t\bar{t}) \rightarrow \gamma H^0$  is still of  $O(1\%)$  and almost comparable to the annihilation into 3 gluons. As a result one can conclude that the most

unfortunate situation would occur if  $|m(t\bar{t}) - m_{Z^0}| < \Gamma_{Z^0}^{tot}$ . However, in this case one has to take into account possible mixing effects between the  $Z^0$  and the  $t\bar{t}$ -resonance<sup>[81,82]</sup> leading to an appreciable enhancement of the production rate. On the other hand, the decay rate to  $\gamma H^0$  is probably not enhanced in the same way, since the  $t\bar{t}$ -state also decays predominantly through the  $Z^0$  channel (Ref.81). However one might still envision a depletion of the dip in Fig.40b around the  $Z^0$  mass.

## 8. Conclusions

An overview over the possible production mechanisms of standard and non-standard Higgs particles in  $e^+e^-$  annihilations up to  $\sqrt{s} \simeq m_{Z^0}$  has been given. For masses of the neutral Higgs less than  $\simeq 10 \text{ GeV}/c^2$  the vector resonances  $J/\Psi$  and  $\Upsilon$  form the best places to look for its production via the Wilczek mechanism. The sensitivity of currently active experiments is not yet sufficient to make definite statements on the existence or non existence of neutral Higgs bosons below  $10 \text{ GeV}/c^2$ .

The Higgs particle production in  $Z^0$  decays (via  $Z^0 \rightarrow l^+l^-H^0$ ) offers reasonable sensitivity for Higgs masses  $10 \text{ GeV}/c^2 \leq m_{H^0} \leq 50 \text{ GeV}/c^2$ , provided the projected luminosities of  $Z^0$  factories like the SLC and LEP are reached. The lower limit on  $m_{H^0}$  is dictated by increasing background, the upper limit is due to the rapidly falling cross section for Higgs production with increasing Higgs mass. Higgs bosons with masses above  $50 \text{ GeV}/c^2$  can best be explored by the process  $e^+e^- \rightarrow Z^0H^0$  providing in principle sensitivity for masses within  $0 < m_{H^0} \leq (\sqrt{s} - m_{Z^0})$  where  $\sqrt{s}$  is the maximal reachable c.m. energy. This reaction however requires a high precision scan above the  $Z^0$  which may not be done in the start-up phases of the SLC and LEP.

For charged Higgs bosons the experimental situation looks entirely different due to the possibility of pair production in  $e^+e^-$  annihilation. As a result of detailed analyses by experiments at PETRA and at PEP, charged Higgs bosons

with masses  $m_{H^\pm} \lesssim 13 \text{ GeV}/c^2$  can be ruled out already. If the evidence for the top quark with properties as expected from the standard model gets stronger, this limit can be pushed up to  $m_{H^\pm} \not\ll m_t$ .

The discussed problematics of Higgs detection in  $Z^0$  decays for Higgs masses below  $\sim 10 \text{ GeV}/c^2$  indicates the need for dedicated high statistics experiments on the  $J/\Psi$  and especially on the  $\Upsilon(1S)$  to either find the standard Higgs or increase the lower limit on its mass from  $O(300) \text{ MeV}/c^2$  to  $O(10,000) \text{ MeV}/c^2$ . In conclusion, one can safely state that the Higgs search has just begun.

## ACKNOWLEDGEMENTS

It is a pleasure to thank A. Fridman, M. Peskin and G. Godfrey for interesting and useful discussions. My special thanks go to F. Gilman for interesting and enlightening suggestions and a careful reading of the manuscript. Last, but not least, I want to thank E.D. Bloom for drawing my attention to this interesting subject.

## REFERENCES

1. Arnison, G. et al., Phys.Lett. 122B (1983) 103, Phys.Lett. 129B (1983) 273, Phys.Lett. 126B (1983) 398, Phys.Lett. 134B (1984) 469;  
Banner, G. et al., Phys.Lett. 122B (1983) 476;  
Bagnaia, P. et al., Phys.Lett. 129B (1983) 130.
2. Glashow, S.L., Nucl.Phys. 22 (1961) 579;  
Weinberg, S., Phys.Rev.Lett. 19 (1967) 1264;  
Salam, A., Proc. 8th Nobel Symp. (Stockholm), ed. N. Svartholm (Almqvist and Wiksell, Stockholm, 1968) p.367.
3. See e.g. Commins, E.D. and P.H. Bucksbaum: Weak interactions of leptons and quarks, Cambridge University Press, Cambridge, 1983.
4. See e.g.: Proceedings of the SLC workshop on experimental use of the SLAC Linear Collider, SLAC Report 247, March 1982.
5. See e.g.: LEP Design Report, CERN-LEP/84-01, June 1984.
6. Goldstone, J.; Nuovo Cimento 19 (1961) 154.
7. Higgs, P.W., Phys.Lett. 12 (1964) 132, Phys.Rev.Lett. 13 (1964) 508, Phys.Rev. 145 (1966) 1156;  
Englert F. and R. Brout, Phys.Rev.Lett. 13 (1964) 321;  
Guralnik, G.S., C.R. Hagen and T.W.B. Kibble, Phys.Rev.Lett. 13 (1964) 585;  
Kibble, T.W.B., Phys.Rev. 155 (1967) 1554.
8. See e.g.: Jarlskog, C., Introduction to the Standard Model, USIP-report 85-02, January 1985.
9. Marciano W. and A. Sirlin, Phys.Rev. D22 (1980) 2695, Nucl.Phys. B189 (1981) 442;  
Llewellyn-Smith, C.H. and J. F. Wheeler, Nucl.Phys. B208 (1982) 27.
10. Coleman, S. and E. Weinberg, Phys.Rev. D7 (1973) 1888;  
Weinberg, S., Phys.Rev.Lett. 36 (1976) 294 ;  
Linde, A.D., JETP Lett. 23 (1976) 64;  
Linde, A.D., Phys.Lett. 70B (1977) 306;  
Veltman, M., Acta Physica Polonica B8 (1977) 475;  
Vayonakis, C.E., Nuovo Cimento 17 (1976) 383;  
Lee, B.W., C. Quigg and H.B. Thacker, Phys.Rev.Lett. 38 (1977) 883, Phys.Rev. D16 (1977) 1519;  
Dicus, D.A. and V.S. Mathur, Phys.Rev. D7 (1973) 3111.
11. Ellis, J., M.K. Gaillard and D.V. Nanopoulos, Nucl.Phys. B106 (1976) 292; and references therein.

12. Willey, R.S. and H.-L. Yu, Phys.Rev. D26 (1982) 3287.
13. UA1 and UA2 collaboration reports cf. Proc. 4th Topical Workshop on  $p\bar{p}$  Collider Physics, Bern (1984);  
Marciano, W.J., BNL-SUNY preprint 35788, 1985.
14. Ellis, J., Invited talk presented at the Royal Society meeting for discussion on the fundamental constants, CERN preprint TH-3616 (1983) and references therein.
15. Maiani, L., in GIF79, Ecole d'Eté de Physique des Particules, Gif-sur-Yvette, 3-7 Septembre 1979.
16. Ellis, J., talk presented at the Summer Institute on Particle Physics, SLAC-PUB-2177, August 1978;  
Langacker, P. et al., UPR-0269T, Sep. 1984, SSC Theoretical Workshop subgroup report, LBL, Berkeley, Jun. 1984. To be published in Proc. of 1984 Div. of Particles and Fields Summer Study Conf., Snowmass, CO, Jun.23-Jul.13, 1984.
17. Kane, G.L., Proceedings of the topical workshop on new particles in superhigh energy collisions, October 1979, University of Wisconsin, Madison, ed. by V. Barger and F. Halzen;  
Haber, H.E., G.L. Kane and T. Sterling, Nucl.Phys. B161 (1979) 493.
18. Einhorn, M. B. and S.D. Ellis, Phys.Rev. D12 (1975) 2007.
19. Savoy, C., in GIF79, Ecole d'Eté de Physique des Particules, Gif-sur-Yvette, 3-7 Septembre 1979.
20. For earlier reviews see e.g.:  
Ref. 11 and references therein;  
Haber, H.E., G.L. Kane and T. Sterling in Ref.17;  
Barbiellini, G. et al., DESY-Report 79/27 (1979);  
Ali, A., DESY-Report 81/60 (1981);  
Vainshtein, A.I., V.I. Zakharov and M.A. Shifman, Sov.Phys.Usp.23(8), Aug.1980, p.429.
21. Ali, A. in Ref. 20; and references therein.
22. Bloom, E.D.; Invited talk presented at the Aspen Winter Physics Conference, Aspen Colorado, January 13-19, 1985, SLAC-PUB-3573; and references therein.
23. MAC-Collaboration, Fernandez, E. et al., 1984, SLAC-PUB-3479, submitted to Phys.Rev. D.
24. Gaemers, K.J.F. and G.J Gounaris, Phys.Lett. 77B (1978) 379.

25. Yu, H.-L., Ph.D.Thesis, Univ. of Pittsburgh, 8312520, 1982, and references therein.
26. Zweig, G., CERN preprints 8182/TH.401 and 8419/TH.412 (1964), unpublished.
27. Wilczek, F., Phys.Rev.Lett. 39 (1977) 1304.
28. Review of Particle Properties, Rev.Mod.Phys.56,No.2,Part II (April 1984).
29. Frampton, P.H. and W.W. Wada, Phys.Rev. D19 (1979) 271.
30. Ellis, J., M.K. Gaillard, D.V. Nanopoulos and C.T. Sachrajda, Phys.Lett. 83B (1979) 339;  
Pantaleone, J., M.E. Peskin and S.-H.H. Tye, Phys.Lett. 149B (1984) 225.
31. See e.g.: Crystal Ball proposal for DORIS II, 1984.
32. For a recent review on the  $\Upsilon$ -system see e.g.: Cassel, D.G., Invited paper presented at the 4th Int. Conf. on Physics in Collision, Santa Cruz, August 22-24, 1984; preprint CLNS-85/644, 1985; and references therein.
33. Wormes, N., Mark III collaboration, private communication;  
Oreglia, M., Ph.D.Thesis, SLAC-Report 236, December 1980, unpublished.
34. Mark III collaboration, Einsweiler, K. et al., 1983, SLAC-PUB-3202, presented at the Int. Europhysics Conf. on High Energy Physics, Brighton, England, July 20-27 1983.
35. Crystal Ball Collaboration, Peck, C.W. et al., 1984, SLAC-PUB-3380 and DESY-report 84-064;  
Trost, H., 1984, Contributed paper to the XXII Int. Conf. on High Energy Physics, Leipzig, July 19-25;  
Niczyporuk, B., 1984, SLAC Summer Institute on Particle Physics, July 23-August 3;  
Coyne, D.G., 1984, Invited talk presented at the Conf. on Physics in Collision IV, University of Santa Cruz, Santa Cruz, California.
36. Mark III collaboration, Wormes, N., 1984, SLAC-PUB-3312; Invited talk presented at the Rencontre de Moriond: New particle production at high energy, La Plagne, France, March 4-10.
37. E.g. the width of the  $\Theta(1690)$  is measured to be  $\Gamma(\Theta) = (130 \pm 25)$  MeV (Ref. 36).
38. See e.g.: Haber, H.E. and G.L. Kane, Phys.Lett. 135B (1984) 196;  
Willey, R.S., Phys.Rev.Lett. 52 (1984) 585.
39. DM2 Collaboration, Szklarz, G., 1984, Contributed paper to the XXII Int. Conf. on High Energy Physics, Leipzig, July 19-25.

40. DM2 collaboration, Augustin, J.E. , Invited talk presented at the Rencontre de Moriond, March 1985.
41. Mark III collaboration, Partridge, R., private communication.
42. Wise, M.B.; HUTP-81/A017, Apr. 1981; Ithaca B-decay Workshop 1981, p.135.
43. CLEO collaboration, Behrends, S. et al., Phys.Lett. 137 B (1984) 277;  
For a review see also:  
Ogg, M., preprint CLNS-84/604, May 1984;  
Kass, R., 1984, Invited talk presented at the Rencontre de Moriond.
44. CUSB collaboration, Youssef, S. et al., Phys.Lett. 139B (1984) 332.
45. Haber, H.E. et al. in Ref. 38; and references therein.
46. This is however in a strict sense relevant only if the  $\xi$  is a pseudoscalar Higgs (Ref.38,42). The data on  $K_S^0 K_S^0$  hinting to a possible  $0^+$  assignment are on the other hand too scarce to discard this option rightaway.
47. Wise, M.B., Phys.Lett. 103B (1981) 121;  
Hall, L.J. and M.B. Wise, Nucl.Phys. B187 (1981) 397;  
Willey, R.S. in Ref.38.
48. For a review see e.g.: Boer, W.d., MPI-PAE/Exp-E1-144, Nov. 1984; Invited talk given at the 4th Int. Conf. on Phys. in Collisions, Santa Cruz, CA, Aug. 22-24, 1984.
49. CLEO collaboration, Avery, P. et al., Phys.Rev.Lett. 53 (1984) 1309.
50. Crystal Ball collaboration, Lowe, S., Invited talk presented at the Rencontre de Moriond, March 1985.
51. Crystal Ball collaboration, Gelfman, D. et al., SLAC-PUB-3563, submitted to Phys.Rev. D; and references therein.
52. Crystal Ball collaboration, Nernst, R. et al., SLAC-PUB-3571, submitted to Phys.Rev. D; and references therein.
53. Glashow, S.L. and M. Machacek, Phys.Lett. 145B (1984) 302;  
Pham, X., PAR/LPTHE-84/38, Nov. 1984;  
Tu, T., BIHEP-TH-84-22, Sep. 1984;  
Gluck, M., DO-TH-84/23, Oct. 1984;  
Shin, M. et al., HUTP-84/A068;  
Georgi, H. et al., Phys.Lett. 149B (1984) 234;  
Rodenberg, R., Print-8-40843 (Aachen), Oct. 1984;  
Lane, K. et al., Phys.Rev.Lett. 53 (1984) 1718;  
Nandi, S., DOE-ER-03992-563 (Texas), Oct. 1984;

- Haber, H.E. and G. L. Kane , Nucl.Phys. B250 (1985) 716;  
 Clavelli, L. et al.,1984, IUHET-96a, Sep. 1984;  
 Pantaleone, Z. et al., 1984, SLAC-PUB-3439 (see Ref.30);  
 Wu, Dan-Di, KEK-TH 97, Nov. 1984.
54. Pantaleone, J., M.E. Peskin and S.-H.H. Tye in Ref.30.
  55. One exception would be to interpret the  $\zeta$  as a  $b\bar{b}$  state, namely the ( $^1S_0$ )  $\eta_B$ . This is however considered to be implausible<sup>[64]</sup> as it would require a hyperfine splitting of an order of magnitude larger than that predicted by QCD.
  56. Tuts, P., Proc. of the 1983 Int. Symp. on Lept. and Phot. Int. at High Energies, Cornell Univ., 1983, p.284.
  57. Note that the spectrum from which these numbers were derived has already been shown in Fig.12.
  58. Franzini, P.,1984, Contributed paper to the XXII Int. Conf. on High Energy Physics, Leipzig, July 19-25.
  59. CUSB Collaboration, Tuts, M.,1984; to be published in the Proc. of the Meeting of the American Physical Society, Dept. of Particles and Fields, Santa Fe, New Mexico, October 31-November 3.
  60. ARGUS collaboration, Albrecht, H. et al., DESY-Report 85-014, 1985.
  61. Coleman, S. and E. Weinberg in Ref. 10;  
 Weinberg, S., Phys.Rev. D7 (1973) 2887.
  62. Marciano, W.J. in Ref. 13.
  63. Willey, R.S. and H.L. Yu, Phys.Rev. D26 (1982) 3086.
  64. Golowich, E. and T.C. Yang, Phys.Lett. 80B (1979) 245.
  65. For a review see e.g.: Fridman, A., DESY-Report 83-131, 1983; and references therein.
  66. For a review see e.g.: Jaros, J.A.; SLAC-PUB-3569, February 1985; Presented at the 12th SLAC Summer Inst. on Part. Phys., Stanford, California, July 23-August 3, 1984.
  67. The same conclusion has been reached in an analysis of data on  $b$ -decays by the CLEO collaboration: Chen, A. et al., Phys.Lett. 122B (1983) 317.
  68. UA1-collaboration, Arnison,G. et al., Phys.Lett. 147B (1984) 493.
  69. Cabibbo, N. and R. Gatto, Phys.Rev. 124 (1961) 1577.
  70. The TASSO experiment e.g. (Althoff, M. et al., Phys.Lett. 122B (1983) 95) quotes an accuracy in their experiment for finding a possible step in

the total annihilation cross section of  $\Delta R < 0.5\beta^3$  at the 95% C.L. for  $12.5 < m_H < 17 \text{ GeV}/c^2$  which is not sensitive enough for the expected rise in  $R$  due to the pair production of charged Higgs particles.

71. For a recent review on the search for charged Higgs bosons in  $e^+e^-$  annihilation see e.g.:  
Wu, S.L., Phys.Rept. 107 (1984) 59;  
Yamada, S., Proc. of the 1983 Int. Symp. on Lept. and Phot. Int. at High Energies, Cornell Univ., 1983.
72. Leveille, J.P., 1981, Ann Arbor-UM-HE-81-11, Ithaca 1981; and Proceedings of the Cornell  $Z^0$  Theory Workshop, ed. by M.E. Peskin and S.-H.H. Tye.
73. Ellis, J., M.K. Gaillard, D.V. Nanopoulos and P. Sikivie, Nucl.Phys. B182 (1981) 529;  
Ellis, J., Lectures presented at the Les Houches Summer School (August 1981) LAPP-TH-48 and CERN-TH-3174;  
see also Ref. 70.
74. Chau, L.L. and W.-Y. Keung, Phys.Rev. D29 (1984) 592.
75. Kim, J.E. and G. Segre, Phys.Lett. 78B (1978) 75.
76. See e.g.: Yamada, S. in Ref. 71.
77. Barbiellini, G. in Ref. 20; and references therein.
78. Bjorken, J.D., 1976 Slac Summer Institute Lect., SLAC-Report-198 (1976) and SLAC-PUB-1866 (1977).
79. See p.127ff in Ref. 4.
80. Lee, B.W. , C. Quigg and H.B. Thacker, Phys.Rev.Lett. 38 (1977) 883 and Phys.Rev. D16 (1977) 1519;  
Glashow, S.L., D.V. Nanopoulos and A. Yildiz, Phys.Rev. D18 (1978) 1724.
81. Chaichian, M. and M. Hayashi, SLAC-PUB-3549, January 1985, submitted to Phys.Rev. D.
82. Franzini, P.J. and F.J. Gilman, SLAC-PUB-3541, January 1985, submitted to Phys.Rev. D;  
Hall, L.J., S.F. King and S.R. Sharpe, Harvard preprint 1985, HUTP-85/A012.

## FIGURE CAPTIONS

1. The lifetime of the Higgs boson as a function of its mass<sup>[11]</sup>.
2. (a) Calculations of  $p\bar{p}(p) \rightarrow H^0 X$  as a function of the Higgs mass<sup>[16]</sup> for different values of  $\sqrt{s}$  and the corresponding Feynman diagrams (Q=quark, G=gluon).  
(b) Production cross section<sup>[19]</sup> for  $p\bar{p} \rightarrow H^0 X$  involving heavy quarks  $Q$  in the final state and the corresponding Feynman diagrams.
3. (a) Feynman diagram for the process  $e^+e^- \rightarrow H^0 \rightarrow X$ .  
(b) Feynman diagram for the Higgs production via bremsstrahlung off a final state quark line ( $f, \bar{f}$ ).  
(c) Feynman diagrams for the process  $e^+e^- \rightarrow \gamma H^0$ .  
(d) Feynman diagrams for the process  $H^0 \rightarrow \gamma\gamma$ .
4.  $R$  values from selected experiments<sup>[22]</sup> which quote a systematic error of less than 7%.
5. Total cross section<sup>[24]</sup> for  $e^+e^- \rightarrow f\bar{f}H^0$  at  $\sqrt{s} = 40$  GeV as a function of the Higgs mass, at fermion masses  $m_f = 1.5, 1.8, 4.5$  and  $15$  GeV/c<sup>2</sup>.
6. (a) The dominant bremsstrahlung diagram<sup>[11]</sup> for  $e^+e^- \rightarrow J/\Psi + H^0$ .  
(b) Feynman diagrams<sup>[27]</sup> for the radiative decay  $V(q\bar{q}) \rightarrow \gamma H^0$  (upper two) and the leptonic decay  $V(q\bar{q}) \rightarrow \mu^+\mu^-$ .  
(c) Feynman diagram for the decay of the vector resonance  $V$  via  $V \rightarrow \gamma gg$ , where  $g$  denotes a gluon.
7. Distribution<sup>[36]</sup> of the invariant mass formed by the two Kaons in (a)  $J/\Psi \rightarrow \gamma K^+K^-$  and (b)  $J/\Psi \rightarrow \gamma K_S^0 K_S^0$ . The curves represent fits to two incoherent Breit Wigner curves plus a quadratic background. Mark III collaboration.
8. Distribution<sup>[36]</sup> of  $m(K^+K^-)$  for the two data samples taken (a) in 1982 ( $\sim 0.9 \times 10^6 J/\Psi$  decays) and (b) in 1983 ( $\sim 1.8 \times 10^6 J/\Psi$  decays). The curve in (a) is what one would expect scaling the signal from the 1983 data as fitted in (b) to the 1982 data. Mark III collaboration.
9. (a)  $K^+K^-$  invariant mass distribution for  $J/\Psi \rightarrow \gamma K^+K^-$  by the DM2 collaboration<sup>[39]</sup>. Result of an analysis of  $\sim 4.4 \times 10^6 J/\Psi$  decays.  
(b) Same as Fig. 9a for the  $\gamma K_S^0 K_S^0$  final state.
10. (a)  $K^+K^-$  invariant mass distribution for  $J/\Psi \rightarrow \gamma K^+K^-$  by the DM2 collaboration<sup>[40]</sup>. Result of an analysis of  $\sim 8.6 \times 10^6 J/\Psi$  decays.  
(b) Same as Fig.10a for the  $\gamma K_S^0 K_S^0$  final state.

11. Invariant mass of candidate  $K^+K^-$  combinations for data taken on (a) the  $\Upsilon(1S)$  and (b) the  $\Upsilon(2S)$  by the CLEO collaboration<sup>[43]</sup>.
12. Inclusive photon spectrum<sup>[44]</sup> from a sample of 112,000  $\Upsilon(1S)$  decays vs.  $Z = E_\gamma/E_{\gamma max}$ ; CUSB collaboration.
13. Flavor changing neutral decay of the  $b$ -quark to the (pseudo)scalar neutral Higgs  $h^0$ , mediated by a charged Higgs  $H^-$ .
14. Invariant mass<sup>[43]</sup> of candidate  $K^+K^-$  combinations for data taken on the  $\Upsilon(4S)$  by the CLEO collaboration.
15. (a) The inclusive spectrum for  $\Upsilon(1S) \rightarrow \gamma +$  multiple hadrons; Crystal Ball collaboration<sup>[35]</sup>.  
 (b) The  $\zeta$ -peak region of Fig.15a with fit (see text) shown as a solid line.  
 (c) Same as Fig.15b with the fitted background subtracted.
16. (a-c) Same as Fig.15 (a-c) but for  $\Upsilon(1S) \rightarrow \gamma +$  low multiplicity sample.
17. Product branching ratio upper limit (90 % C.L.) for the process  $\Upsilon(nS) \rightarrow \gamma X$ ,  $X \rightarrow \tau^+\tau^-$ ; Crystal Ball collaboration. The decays  $\tau^\pm \rightarrow e^\pm\nu\bar{\nu}$  and  $\tau^\mp \rightarrow \mu^\mp\nu\nu$  have been used in the analysis.
18. (a-c) Same as Fig.15 (a-c) but for  $\Upsilon(2S) \rightarrow \gamma +$  multiple hadrons.
19. (a) The 90% C.L. upper limit for  $Br(\Upsilon \rightarrow \gamma H^0)$  derived from the data shown in Fig.12; CUSB collaboration<sup>[44]</sup>.  
 (b) Prediction of the standard model with a single Higgs doublet.
20. The 90% C.L. upper limit for  $Br(\Upsilon \rightarrow \gamma X)$  vs.  $M_X$  by the CUSB collaboration (Ref.58) presented at Leipzig in the summer of 1984. Indicated also is the result of the Crystal Ball collaboration<sup>[35]</sup> for  $\Upsilon(1S) \rightarrow \gamma\zeta(8.3)$ . The hatched area indicates the newest results from the CUSB collaboration presented in the fall of 1984 (Ref.59).
21. The 90% C.L. upper limit for the product branching ratio  $Br(\Upsilon \rightarrow \gamma H^0) \cdot Br(H^0 \rightarrow 2 \text{ charged particles})$  derived by the CUSB collaboration (Ref.44)  
 (a) from  $\Upsilon$ -decays, (b) from  $\Upsilon'$ -decays. (c) shows the standard model prediction for  $Br(\Upsilon \rightarrow \gamma H^0)$ .
22. The 90% C.L. upper limit for the product branching ratio of the decay  $Br(\Upsilon \rightarrow \gamma X) \cdot Br(X \rightarrow \tau^+\tau^-)$  by the ARGUS collaboration<sup>[60]</sup>. The decays  $\tau \rightarrow \mu\nu\bar{\nu}, e\nu\bar{\nu}, \pi\nu$  and  $K\nu$  have been used in the analysis.
23. The inclusive photon spectrum from the 22  $pb^{-1}$  of data taken by the Crystal Ball collaboration in the fall of 1984<sup>[60]</sup>. The best fit is shown with the mean constrained to  $\pm 1.0\%$  of that expected for the  $\zeta(8.3)$ .

24. The 90% C.L. upper limit from the data shown in Fig.23 for the process  $\Upsilon(1S) \rightarrow \gamma X$ , where  $X$  decays hadronically. The hadronic decay mode is modeled by  $c\bar{c}$  jets ( $c$  is the charmed quark). The vertical dashed lines show the expected position of the  $\zeta(8.3)$ .
25. Branching ratios for decays of the  $\Upsilon$ -states into a Higgs boson with mass  $\sim 10 \text{ GeV}/c^2$  as calculated in Ref.30.
26. Feynman diagram for the  $H^0$ - ${}^3P_0(b\bar{b})$  mixing.
27. (a) Feynman diagrams<sup>[63]</sup> for  $Q \rightarrow H^0 q'$ . Solid line, quark ( $Q, Q_i, q'$ ); wiggly line, gauge vector boson ( $W^\pm$ ); dashed line, physical Higgs boson ( $H^0$ ); dash-dot line, unphysical Higgs boson ( $\phi^\pm$ ).  
 (b) An example of the Feynman diagrams of Fig.27a involving the  $t$ -quark.  
 (c) Feynman diagrams<sup>[63]</sup> for the bremsstrahlung of  $H^0$ . The notation is the same as in Fig.27a.
28. Disallowed values of  $m_t, m_{H^0}$  (from Ref. 63) deduced from data published in Ref.67. The single hatched and double hatched areas for  $1.0 \leq m_{H^0} \leq 3.5 \text{ GeV}/c^2$  come from the assumption  $Br(H^0 \rightarrow \mu^+\mu^-) = 0.2$  and  $Br(H^0 \rightarrow \mu^+\mu^-) = 0.02$  respectively. The authors of Ref.63 emphasize that these results are illustrative, not optimal, because they are obtained by analyzing an experiment (Ref.67) which was not designed nor analyzed for this purpose.
29. Diagrams contributing to  $e^+e^- \rightarrow H^+H^-$ . (a) via an intermediate virtual photon, (b) via coupling to the  $Z^0$ .
30. Main decay modes of a charged Higgs boson  $H^\pm$ .
31. Expected event patterns<sup>[76]</sup> for the  $e^+e^- \rightarrow H^+H^-$  reaction for different decay modes of  $H^\pm$ . See text.
32. The combined<sup>[76]</sup> limit on the mass of charged Higgs as a function of its branching ratio into  $\tau\nu_\tau$ , obtained by  $e^+e^-$  experiments. Combinations of  $[Br(H^+ \rightarrow \tau^+\nu_\tau), m_{H^+}]$  that lie within the area surrounded by the shaded band are excluded by experiment at 95 % C.L..
33. Feynman diagrams for the decay  $Z^0 \rightarrow \gamma H^0$ .
34. Decay rates<sup>[77]</sup> for  $Z^0 \rightarrow \gamma H^0$  and  $Z^0 \rightarrow \mu^+\mu^-H^0$  (or  $Z^0 \rightarrow e^+e^-H^0$ ) in terms of the decay width  $Z^0 \rightarrow \mu^+\mu^-$  for different values of the Higgs mass.
35. (a) The decay  $Z^0 \rightarrow \mu^+\mu^-H^0$ .  
 (b) The process  $e^+e^- \rightarrow Z^{0*} \rightarrow H^0 Z^0$ .
36. Mass spectrum recoiling against high mass ( $> 50 \text{ GeV}/c^2$ )  $e^+e^-$  pairs from a Monte Carlo simulation<sup>[79]</sup> of  $Z^0 \rightarrow e^+e^-H^0$  and  $e^+e^- \rightarrow e^+e^-X$ .

37. Calculations<sup>[80]</sup> of  $\sigma(e^+e^- \rightarrow H^0 Z^0)/\sigma_{\mu\mu}$  for different values of  $\sqrt{s}$ ,  $m_{H^0}$  and  $\sin^2\theta_W$ .
38. Cross section<sup>[77]</sup> for  $e^+e^- \rightarrow H^+H^-$  (including  $Z^0$ -exchange) as a function of  $\sqrt{s}$ . The dashed line shows the electromagnetic contribution whereas the full line includes also the effect of  $Z^0$  exchange.
39. (a) Feynman diagrams for the dominating decay modes of  $J/\Psi$  and  $\Upsilon$ .  
(b) Feynman diagrams which gain importance for very heavy vector resonances (see text).
40. (a) Calculated<sup>[81]</sup> decay widths of a vector resonance  $V$  into various channels vs. the mass  $m_t$  of the constituent quarks. ( $\Gamma_{W1}$  is the partial width for the (spectator like) weak decay of one of the constituent quarks; the other partial widths are selfexplanatory).  
(b) Branching ratios of  $V$  decays vs.  $m_t$ . See also Fig.40a.

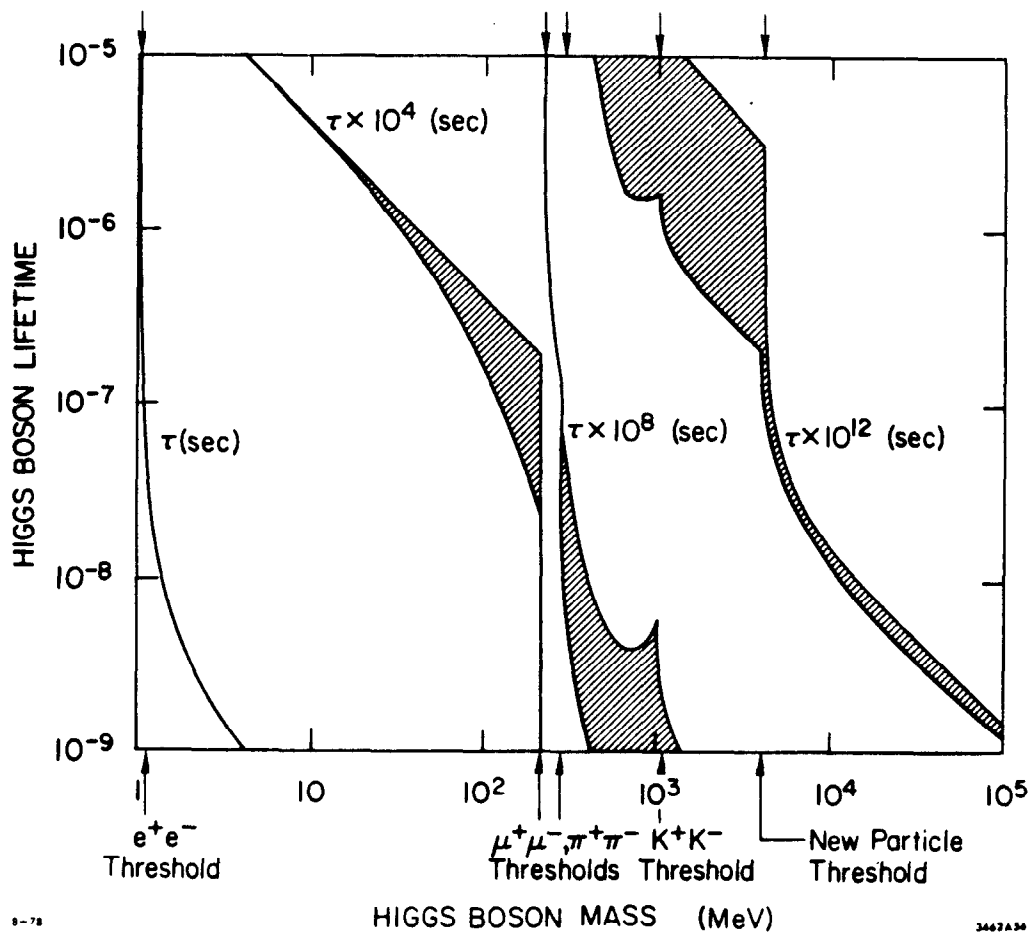
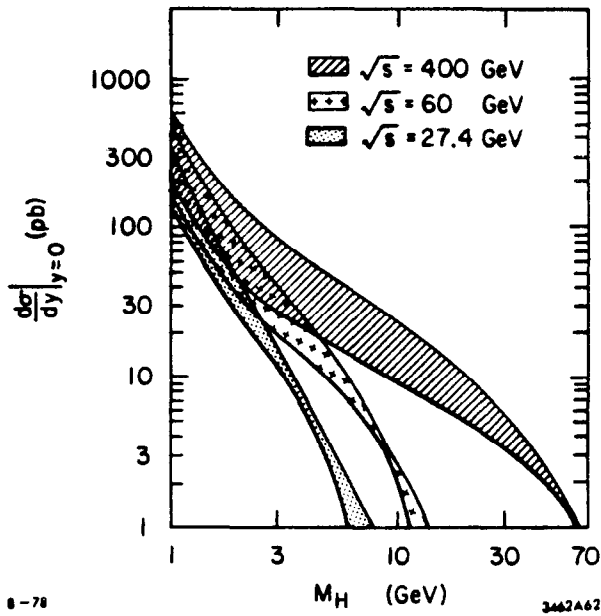


Fig. 1



8-78

3462A62

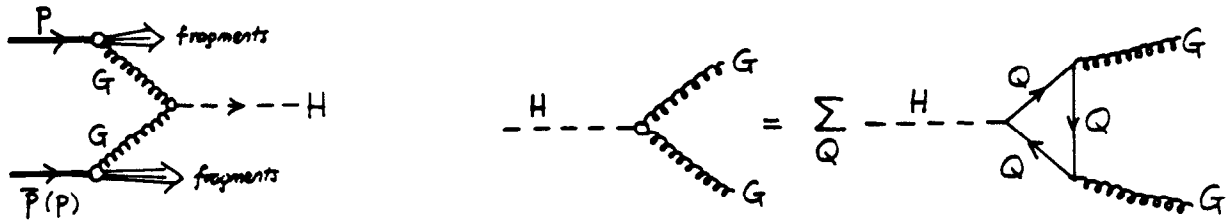


Fig. 2a

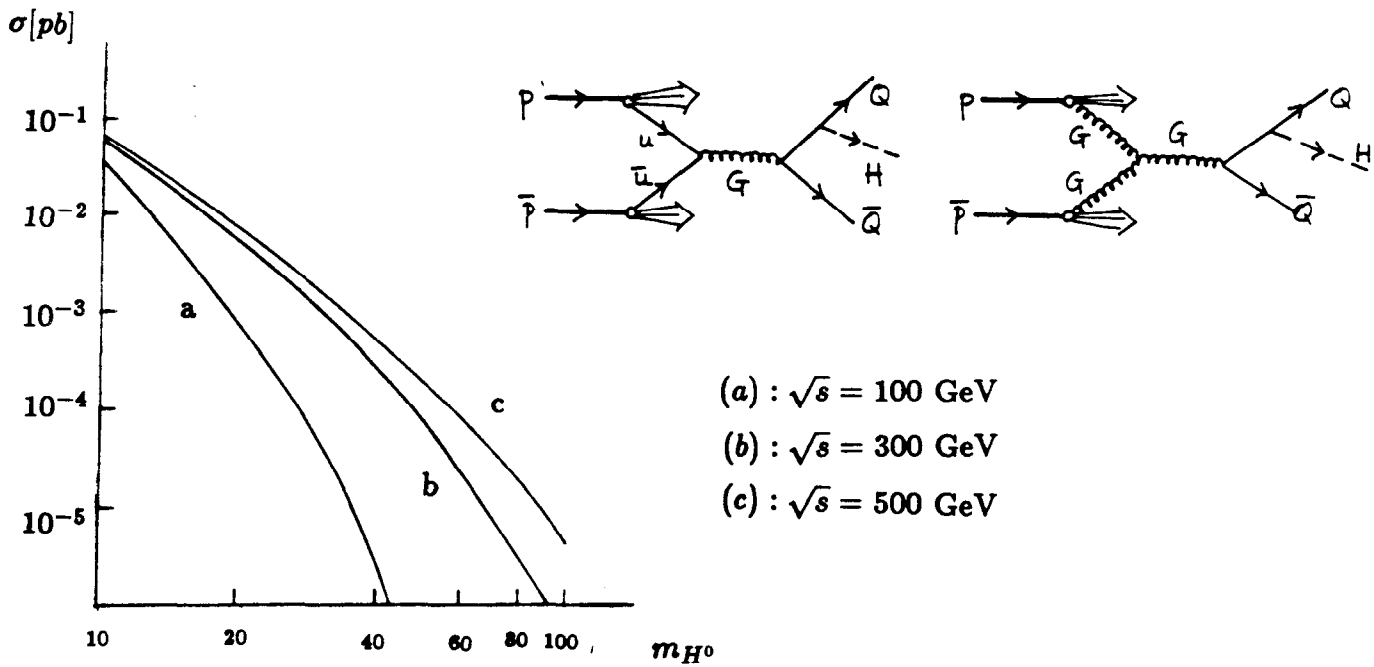


Fig. 2b

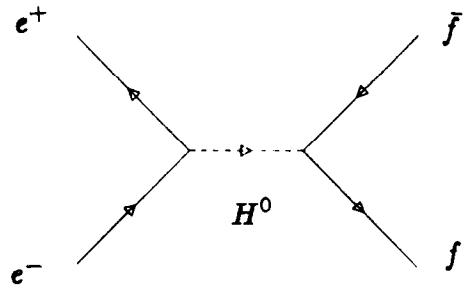


Fig. 3a

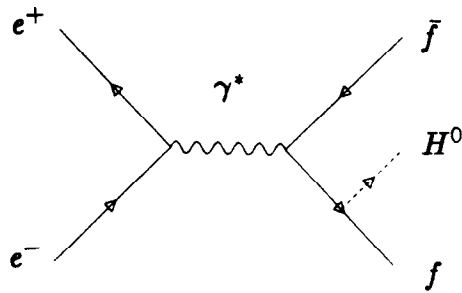


Fig. 3b

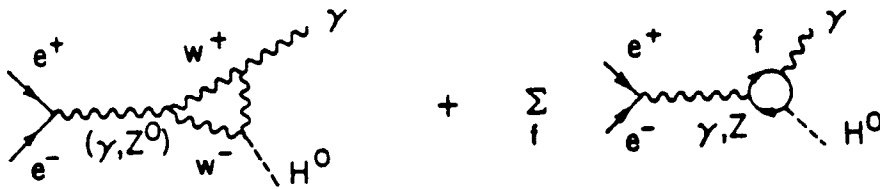


Fig. 3c

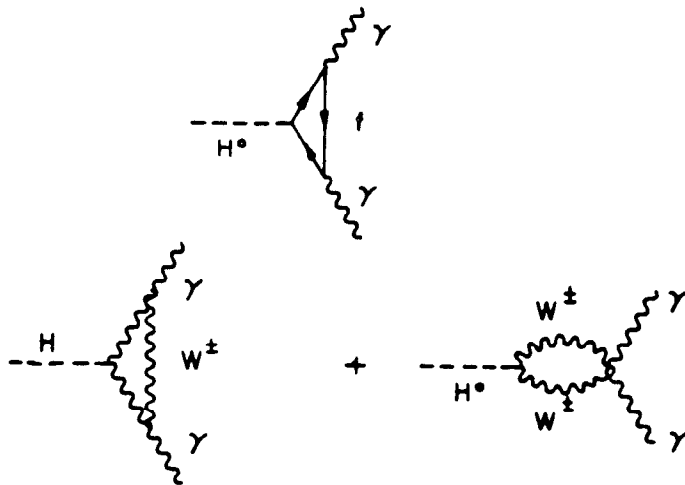


Fig. 3d

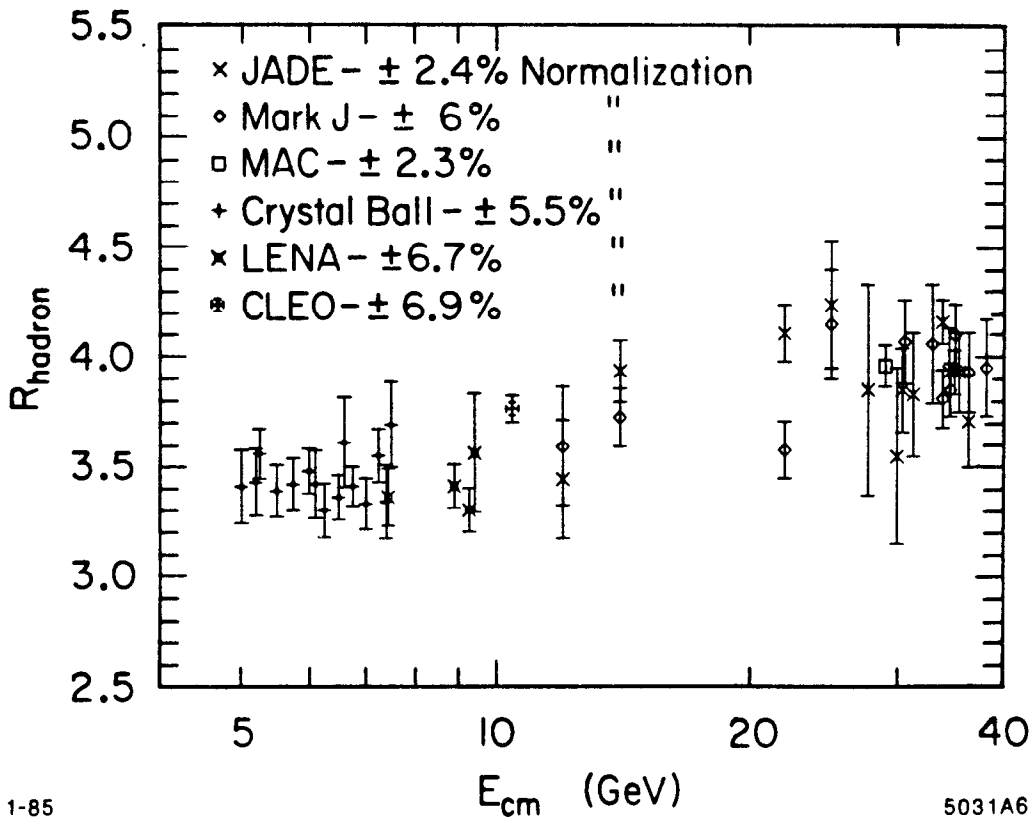


Fig. 4

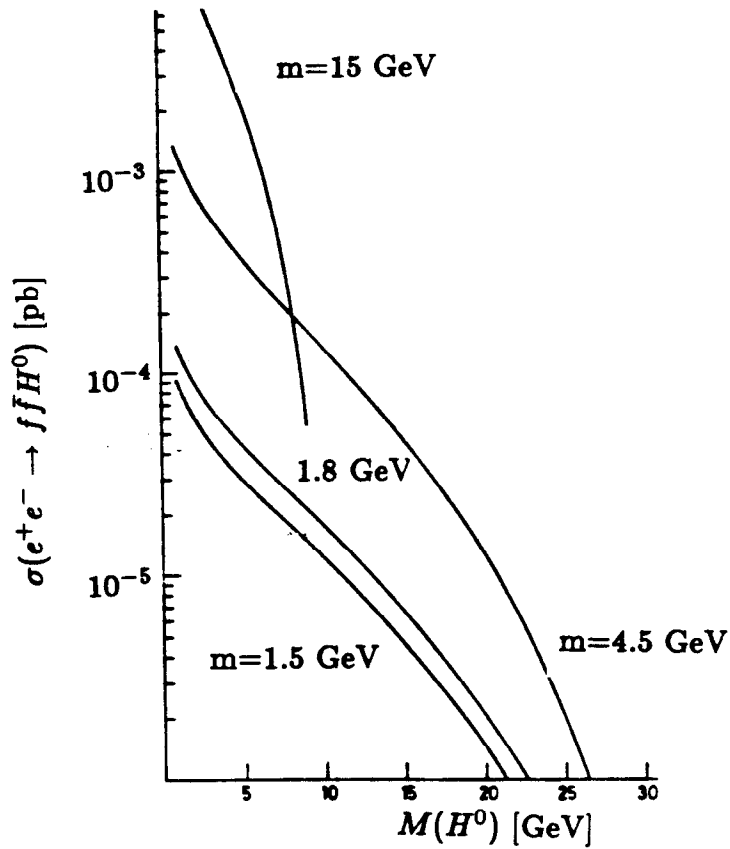


Fig. 5

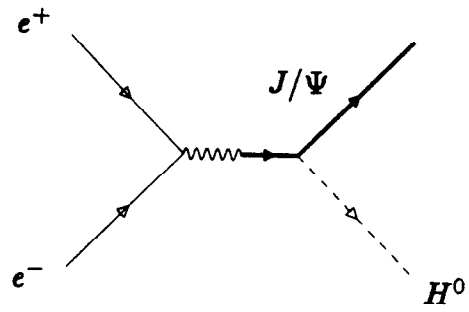


Fig. 6a

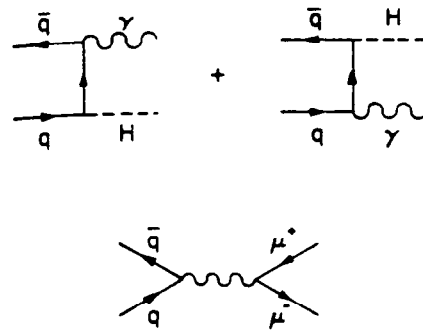
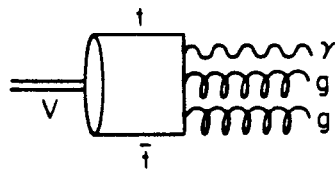


Fig. 6b



1-85

5016A5

Fig. 6c

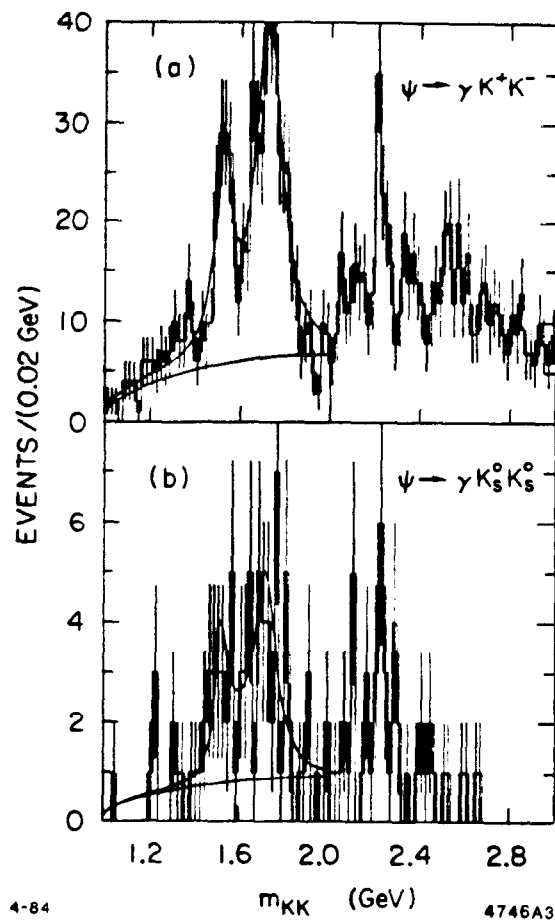


Fig. 7

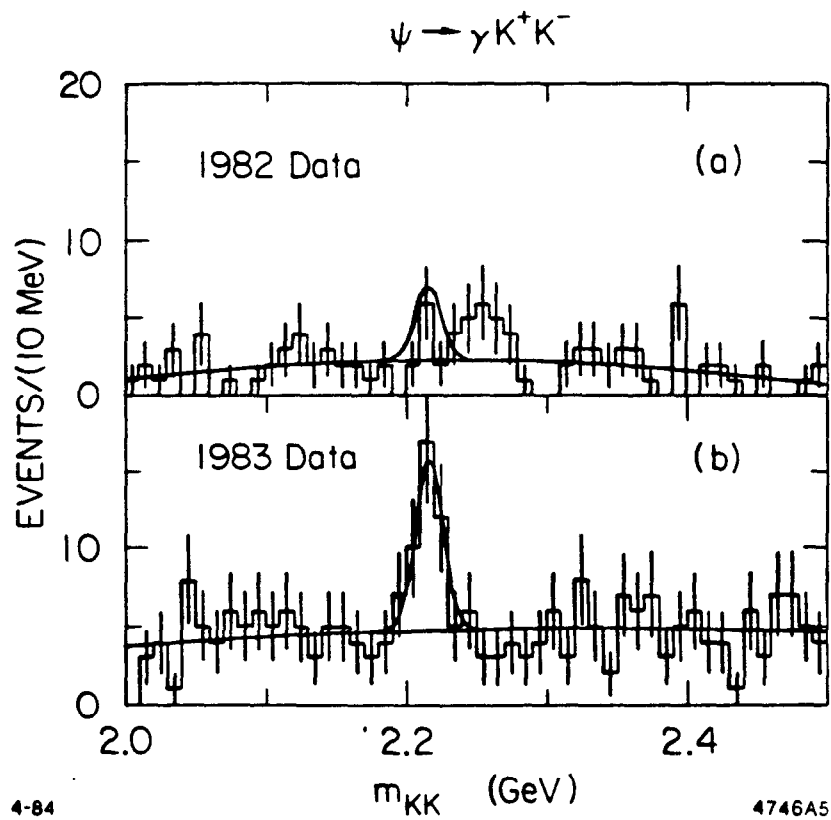


Fig. 8

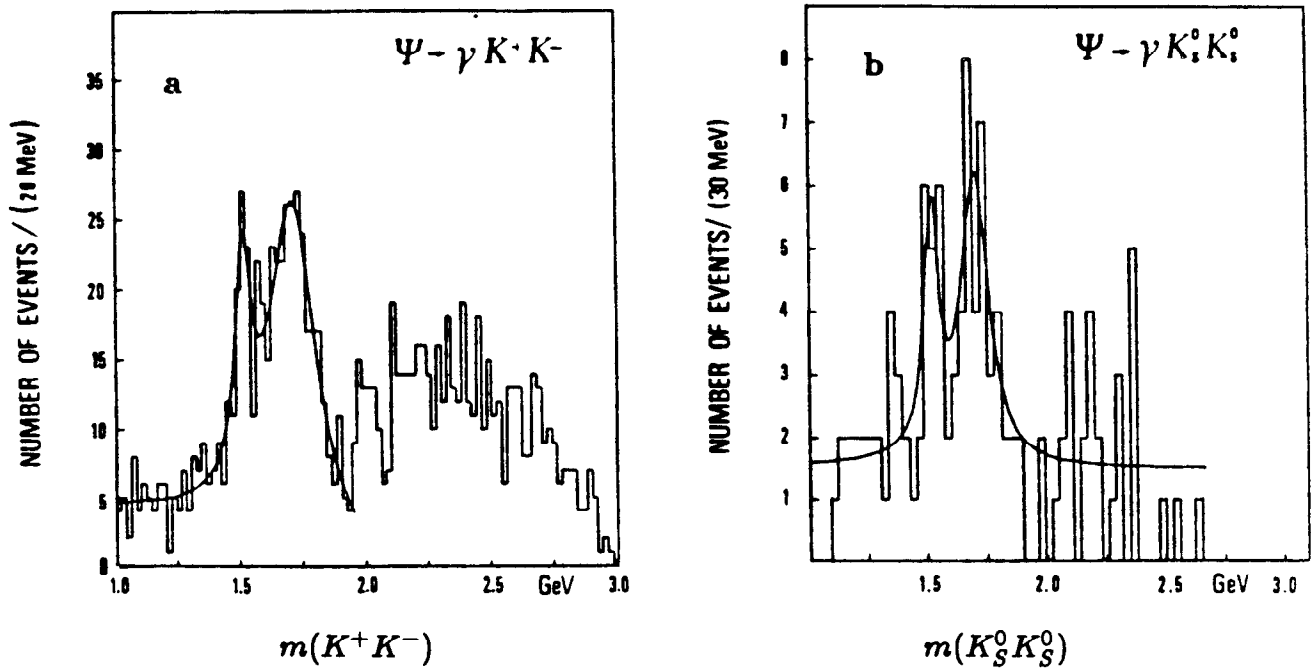


Fig. 9

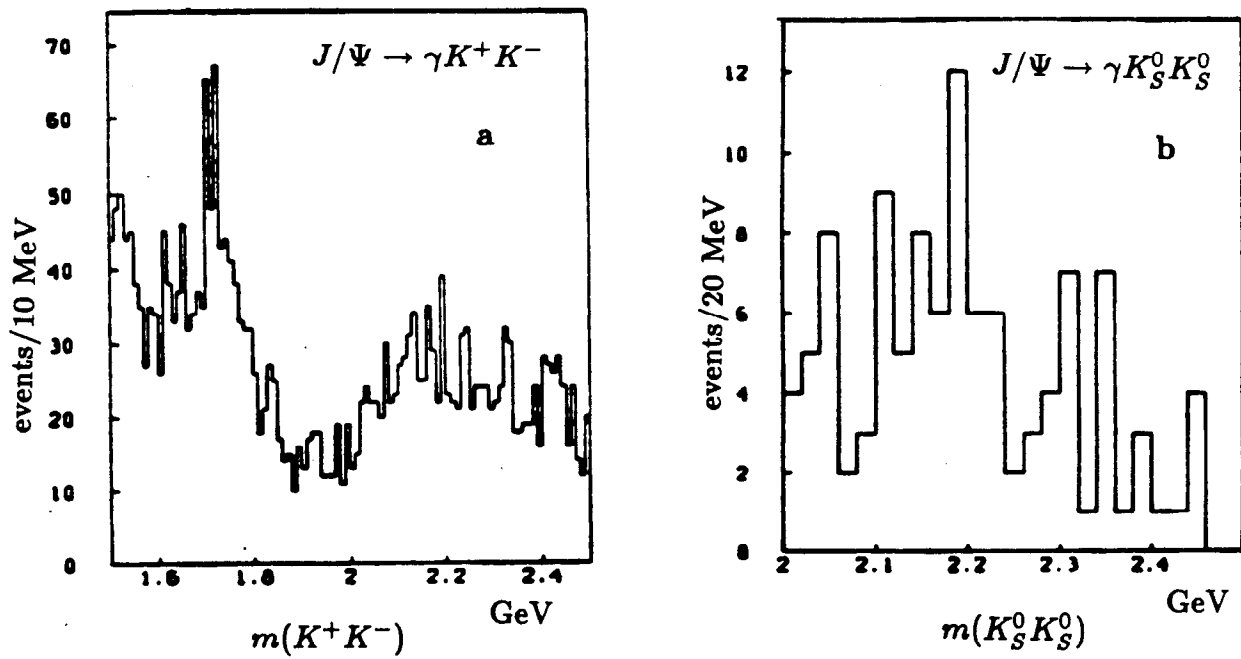


Fig.10

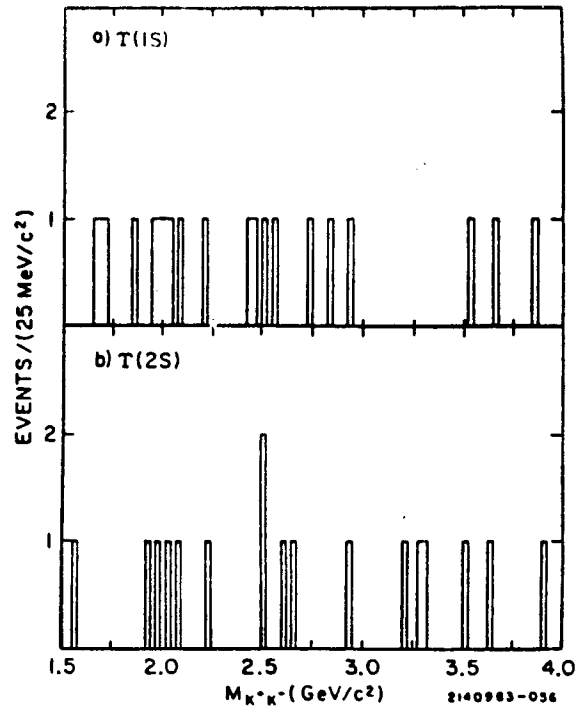


Fig.11

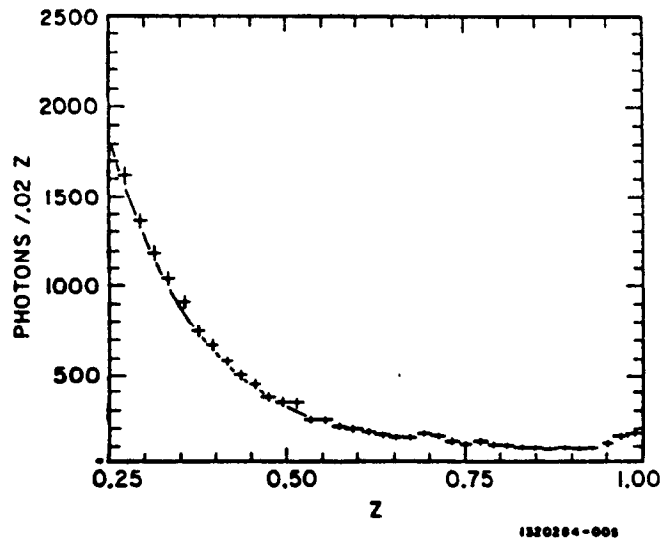


Fig.12

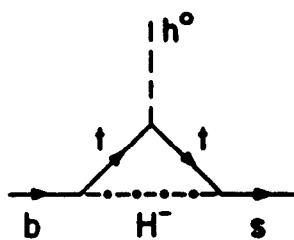


Fig.13

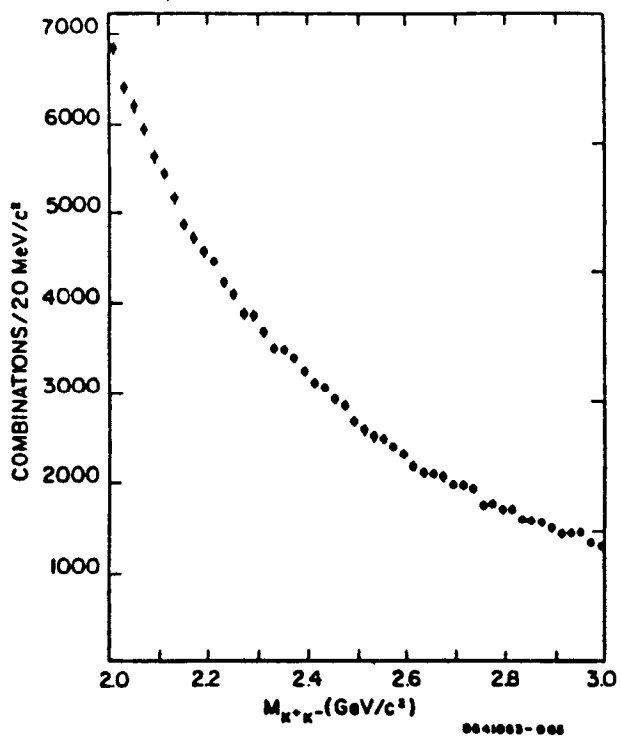


Fig.14

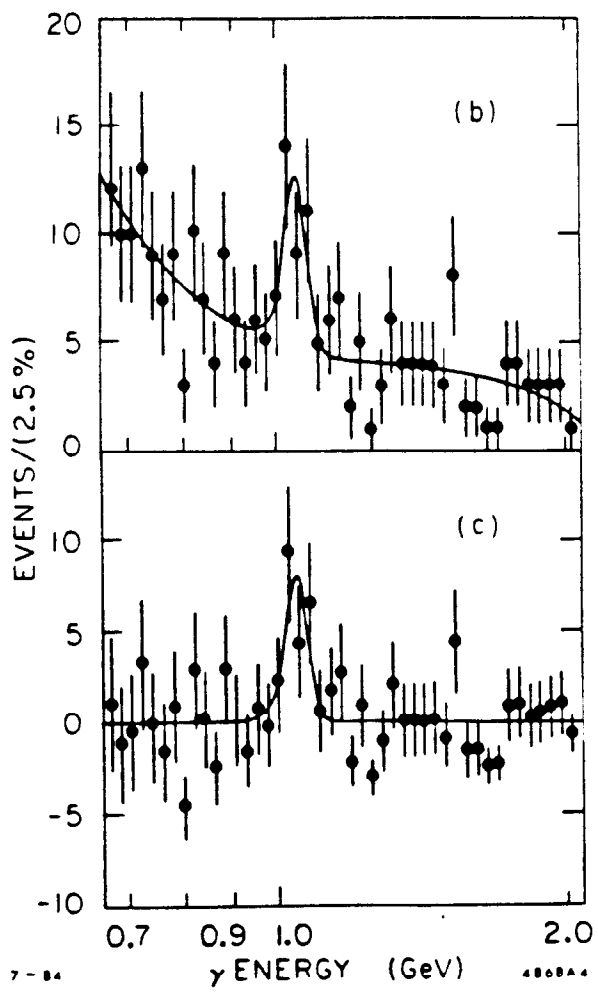
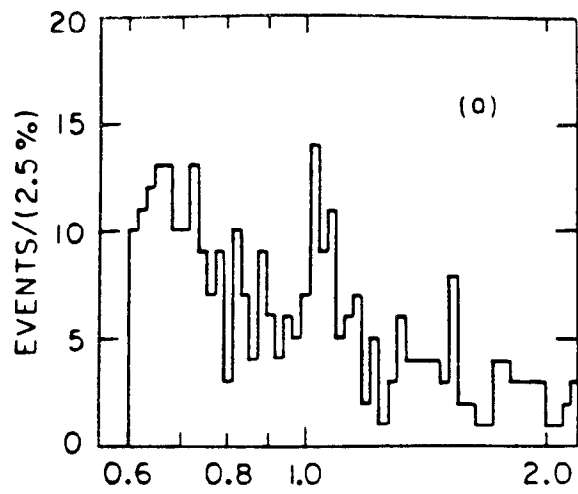
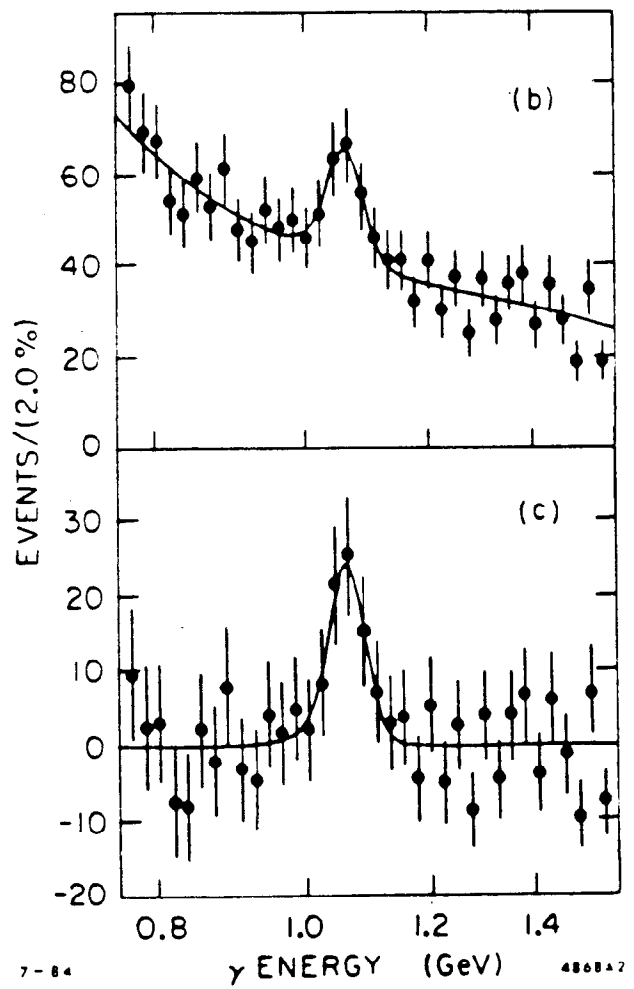
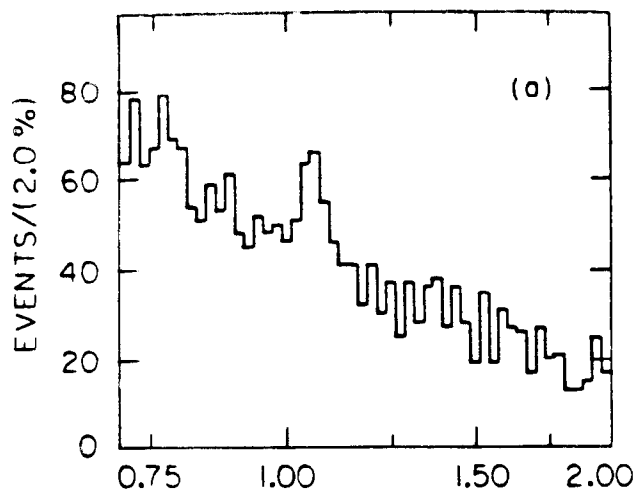


Fig.15

Fig.16

Crystal Ball preliminary

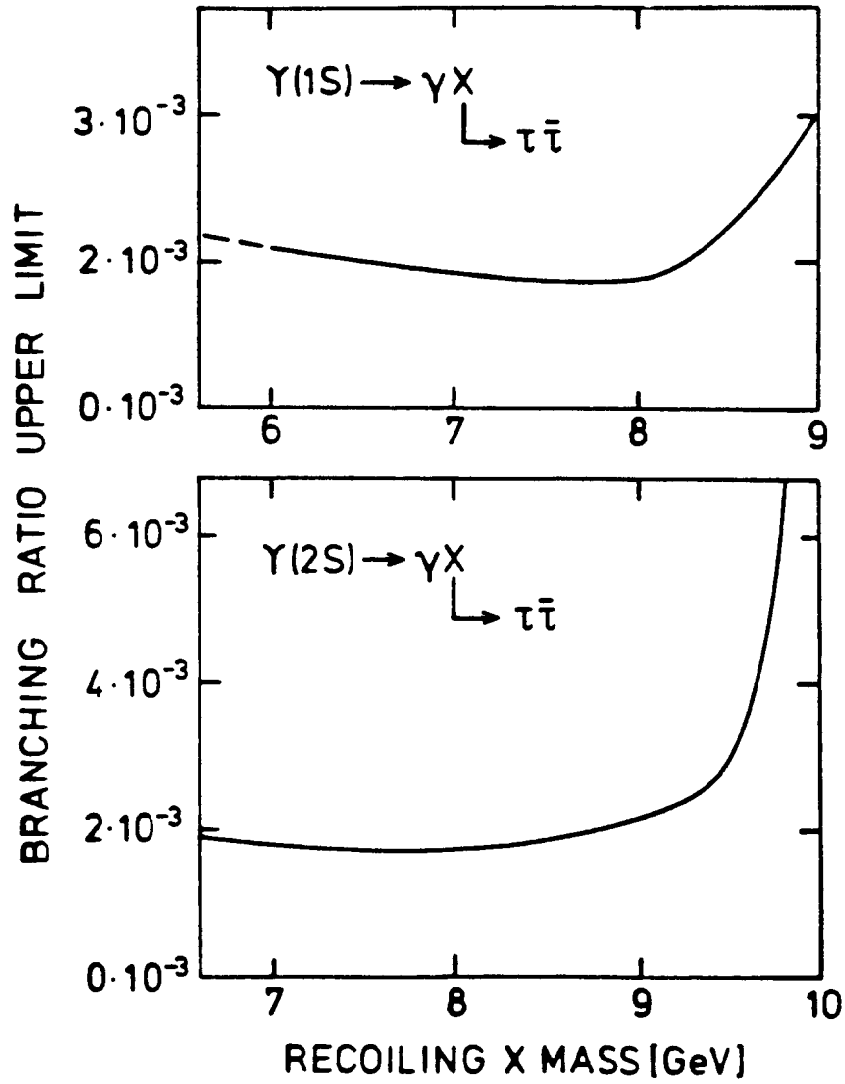


Fig.17

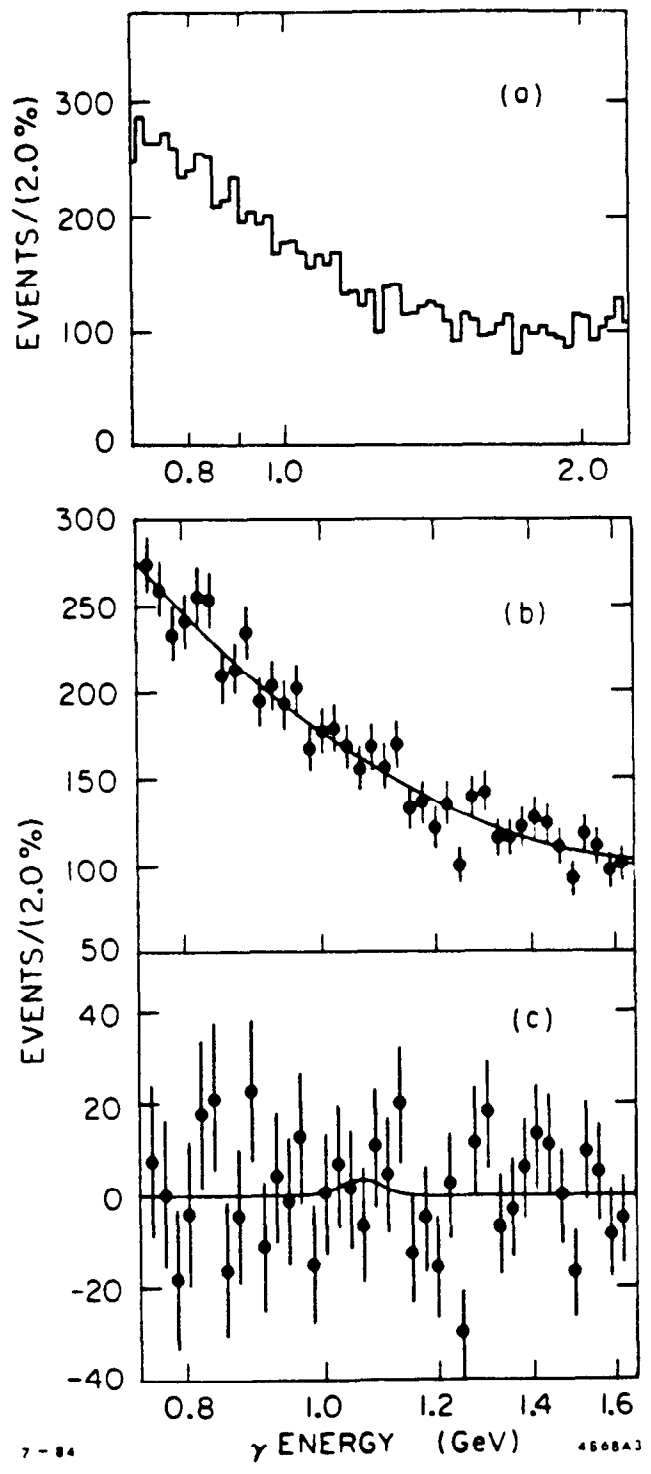


Fig.18

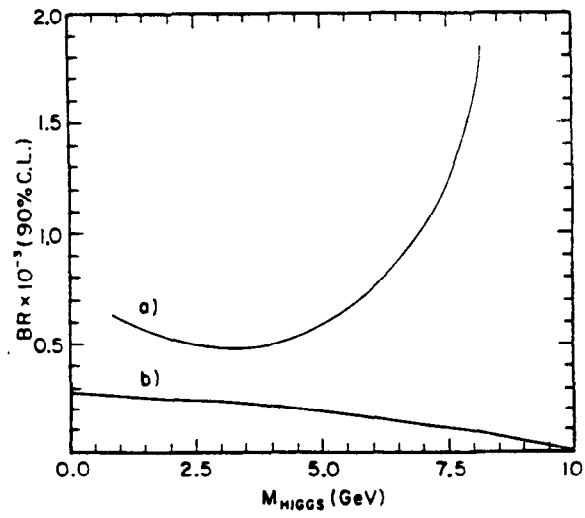


Fig.19

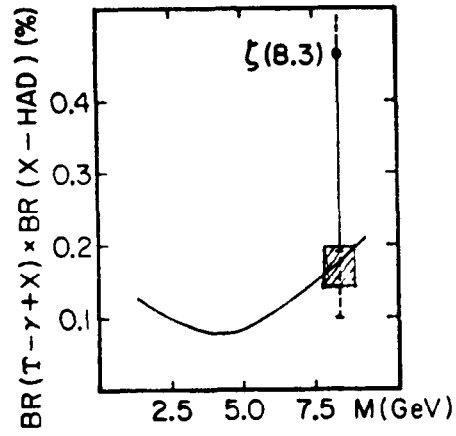


Fig.20

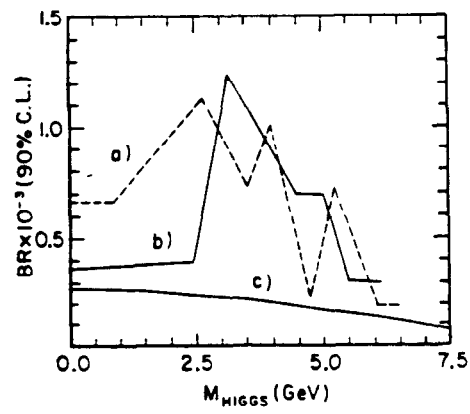
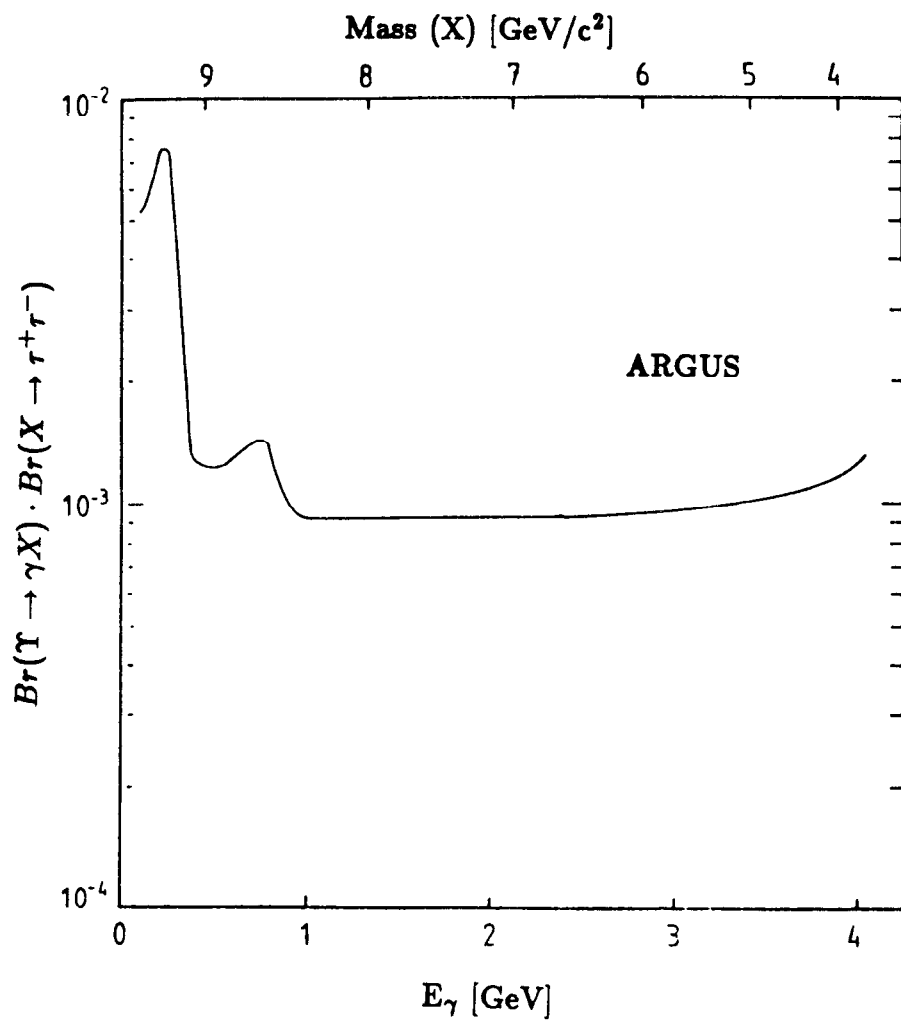


Fig.21



**Fig.22**

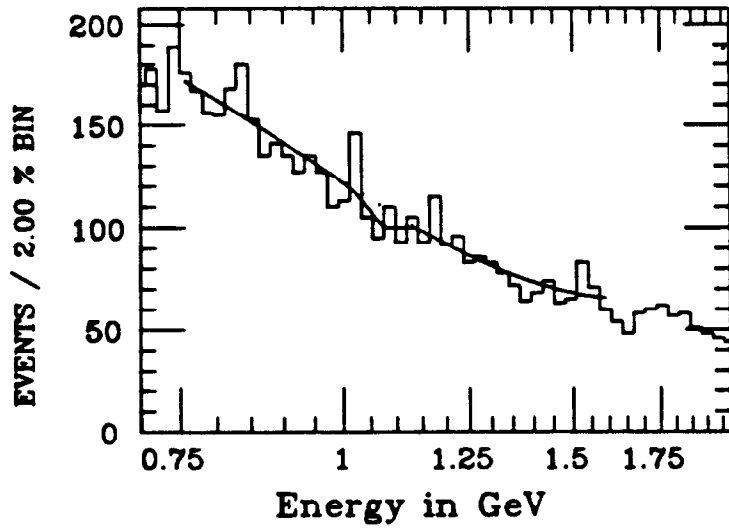


Fig.23

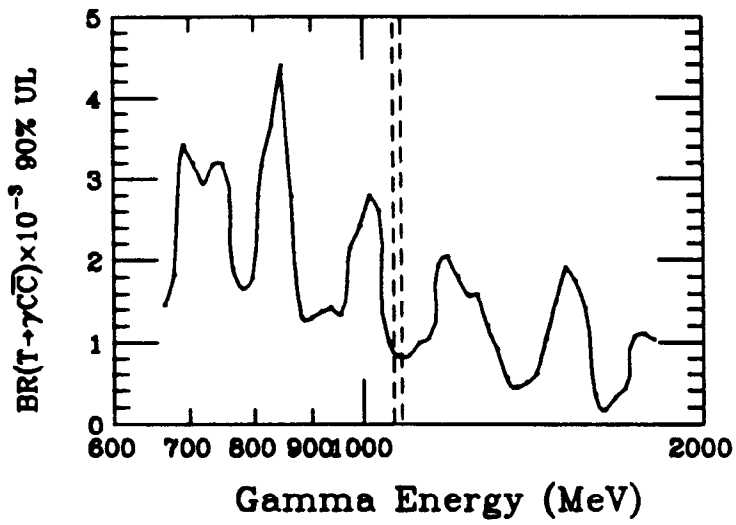


Fig.24

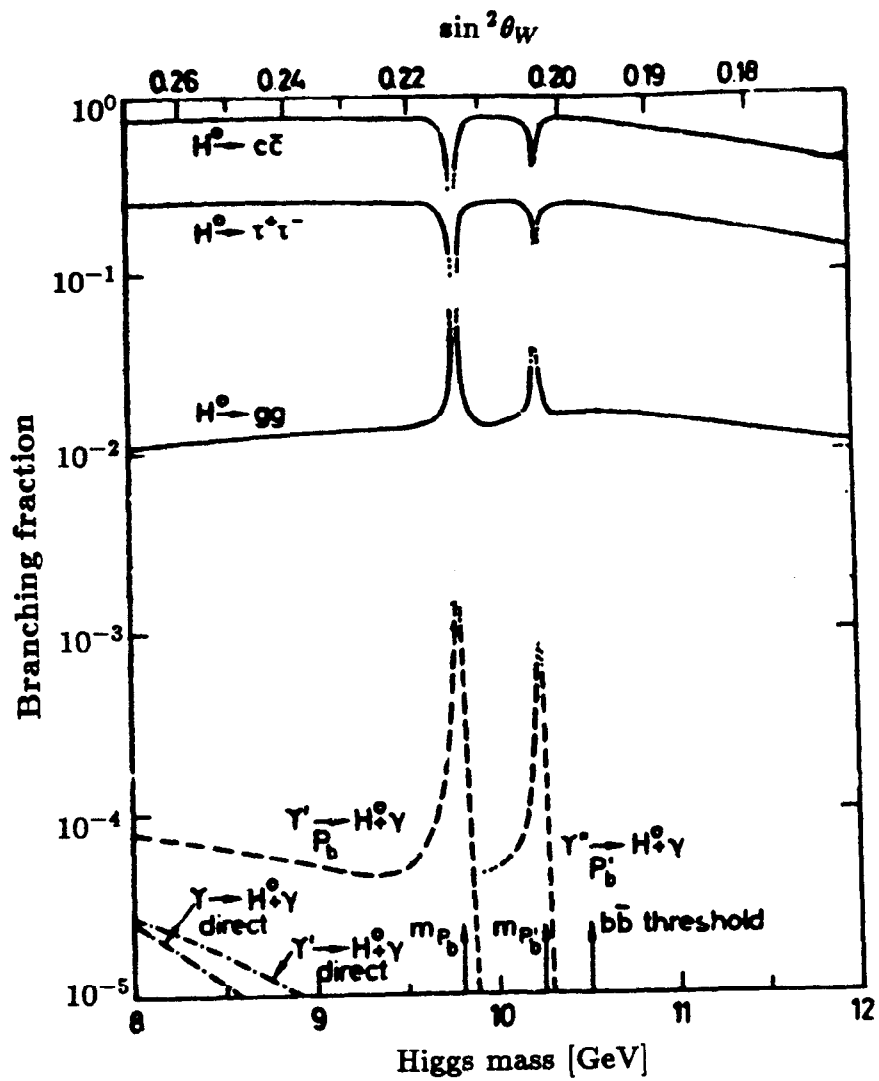


Fig.25

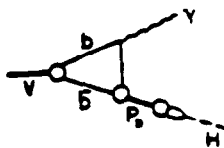


Fig.26

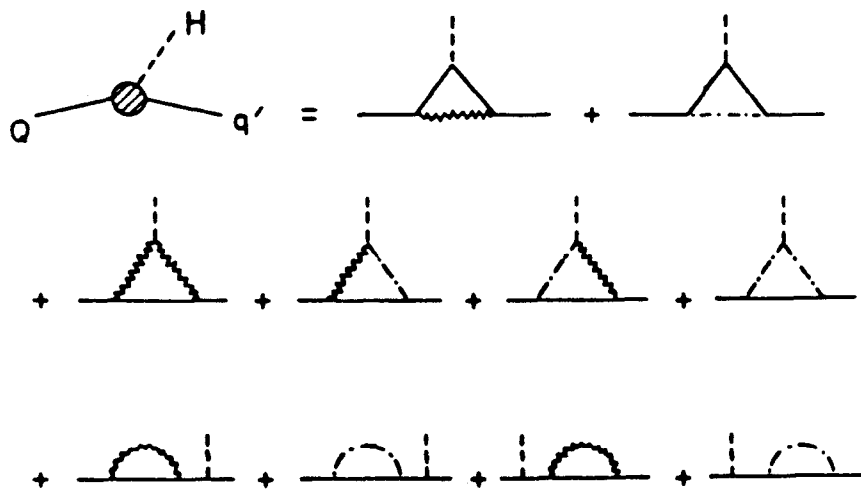


Fig.27a

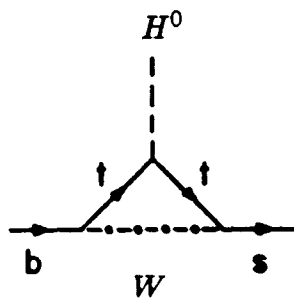


Fig.27b

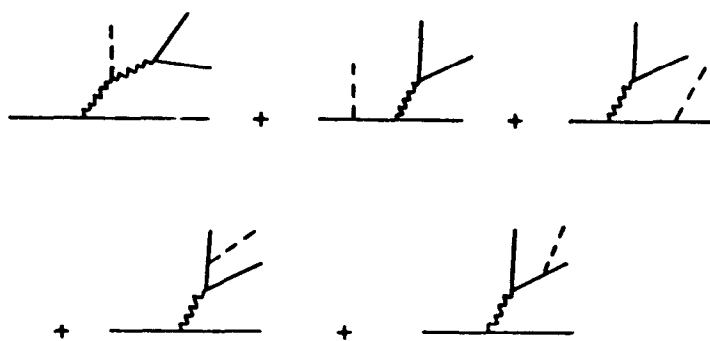


Fig.27c

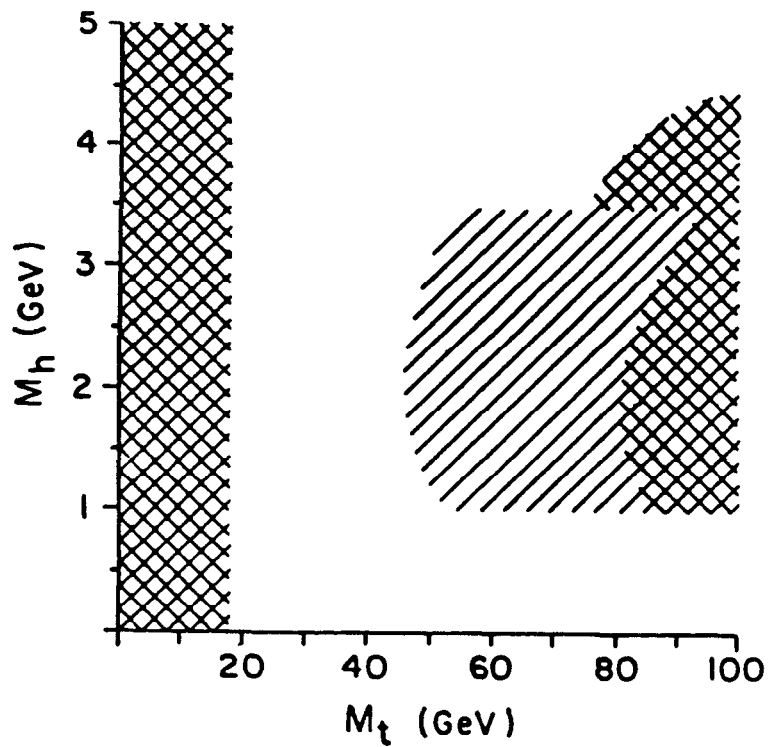


Fig.28

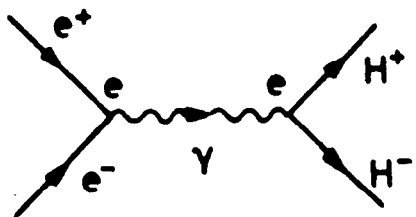


Fig.29a

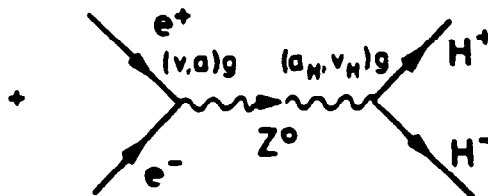


Fig.29b

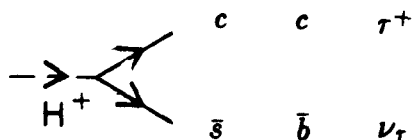


Fig.30

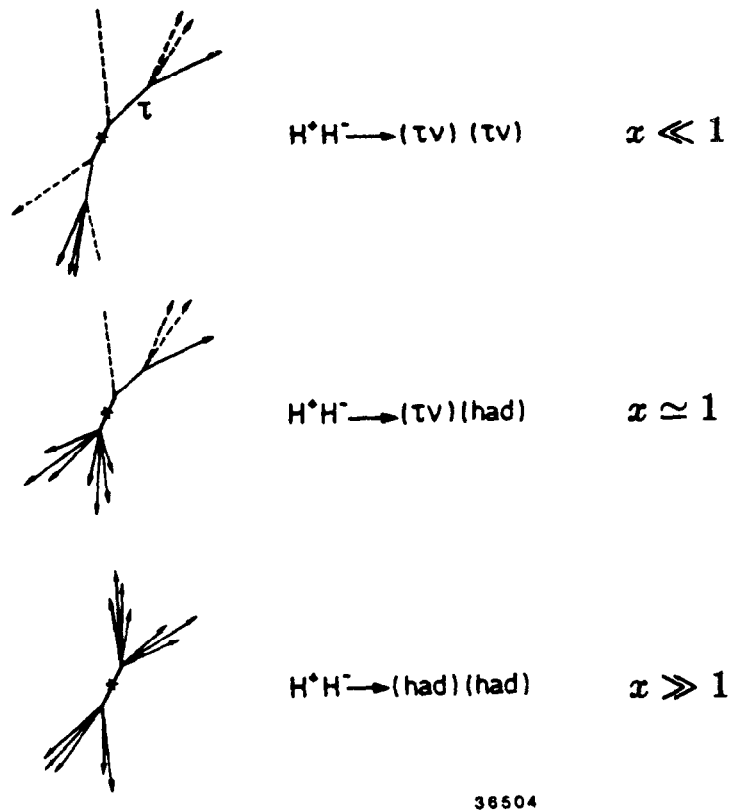


Fig.31

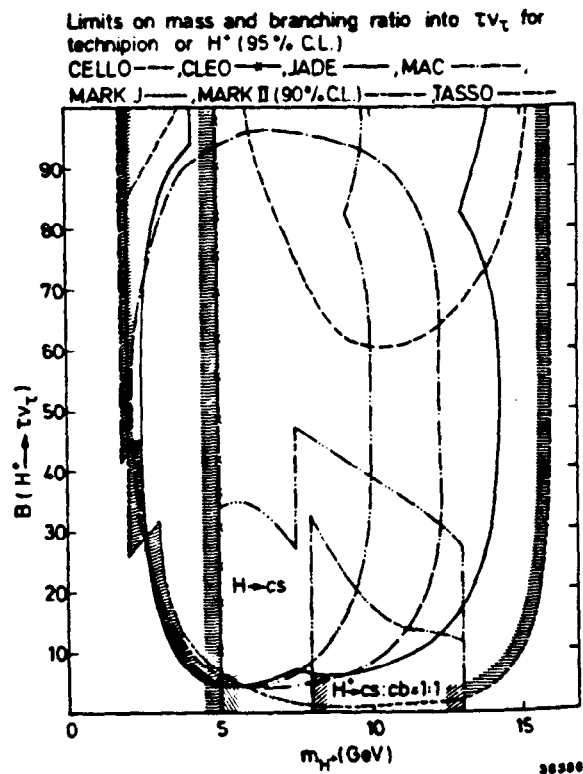


Fig.32

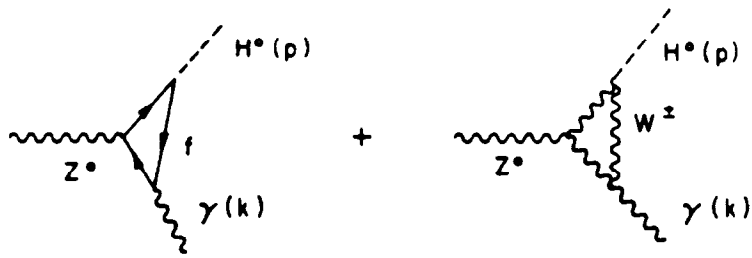


Fig.33

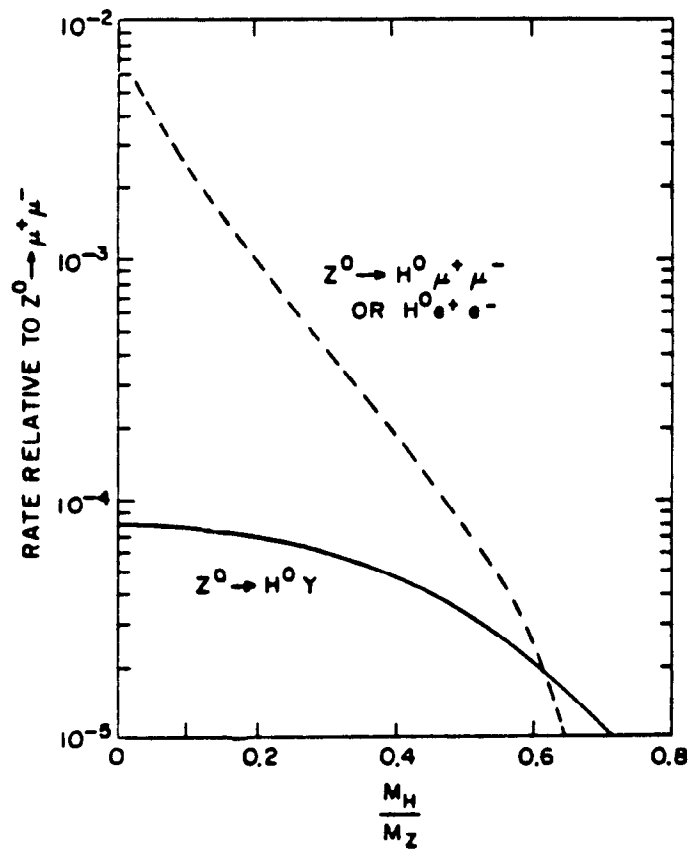


Fig.34

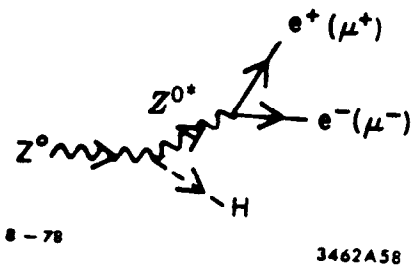


Fig.35a

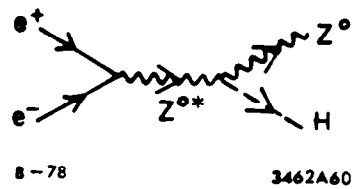


Fig.35b

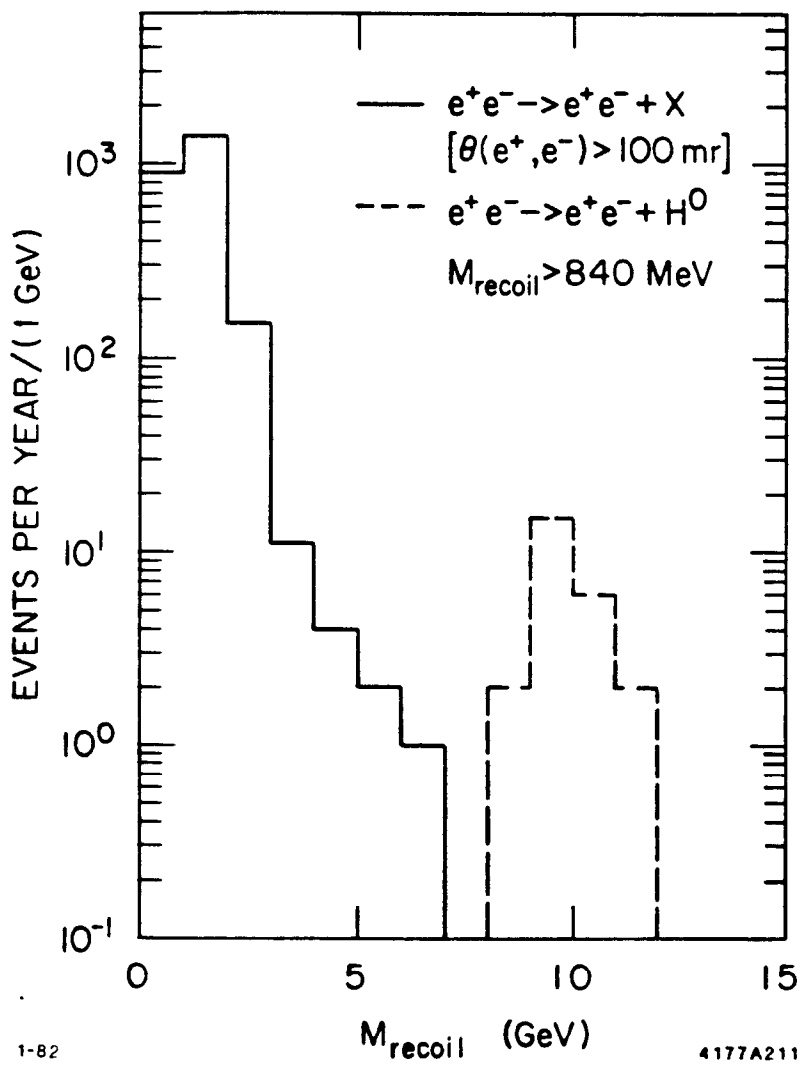


Fig.36

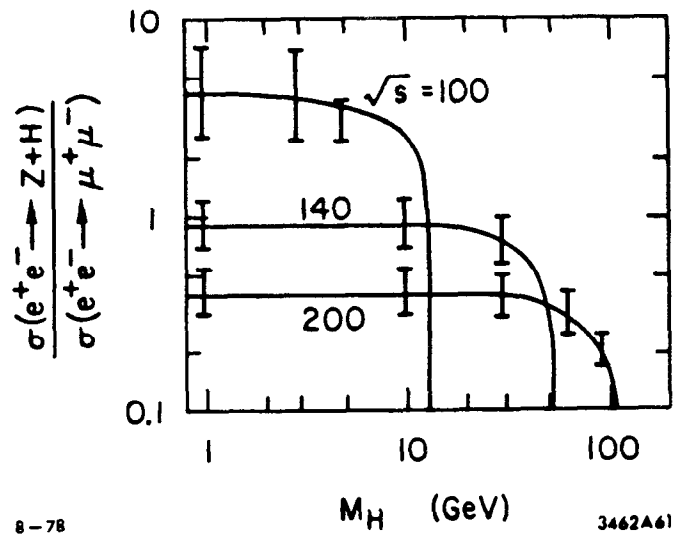


Fig.37

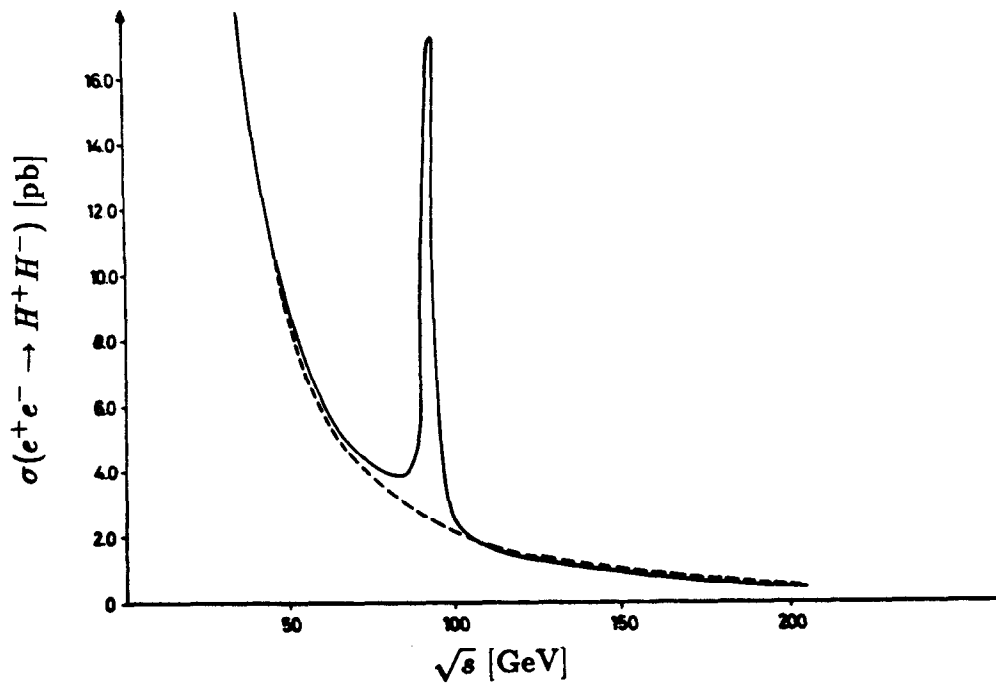
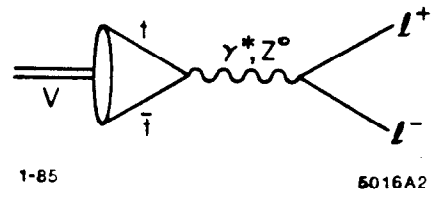
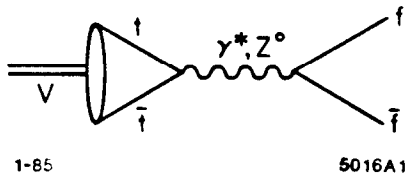
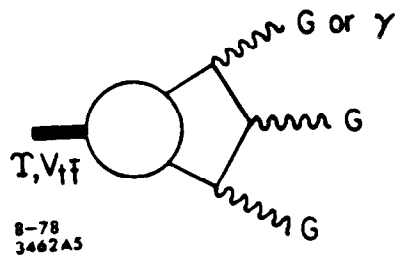
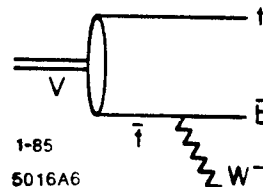
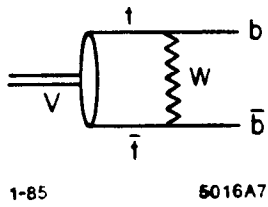
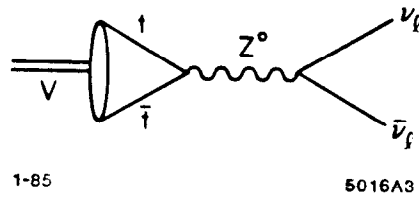


Fig.38



**Fig.39a**



**Fig.39b**

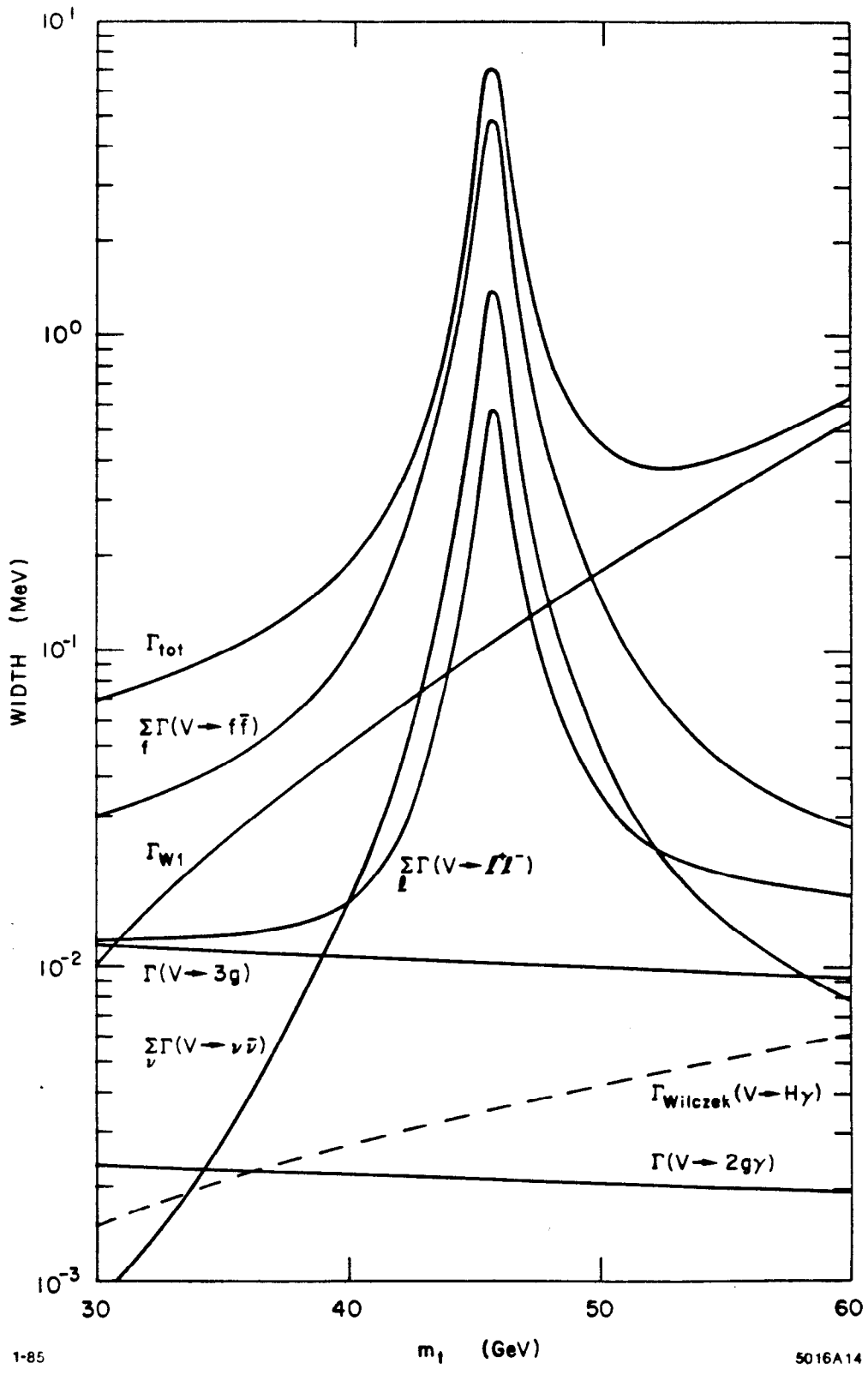


Fig.40a

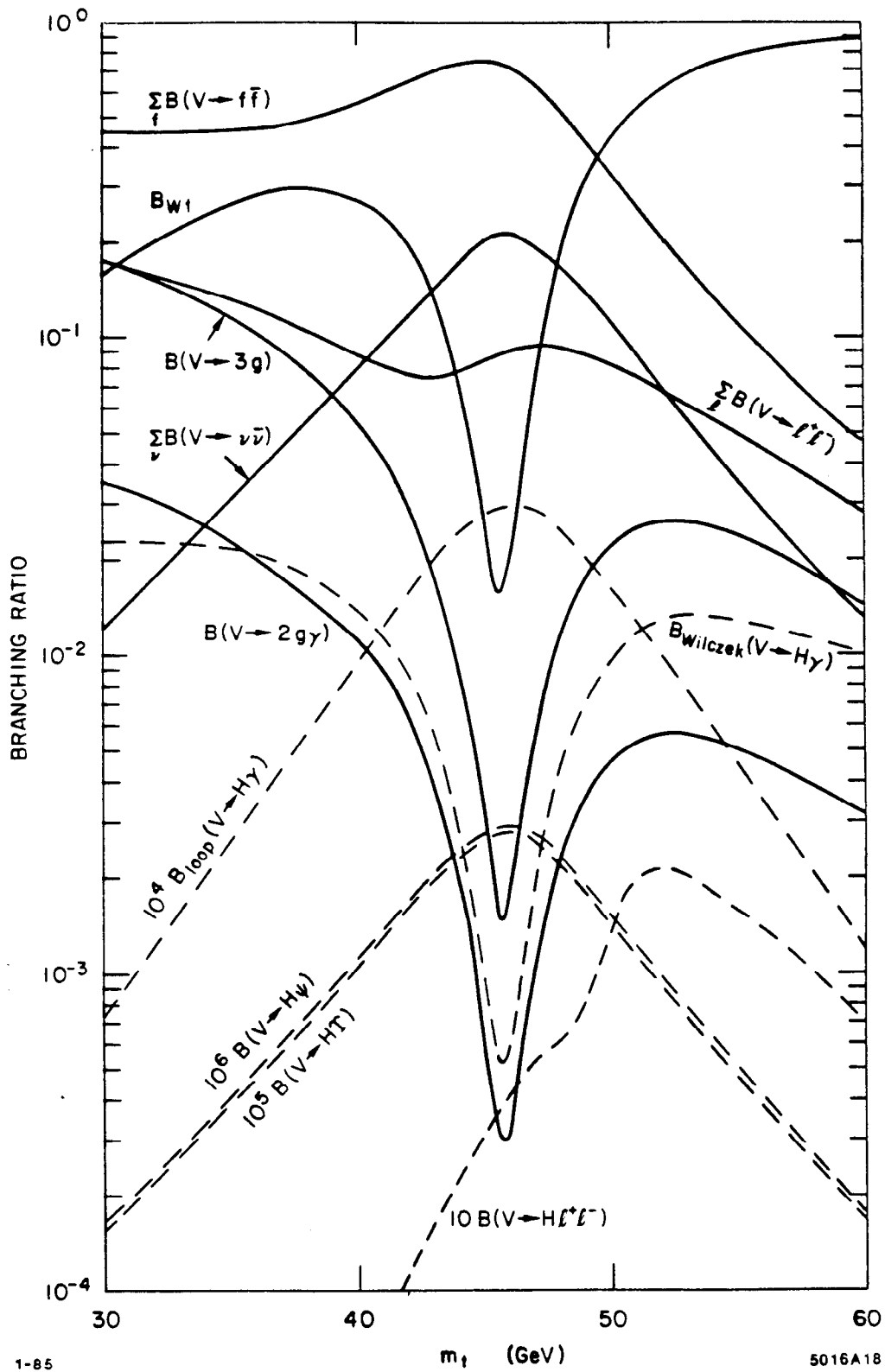


Fig.40b